NASA CR-121146

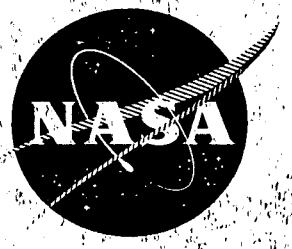

LF460 DETAIL DESIGN

FINAL TECHNICAL REPORT

ON AIRCRAFT SUPPORT ACTIVITY

by

GENERAL ELECTRIC COMPANY

prepared for

NATIONAL AERONAUTICS AND SPACE ADMINISTRATION

NASA-Lewis Research Center
Contract NAS2-6056
L. W. Gertsma - Project Manager

1. Report No.	2. Government Accession No.	3. Recipient's Catalog No.
CR121146		

4. Title and Subtitle	5. Report Date
LF460 Detail Design Final Technical Report on Aircraft Support Activity	April, 1973
	6. Performing Organization Code
7. Author(s)	8. Performing Organization Report No.
	10. Work Unit No.
9. Performing Organization Name and Address General Electric Company Aircraft Engine Group Cincinnati, Ohio 45215	11. Contract or Grant No. NAS2-6056
	13. Type of Report and Period Covered Contractor Report June 1971 to March 1972
12. Sponsoring Agency Name and Address National Aeronautics and Space Administration Washington, D. C. 20546	14. Sponsoring Agency Code

15. Supplementary Notes

Project Manager, L. W. Gertsma
Lift Fan Project Office
NASA Lewis Research Center, Cleveland, Ohio

16. Abstract

This is the final report presenting the results of various studies and analyses that were performed in support of the V/STOL research transport design effort. The propulsion system specified for these studies was the LF460/YJ97-GE-100 turbotip lift fan. Strong emphasis was placed on achieving low fan noise while maintaining the high thrust/weight capability of the high pressure ratio lift fan system. The work was divided into cycle analysis and performance studies, installation and systems support, acoustic analysis and preliminary or conceptual design studies.

17. Key Words (Suggested by Author(s))	18. Distribution Statement
Propulsion, Lift Fan, V/STOL, Connecting Duct, Aerodynamic Design	Unclassified - Unlimited

19. Security Classif. (of this report)	20. Security Classif. (of this page)	21. No. of Pages	22. Price*
Unclassified	Unclassified	121	3.00

* For sale by the National Technical Information Service, Springfield, Virginia 22151

TABLE OF CONTENTS

LIST OF TABLES

LIST OF ILLUSTRATIONS

LIST OF ILLUSTRATIONS

LIST OF ILLUSTRATIONS

LIST OF ILLUSTRATIONS

LIST OF ILLUSTRATIONS

SECTION I

SUMMARY

This is the final report presenting the results of various studies and analyses that were performed in support of the V/STOL research transport design efforts. This activity covered the period from June 1971 to March 1972 and was performed under an amendment to Contract NAS2-6056.

In June 1971, three aircraft companies were contracted to perform conceptual design studies of a V/STOL research transport that employed the LF460 turbotip lift fan as the prime V/STOL propulsion component. Prior to this aircraft study contract, the detail design of the LF460 had been completed, and additional design studies were being performed for remote lift units employing heavy exhaust suppression and low fan pressure ratios for reduced noise generation. The aircraft support activity included studies and analysis of this complete LF4XX family of lift fans. The designation "4" denotes the fourth design generation and the "XX" denotes the fan size in terms of tip diameter.

The support activity can be separated into four major categories:

- Cycle analysis and performance
- Installation and systems
- Acoustic Analysis
- Preliminary and conceptual design studies

This report presents the results of those studies and analyses where significant contributions were derived during the airframer support activity.

SECTION II

INTRODUCTION

Studies were initiated by NASA and the General Electric Company in 1968 to define an advanced, high pressure ratio, turbotip lift fan system which would take advantage of available higher energy gas generator sources. The initial studies of this advanced system were directed towards a potential application in a modified XV-5 aircraft for flight research testing. The proposed system, a LF446 lift fan was driven by the discharge gas of an advanced engine (GE1/10); however, recognizing that this cycle would not be available in time for the planned flight demonstration, the YJ97-GE-100 turbojet gas generator was selected as the most promising candidate for the flight demonstration program.

In late 1969, the program was redirected by NASA toward a research transport aircraft that would provide technology information applicable to the design of future V/STOL commercial transports. With this change in program direction, the LF446 was scaled-up in size to take advantage of the full discharge flow of the YJ97 engine. This resulting 60-inch lift fan configuration was called the LF460 advanced turbotip lift fan.

Preliminary design studies of the LF460/YJ97-GE-100 system were conducted in the late 1969, early 1970 time period of an advanced lift fan that would satisfy the V/STOL transport research aircraft requirements. Strong emphasis was placed on achieving low fan noise while maintaining the high thrust/weight capability of the high pressure ratio lift fan systems. The detailed design of the LF460 was initiated in April 1970 and was completed in May 1971. The final fan layout is shown in Figure 1. The program summary and results of the detailed design of this LF460/YJ97-GE-100 system are presented in Reference 1.

Performance of the LF460/YJ97-GE-100 system was also estimated and presented in a customer deck for use on electric data processing equipment. This customer deck represented a complete lift fan-engine system, and included, representative interconnect ducting, inlet, exhaust nozzles and power transfer control systems.

The next phase in development of a V/STOL research transport, using lift fan as the method of propulsion, was initiated by NASA in June 1971. At that time, three separate aircraft companies were contracted to study research V/STOL aircraft designs that would provide the needed technology for an advanced

V/STOL commercial transport system. The propulsion system specified for these studies was the LF460/YJ97-GE-100 turbotip lift fan.

Coincident with this additional aircraft design activity, the scope of the LF460 program was expanded to provide propulsion system support for the selected aircraft companies. This activity covered the time period from June 1971 to March 1972. This report documents the significant work items or tasks performed during this programed support activity of the V/STOL research aircraft studies.

The work items will be divided into four major categories as listed below:

- Cycle analysis and performance studies
- Installation and systems support
- Acoustic analysis
- Preliminary or conceptual design studies

SECTION III

CYCLE ANALYSIS AND PERFORMANCE

In support of the V/STOL research transport studies, performance and cycle studies were conducted for the LF460-YJ97-GE-100 propulsion system. Much of the activity was involved in verification of system performance as estimated by the users of customer deck and development of routine performance data as requested by the particular airframe companies. The following discussion presents some of the studies where significant contributions were made to enhance the understanding of lift fan performance particularly for the unique interconnect power transfer methods incorporated in the LF460/YJ97-GE-100 system and corresponding cycle deck.

Expanded Performance Deck Operation

Performance of the LF460/YJ97-GE-100 turbotip lift fan system was represented in a customer deck developed as part of the basic LF460 design studies. This performance deck was provided to each of the aircraft companies involved in the preliminary design of the V/STOL research transport. The basic deck included a representative duct for transferring the hot gases from the YJ97-GE-100 gas generator to the LF460 and representative convergent nozzles and exit louver exhaust systems for customer usage. The option was also provided for the customer or user to supply their own connecting duct and exhaust systems computational procedure.

During the conduct of the aircraft design studies, customer usage indicated a desire to expand the deck capability in several areas. The following discussion presents the expanded capability provided during this effort. Appendix A presents the instructions required to incorporate these changes into the original cycle deck representation.

Turbine Temperature Limit

The YJ97-GE-100 engine had an established steady state exhaust gas temperature limit of 1835 degrees Rankine. Engine operation at above standard day conditions would require an engine speed cut-back in order to maintain operation within this limit. A tentative revised temperature limit of 1870 degrees Rankine has been established for the engine during the above standard

day operation. The new limit permitted rated speed (101.5%) operation at above standard conditions only and does not represent a revised limit for engine trimming on a standard day. The procedures for revising the present customer deck to include this capability is given in Appendix A.

Sizing with Customer Bleed and Power Extraction

The original customer deck sizes the system for operation at the engine design point with no power extraction or compressor bleed. Bleed and power extraction would produce engine speed cut-back consistent with the established exhaust gas temperature limit of 1835 degrees Rankine. An alternate method of sizing the system was provided to include corrections for continuous levels of power extraction and customer bleed. The procedure for resizing the system with bleed and power extraction was developed using a design point (Z2CRSN) correction factor.

Nozzle Performance

The customer deck includes representative performance of nozzle configurations for use with the LF460 lift fan. The deck user originally had the option of providing his own nozzle subroutine to replace the built-in systems. The expanded procedures define the nozzle parameters presently in the deck and provided the customer an option of revising these parameters to represent his particular nozzle system. This expanded capability permitted the deck user to represent his nozzle configuration using the computational procedures included in the existing customer deck.

Ducting Systems Representation

The customer deck includes a representative ducting system with a diffuser, close-coupled ducting, throttling valve and interconnect duct systems. The option of using this method of representation, with modifications, was provided in the expanded deck capability. Provisions were given for adjustment of the ducting system performance and input parameters to match the particular LF460/YJ97-GE-100 system installation. The aircraft propulsion designers could then make use of customer deck procedures without developing their own ducting representation.

B

System Operation with Speed Unbalance

The power transfer method used in the LF460/YJ97-GE-100 system employs a pair of interconnected gas generators. Operation of the two engines at equal power levels can readily be determined by treating each engine separately using a conventional cycle analysis methods. The case of operation at unequal power levels requires an evaluation of the mutual interaction of the two engines through the interconnect duct system. This condition of unbalanced power operation was experimentally investigated as part of a NASA sponsored program for tests of two interconnected YJ97 engines. These tests for demonstration of the feasibility of the power transfer control concept were performed by the McDonnell Douglas Corporation at St. Louis, Missouri.

This test program demonstrated that the interconnected engines do have a large tolerance for power or speed unbalance. In addition to the test program, a parallel analytical cycle study was undertaken to investigate operation with speed unbalance. For this study, the interconnect ducting system was assumed to be accurately represented by the system included in the LF460 cycle deck. References 2 and 3 describe the ducting arrangement and the associated ducting loss parameters.

The results of this analysis are presented in Figure 2 through 8, and verify that operation is possible with quite large speed unbalances. The limits of the speed unbalance can be estimated based on the levels of compressor stall margin presented in Figure 7. This data indicates that adequate stall margin exists for the maximum attainable range of speed unbalance as long as the high engine speed is below about 92.5 percent. The maximum speed unbalance occurs when the low engine is at the idle power setting of 60 percent speed. The range of speed unbalance where stall of the low speed engine will occur is presented in Figure 8. This characteristic is based on cycle calculations for identical engine systems with no allowance for engine acceleration to higher speeds. The analytical stall characteristic agrees with the experimental test program where engine stall occurred with the high speed engine at 97.5 percent and the low speed engine at idle.

Effect of Variable Scroll Arc on Engine-Out Operation

The LF460/YJ97 lift fan system was designed for operation with interconnect between two engine and two lift units. The interconnect system provides a

method of power transfer between the pair of engines, thus, lift fan thrust can be modulated to provide aircraft control moments.

The interconnect ducting system, as included in the cycle deck representation is presented schematically in Figure 9. This ducting system represents an estimate of the system as proposed during the initial V/STOL research studies.

Operation of the ducting system to provide differential thrust for aircraft control proved quite adequate for the case of both engine systems operating. Investigations of operation of engine ducting system during engine-out operation showed a considerable fan thrust mis-match in addition to an increased engine discharge temperature. This increased engine temperature reduced the level of control thrust available based on the engine exit temperature limit of 2060 degrees Rankine.

The problem of engine-out operation initiated a study to investigate the effects of variable scroll arc on the magnitude of fan thrust mis-match. The LF460 lift fan was designed for equal or 180 degree scroll arcs as supplied by each inlet duct. For this study, the scroll arc was permitted to vary between 180 and 240 degrees for the unpowered or engine-out fan and between 180 and 120 degrees for the powered lift fan. The total scroll arc for each fan was held constant at 360 degrees as required to achieve design operation with two functional engines.

The performance assumed for the representative ducting system is summarizes in Table I and Figures 10 and 11. Table I lists the assumed loss coefficients for each of the major ducting components as identified in Figure 9. Figures 10 and 11 present the losses associated with the interconnect bleed flow extraction and injection processes. These assumed losses are reasonable estimates for a representative ducting system. Verification of these losses for the particular aircraft system will be required after the final aircraft system is selected. For this study, these losses were assumed to apply for the initial study. In addition, the losses were reduced by one half of the initial level to observe the changes of single engine performance levels.

Figures 12 through 15 present significant performance parameters as a function of the scroll admission arc. For the equal scroll split configuration, 180 degrees, the fan thrust mis-match is apparent. For this case, the fan directly connected to the operating engine would develop about 8200

pounds while the remote or engine-out unit would develop about 6400 pounds, and the engine exhaust gas temperature is 2000 degrees Rankine. Compared to a limiting temperature of 2060 degrees Rankine, the overtemperature range for control is very low, and thus the potential for control force development is at an unacceptable low level.

The scroll arc required for equal fan thrust is a 210-150 degree split. For this condition, the engine operation has moved into a speed cut-back condition due to the limiting exhaust gas gemperature and therefore there is no margin for control with power transfer. In order to provide control, additional engine speed reductions could be employed to reduce the exhaust gas temperature at some sacrifice of total fan thrust.

The analysis was extended to investigate the effects of reducing the interconnect losses. For this study, the losses of the cross-duct, including bleed-in and bleed-out ports were set at 50 percent of the original value. The performance for a range of scroll arcs is presented in Figures 16 through 19. Comparison of this performance with data with the original loss estimates shows a considerable improvement in the levels of control capable with scroll arcs adjusted for trimmed for thrust. The scroll arcs for trim are about 197/163 degrees and the engine discharge temperature is about 1930 degrees Rankine.

The results of this analysis show the extent of the ducting design problems for the particular case of engine-out or single engine operation. Low duct pressure losses and a selected scroll arc split are a requirement for achieving control capability with no change of trim requirements in the axis where the engine-out condition occurs.

SECTION IV

INSTALLATIONS AND SYSTEMS

The installation of propulsion systems into V/STOL aircraft requires close liaison between the propulsion and aircraft system designers. The installation problem is particularly critical in the area of propulsion system control, since the propulsion system is the only source of lift at hover, and in the methods of installation, because the volume of the propulsion components occupy a significant part of the aircraft structure. Throughout the preliminary and final design phases of the LF460 lift fan system, considerable effort was applied to develop a system that would meet the aircraft requirements and at the same time develop a lightweight high efficiency propulsion system.

The following discussion presents some of the significant results obtained during installation and system studies as requested by the concerned airframe design groups.

Fan Stall Envelope

Previous experience with fan-in-wing operation has shown that a stall condition can occur at high angles of attack and high cross-flow velocities. This stall condition appears as a breakdown of the flow into the fan inlet and over the surrounding wing or lifting surface. One of the initial studies undertaken was to define a criteria for stall of lift fans when installed in typical shallow inlet configurations.

The basic source of fan-in-wing stall data was tests performed by NASA with the LF336/A fan installed in a two fan model. During these tests, one hard stall condition and two points of approaching or soft stall were observed. These stall points are identified in Figure 20 and provided the basis for evaluation of the stall boundary. The stall boundary is defined in terms of a velocity ratio, q_o/q_f, and applies only to the particular wing and fan configuration as tested. However, additional experience with fan-in-wing systems has shown that the distance from the fan centerline to the wing leading edge influences the stall boundaries. Short leading edge systems tend to have a narrower range of stall free operation.

Using the data presented in Figure 20, and the trend of reduced stall margin for short leading edge systems, the general shallow inlet stall criteria

is defined in terms of the surface geometry, angle of attack and velocity ratio parameters. The estimated criteria, although based on a minimum amount of data, provides a method of estimating the operational limitations of particular installations during the preliminary design studies. Actual definition of these stall characteristics can only be determined by tests of the final fan and wing installation system.

Exit Louver Throttling Characteristics

A common method of thrust vectoring and thrust modulation for lift fans employs an exit louver cascade located in the fan exhaust flow. Figure 22 depicts a typical exit louver system where both thrust vectoring and modulation are possible. Thrust vectoring is achieved by orienting all louvers in the same direction. Similarily, thrust modulation is obtained by orientation of every other louver in opposite directions or by staggering the louvers. The louver vector angle and stagger angle, as defined in the figure, are the average louver angles and the differential louver orientation angles, respectively.

For this type of exit louver system, it is apparent that the fan exit effective area may be reduced to an area small enough to produce fan stall. This is particularily the case for fan systems designed for high pressure ratios. Model tests of fans with exit louvers has shown that the area reduction due to the louvers can be relieved by increasing the space between the fan exit and the louver leading edge. Dropping the louvers in this manner relieves the fan stall problem, but, in the process, increases the mechanical complexity of the louver mounting and actuation system. It is therefore desirable to maintain a minimum louver drop distance for a particular set of thrust vector and modulation requirements.

In order to establish the minimum drop height, three parameters must be known or specified:

- Blockage or throttling tolerance of the fan design.
- Maximum blockage of the louver system based on vector and thrust spoiling requirements.
- Variation of effective blockage with increased spacing or drop distance.

The first two items are a function of the selected designs. The final items, or effects of drop distance, are a generalized parameter independent of the specific design. In order to investigate blockage downstream of a free jet, a simple test program was conducted using an existing facility and nozzle configuration. Blockage was simulated by an array of 0.250 inch diameter rods mounted in a frame at various locations in the free jet. Tests were performed for both a round and a 0.5 radius ratio annular jet. The correlation of these test results are shown in Figures 23 and 24.

This blockage criteria was used as a basis for the estimated louver stagger blockage characteristics given in Figure 25. The louver performance at zero drop distance is based on experimental louver performance obtained during tests of the X-353-5, the 26-inch low speed scale model fan and the 15-inch scale model high pressure ratio fans. The characteristics are typical of louvers with about 8 to 10 percent thickness and 1.4 to 1.6 solidity.

The louver characteristics incorporated into the LF460/YJ97-GE-100 performance deck were based on this louver performance criteria. These characteristics, showing a typical louver performance maps, are presented in Figures 26 and 27. Performance obtained for the LF460 lift fan with this louver system installed is summarized in Figure 28.

Control of Multi-engine Common Manifold Systems

The LF460/YJ97-GE-100 lift fan system was designed for operation with interconnect between a two engine and two fan system. Some of the early V/STOL research aircraft studies considered multi-engine interconnect configurations. The problem then was to estimate the lift control capabilities for these systems.

During analysis of the problem of multi-engine interconnect, a simple method was developed for prediction of the amount of lift control available for the general interconnected arrangement. The generalized throttling or control characteristics are presented in Figure 29. The throttling parameter is a product of the number of interconnected units and the percent of the total system control applied to each fan.

The procedure for estimating the control capabilities of a six fan, six engine interconnected LF4XX/YJ97 system is given in Figure 30. The example, as presented, applied to the case where all engines are operating at the

maximum temperature level or the maximum control condition. Negligible losses are assumed for the interconnect ducting system. The fan lifts as estimated do not include any thrust spoiling for control. Additional lift changes due to thrust spoiling could be employed to increase the control forces of the sytem and to maintain a constant total system lift.

Acceleration Time of LF460 Lift Fans

During the studies of the V/STOL research aircraft, the need existed for an estimate of the time for the LF460 to accelerate from standstill following an instantaneous input of gas energy. For this analysis, two input energy levels were assumed. One condition was constant gas conditions at the fan turbine inlet. For this case, the turbine torque was estimated to vary linearly with speed as shown in Figure 31. The fan torque was estimated, based on cycle calculations, to vary with rotational speed squared. The differential fan-turbine torque is the available torque to accelerate the rotational inertia. The rotor polar moment of inertia was selected as the calculated design value of 19.6 (pound-ft-sec^2). A second analysis was performed and assumed a constant design turbine torque of 186,700 inch-pounds.

The calculated variation of fan speed with time for these two instantaneous torque inputs to the turbine rotor are presented in Figure 32. The effective time constants are 0.28 seconds and 0.42 seconds for the two cases analyzed.

Cruise Fan Inlets

The LF4XX family of lift fans incorporate fan aerodynamic designs that are matched to the rotor inflow conditions inherent to shallow fan-in-wing types of installations. These shallow inlets develop inlet velocity profiles that are higher at the tip than over the remainder of the inlet annulus. The fan rotor blades are then designed to accept this high velocity by increasing the blade camber and orientation angle above that required for a cylindrical inlet flowpath as exists with most conventional engine installations.

When a shallow inlet fan system is operated in a simulated cruise fan system, the inlet velocity profiles will deviate from the shallow inlet design conditions. The level of deviation will depend on the diameter of the cylindrical inlet that transitions into the fan rotor inlet. A small diameter inlet is desirable for a cruise fan type of installation, and also produces the greatest inlet flow deviation.

Studies were performed to determine the minimum cylindrical inlet diameter that could be used with the LF460 lift fan. This analysis was performed using the off-design features of the aerodynamic design program originally employed to design the LF460 system. A series of various inlet diameters were analyzed and the results showed a minimum tolerable inlet diameter of 69.0 inches. The criteria for selection of this inlet diameter was a moderate increase in aerodynamic risk attendant with the increased rotor blade incidence in the vicinity of the fan tip. This large cruise inlet requirement for the LF460 lift fan system could not yield attractive cruise fan inlet designs.

As the installation studies progressed, more emphasis was placed on low fan noise generation and thus the trend was towards fans incorporating lower pressure ratios than the LF460. A similar cruise fan inlet analysis was performed for the LF467, a 1.30 pressure ratio lift fan system. For this fan design, the minimum tip diameter was only about 2 percent larger than the fan inlet tip diameter. This smaller cylindrical inlet diameter was much more adaptable to cruise fan installation, and is shown in Figure 33.

Impingement of an Annular Jet on a Ground Plane

When flow issuing from an annular jet nozzle impinges on a ground plane normal to the jet axis, the back pressure effect of the ground plane is felt upstream at the nozzle exit plane. Of particular significance for lift fans, the presence of the ground plane may have very large effects on the mass flow, jet velocity and thrust produced by the jet. Also of interest is the effect of the ground plane on the centerbody base pressure. A study was directed toward determining these effects for a wide range of ground plane "height jet diameter" ratios.

Besides the ground plane "height/diameter" ratio, a number of other variables may be assumed to have a significant effect on the back pressure produced by the ground plane. Among these are:

- Radius ratio of the annular nozzle.
- Nozzle pressure ratio.
- Reynold's number.
- Average angle of inclination of the flow to the jet axis at the nozzle exit plane.
- Swirl angle

Previous studies and analysis have investigated various combinations of the above variables both analytically and experimentally, however they have fallen generally into two classes:

1) Very high radius ratios when the jet is essentially a thin curtain and the centerbody wake is large and in intimate contact with the ground plane or,
2) Zero radius ratio cases where there is no centerbody or centerbody wake.

For application to lift fans, it is desirable to study jets with radius ratios in the range of 0.3 to 0.7. Analysis of jets in this range of radius ratios has proven to be considerably more difficult than is the above mentioned cases for two reasons. First, some of the simplifying assumptions which can be made for high radius ratios are no longer realistic. Second, two possible flow patterns may exist for many interesting combinations of variables, and prediction of which of the two will occur and when transition from one to the other will occur becomes an important part of the problem.

Figures 34a and 34b show pictorially the two flow patterns which may exist for a single set of variables. Figure 34a shows the wake of the center-body closing before reaching the ground plane. In Figure 34b, the centerbody wake does not close at all but spreads to contact a large area of the ground plane.

In general, these two flow patterns will produce different base pressures on the center-body and will cause the jet to produce different thrusts and mass flows. Transition from one flow pattern to the other could be partially responsible for the difficulty experienced in flying lift fan powered V/STOL aircraft in "ground effect".

Analysis

An analysis was made for the following two cases:

- o The case shown in Figure 34a with a ground plane height/diameter ratio of infinity.
- o The case shown in Figure 34b with variable height/diameter ratio.

Details of these analyses will not be given in this summary but the following is a discussion of the general approach and assumptions.

The basic assumptions used in the analysis are as follows:

- Within the range of pressure ratios of interest for lift fans compressibility would not be a significant factor.
- Within the body of the main stream flow viscosity would be insignificant.
- Viscous forces on the outer surface of the jet could be ignored as far as their influence on ground plane effects and centerbody base pressures.
- Viscous shear forces between the centerbody wake and main stream flow were constant per unit of interface area.
- The flow was axisymetric.
- Swirl angles were zero.

Consider first the case illustrated in Figure 34b. If an initial base pressure and flow angle β are assumed and the appropriate momentum and continuity equations are applied to the jet and the centerbody wake, then the trajectory of the wake can be calculated by stepwise integration in the direction of flow. A time sharing computer program was written to do these computations. The minimum base pressure which can be assumed for this flow pattern is the value which results in a flow as shown in Figure 34c, where the centerbody wake nearly closes and then opens up again. Higher assumed base pressures result in flow patterns more like that shown in Figure 34b. The ground plane height for this case was assumed to be at the point where the flow trajectory of the inner surface of the jet becomes normal to the jet axis.

Next consider the case illustrated in Figure 34a but with the ground plane at downstream infinity. In this case, the base pressure cannot be arbitrarily specified but must satisfy momentum relationships involving the viscous forces between the centerbody wake and the jet. A second time sharing computer program was written for this case which iterated on the base pressure until these relationships were satisfied.

It has been postulated in this study that the higher and lower critical height/diameter ratios at which transition from one flow pattern to the other will occur may be approximated by the values of $(H/D)_H$ and $(H/D)_L$ shown in Figure 34c.

In order to check the above analysis, experimental data was used from tests of a 26-inch diameter low speed scale model of a lift fan, where data existed in ground plane effects. This fan had a radius ratio of 0.4 and the angle β equal to zero. With no ground plane, the fan had a measured hub static

pressure coefficient of -0.1. The viscous shear force term in the analysis was adjusted until this result was duplicated by the analysis with the ground plane at downstream infinity. This same viscous term was then used as the ground plane height was varied. The resulting comparison between these calculations and the measured values are shown in Figure 35. This agreement was considered satisfactory. In full scale lift fans, hub base pressure coefficients with no ground plane have been consistently measured at -0.125 for similar geometrics. The viscous term was adjusted to give this value for a radius ratio of 0.4 and the angle β equal to zero for the remainder of the results presented in this study.

Results

Figures 36 through 40 present the results for the case with no ground plane. Figure 36 shows the hub drag coefficient as a function of radius ratio and β, where the drag coefficient is defined as

$$C_D = F_D / (\tfrac{1}{2} \rho V_1^2 A_B)$$

Figure 37 shows the hub static pressure coefficient based on the total-to-ambient head of the jet.

$$C_P = (P_1 - P_o) / (\tfrac{1}{2} \rho V_o^2)$$

Figure 38 shows the jet velocity coefficient as a function of radius ratio and β and is defined as

$$C_V = \frac{F_N}{\dot{m} V_o}$$

Figure 39 shows the flow coefficient as a function of radius ratio and β and is defined as

$$C_F = \frac{\dot{m}}{\rho V_o A_n}$$

This flow coefficient does not include the effect of any boundary layer in the jet nozzle but includes only the effects of the base pressure coefficient and angularity effects when $\beta \neq 0$. Figure 40 shows the thrust coefficient as a function of radius and β and is defined as

$$C_T = C_V C_F$$

Figures 41 through 50 present results for the case with ground plane illustrated in Figure 34b. These results have been presented as carpet plots where β is a constant, radius ratio and C_P are parameters, ground plane "height/diameter" ratio is the abcessa and C_V, C_F, or C_T is the ordinate. It will be noticed that C_V and C_T are often above unity for these cases. This is a result of thrust augmentation provided by the ground effect. It will be noticed that as a general rule positive thrust augmentation results from the ground plane for radius ratios over 0.6 and negative augmentation results for radius ratios less than 0.55.

Figure 41 shows how the higher and lower critical "height/diameter" ratios vary with radius ratio and β. These critical values are as defined in Figure 34c. It should be noted that these critical values are hypothetical only and are substantiated by a minimum of experimental data but should give general trends. It is quite likely that flow unsteadyness and other factors in a real case could have a substantial effect on the results shown in Figure 41.

SECTION V

ACOUSTIC ANALYSIS

In support of the NASA V/STOL research aircraft program, noise footprints were calculated for the three proposed aircraft designs. Figure 51 is a photograph of models of these three aircraft. The footprints were determined on as consistent basis as possible to allow a direct comparison to be made of both the sideline noise levels and the total exposure acreage for 95 PNdB. Some of the more critical assumptions were:

- All aircraft use the LF460/YJ97-GE-100 with suppression
- Common takeoff flight path and velocity schedule as shown in Figures 52 and 53.
- McDonnell and North American thrust vectoring schedule as shown in Figure 54.
- Boeing thrust vectoring modified as shown in Figure 55 to account for canted cruise engine.

Several differences were apparent in the three aircraft designs. The McDonnell configuration is the largest gross weight aircraft with six LF460 lift fans operating at the noise rating point (80% maximum thrust). Next in size is the North American configuration which also utilizes six lift fans. Due to the lower gross weight, the aircraft is capable of taking off with reduced thrust on all engines, or if aircraft balance is maintained with noise rating point thrust on 4 lift fans and very low thrust on the remaining two fans. The effects of these thrust variations are shown by configurations 4 and 5, Table II. The smallest aircraft is the Boeing configuration which requires only four lift units at noise rating point thrust. Two of these fans are oriented such that cruise and lift thrust may be obtained without a vectoring exhaust nozzle as used on the preceding two configurations.

To evaluate the effect of adding suppression, the North American and McDonnell configurations were assumed to have the following:

- Lift cruise fan inlet, -5 PNdB
- Lift cruise gas generator inlet, -5 PNdB
- Lift and lift cruise fan exhaust, -6 PNdB

The McDonnell research aircraft was also assumed to have varying degrees of lift/cruise fan inlet and gas generator inlet suppression as follows:

L/C Fan Inlet	Gas Gen. Inlet
-5	No noise
No noise	No noise

Results of the study are presented in Figures 56 through 63 and summarized on Table II. The footprints are generally of the same shape with the maximum sideline noise occurring during the vertical rise portion of the takeoff represented by the almost circular constant contour lines. An elongated tongue is then created as the aircraft transistions to horizontal flight.

The effect of installation suppression is seen primarily as a large reduction of the 95 PNdB exposure acreage. Sideline noise is reduced by 2.5 PNdB, for both the high thrust McDonnell (configurations 1 and 2) and low thrust North American (configurations 4 and 6 aircraft).

Figure 63 shows the effect of providing installation suppression sufficient to eliminate the lift cruise and gas generator inlets as noise sources. These are configurations 8 and 9 on Table II. For this case of both noise sources eliminated, the exposure acreage is reduced to only 81 acres. The maximum 500 ft. sideline noise, however, is still in excess of 95 PNdB. This points out the problem in evaluating aircraft noise on a single point basis.

The effect of takeoff profile, configurations 2 and 3, was found to be small for the two types evaluated. Both the maximum sideline PNdB and 95 PNdB exposure acreage were similar. It is significant that the low altitude transistion reduced the sideline noise by 0.5 PNdB but increased the exposure area by 20 acres. From these results, it is evident that the sideline noise near the point of liftoff may show little improvement while the exposure acreage may be reduced significantly by controlling the engine vectoring and power during the horizontal flight portion of the takeoff profile.

As expected, sideline noise was reduced with the lower takeoff thrust configurations. The change was proportional to thrust to the first power $\Delta db = 10 \log$ (Thrust Ratio).

Varying the number of engines from 6 to 4, configurations 1, 5, and 7, provided a maximum of 1 PNdB reduction. This is slightly less, 0.5 to 1 PNdB,

than expected and the difference is thought to be the effect of inlet radiated noise from the lift cruise fans which is constant for the 4 and 6 fan configurations.

In summary, the footprints calculated for the three research aircraft showed the flight path and level of inlet suppression on the lift cruise and gas generator inlets could result in a very low level of 95 PNdB exposure acreage. Achieving the 500 ft. sideline goal of 95 PNdB, however, will require extensive suppression and perhaps be unrealistic when the noise is evaluated on an airport usage basis due to the low exposure acreage.

SECTION VI

PRELIMINARY AND CONCEPTUAL DESIGN STUDIES

The LF460 lift fan configuration was designed for minimum weight consistent with minimum overall fan thickness and low noise generation. These criteria produced a lift fan design that incorporated the following features:

- Triple bubble scroll with gooseneck to provide minimum fan installation diameter consistent with minimum thickness.
- A double mid-span rotor with 88 blades incorporating integral tip turbine carriers. The large number of blades was selected based on light weight and low noise generation.
- Two chord rotor-stator spacing for minimum noise generation. Moderate interstage acoustic treatment was applied to the design.
- A four strut front frame with an integral shallow inlet bellmouth contour.
- Leaned exit stator vanes for low rotor-stator interaction noise generation.

This basic LF460 lift fan design was selected as the propulsion system, with the YJ97-GE-100 turbojet as the gas generator, for use in the studies of a V/STOL research aircraft. Early in the program, parallel studies of more advanced remote lift units incorporated novel features consistent with improved design that were readily adaptable to the LF460 design. For example, a three strut front frame design and simplified scroll represented a substantial weight savings over the LF460 design at a small increase in overall thickness.

The need for aircraft adaptability and the desire for further design optimization initiated several preliminary and conceptual design studies of modified LF460 systems. The following sections of this report describe the results of some of the more important design studies.

Modified Three-Strut Front Frame

The basic LF460 lift fan included a four strut, major and minor, front frame design and the triple bubble scroll. This design is described in detail in Reference 1. During the conceptual design studies of advanced remote lift fans, a new approach was conceived that incorporated a three-strut frame single bubble scroll system. This design concept was carried through a concept

definition phase that developed approximate system weight and installation dimensions for the modified LF460 system.

The installation sketch of the modified LF460 design is shown in Figure 64. The significant installation dimensions for this modified system are compared with the original LF460 design in the figure. The effects of the design change increased the fan depth by about 20 percent, with some decrease in the overall planform dimensions.

This design change represents a weight reduction of about 62 pounds from the original LF460 weight of 789 pounds. Thus, a modified three-strut front frame design of the LF460 has an estimate weight of 717 pounds.

Modified 75/25 Split Scroll Arc

The basic LF460 lift fan system was designed to operation as a two engine, two fan interconnected system. For this configuration, each scroll inlet would supply 180 degrees or one-half of the turbine arc. In the event of an engine failure, one scroll inlet on each of the interconnected fans would be closed off, and, the remaining engine would operate into two 180 degree scroll segments, one in each fan. The total scroll arc would then reflect a nozzle area near design for one engine system.

A special case was proposed where four engines, four fans were interconnected. For this system, a single engine failure would represent a 25 percent loss in total gas supply, and, scroll area of each fan would require a 25 percent or 90 degree reduction in scroll arc.

A conceptual design was performed to study this 75/25 scroll split configuration. The approximate installation dimensions for this configuration, with the two scroll inlets located diametrically opposite, is shown in Figure 65. This preliminary configuration incorporated the three-strut front frame and single bubble scroll designs as discussed previously. The estimated weight for this configuration was 717 pounds, or the same weight as a 50/50 scroll split configuration that incorporated similar design concepts.

Parametric Lift Fan Study

The guidelines for the design studies of the V/STOL research aircraft specified the LF460/YJ97-GE-100 system as the available propulsion system. The LF460 had been designed for maximum thrust-to-weight consistent with low noise generation. As the aircraft design studies progressed, the emphasis

shifted to lower noise levels, and thus decreased the attractiveness of the LF460 because of the inherent noise associated with the design fan stage pressure ratio of about 1.40. With the trend to lower noise and thus lower pressure ratio, a preliminary study was performed to evaluate the effects of pressure ratio on fan performance and size. Other parameters such as levels of fan internal exhaust suppression, radius ratio, tip speed and design ambient temperature were included in the analysis. Because of the depth of this study and the number of variables involved, the analysis was performed using time sharing design point programs and maximum engine discharge gas conditions. This method of analysis gave approximate performance data that later provided the basis for a more accurate analysis using a modification to LF460/YJ97-GE-100 customer deck.

The parametric study was performed for sea level standard day and a 90 degree Fahrenheit ambient temperatures. The YJ97 discharge gas conditions used for this analysis are listed in Table III. The results of this parametric study are presented in Figures 66 and 67. Performance for two families of lift fans are presented; one basic unsuppressed and the other with heavy exhaust suppression incorporating four acoustically treated splitter rings. Performance and size are shown for both a constant tip speed of 1125 feet per second, radius ratio being variable, and for constant radius ratio of 0.454, tip speed being variable. The performance of the standard day fan designs is shown in Figure 66. Comparable data for the 90 degree Fahrenheit day designs is shown in Figure 67.

This study was then used as a basis for a more accurate performance evaluation using modifications to the LF460/YJ97-GE-100 customer deck. The selected fan diameter, based on airframe study inputs, had a 64.0 inch tip diameter. Performance was calculated for the maximum control conditions, with interconnect duct transfer flow, and for the nominal rated operating conditions of the engine. The results of this analysis are summarized in Table IV for two levels of exhaust suppression, two tip speeds and two radius ratios. Performance for fan systems designed to the standard day conditions is also tabulated during off-design operation on the hot day.

A conceptual study was performed to define the approximate weight and installation dimensions for a typical 64-inch lift fan system. This study showed the weight of the LF464 lift fan to be 800 pounds for a lightly

suppressed configuration and 880 pounds for a heavily suppressed configuration. Figure 68 shows the significant installation dimensions for a heavily suppressed LF464 lift fan employing the three-strut front frame, single bubble scroll concepts.

Lift Fan Parametric Correlation

During the research aircraft and propulsion integration studies, conceptual or preliminary designs were completed for several lift fan systems of the LF4XX family. These studies were either performed as part of the aircraft support activity or under separate contracts with NASA. These studies produced preliminary designs for the LF464, LF467 (Reference 4) and the LF468 (Reference 5) remote lift fans. A detailed design of the LF460 was also completed and is described in Reference 1. A separate design study for a family of unsuppressed, close rotor-stator spacing, lift fans was also carried through an initial concept definition phase and was included in the development of the parametric correlation.

It has been very difficult to compare these systems on an equal basis because of the numerous differences in installation and design assumptions. In addition, the performance of the YJ97 gas generator has also been modified to incorporate more recent performance levels. Because of this apparent lack of commonality in the various designs, a study was undertaken to correlate the significant performance and geometric parameters for the LF4XX lift fan family. The following discussion presents the results of this study and should provide a valuable link in understanding the trade-offs of such items as fan pressure ratio, tip speed and level of noise suppression.

For this study certain ground rules were assumed concerning the installation. Ducting and gas generator installation effects were considered and established as follows for reference:

- Gas generator inlet recovery 0.985
- Compressor bleed 0.5%
- Horsepower extraction. 25
- Ducting loss without flow transfer . . 10.7%

The assumptions concerning the lift units include:

- A three-strut front frame
- A single gooseneck scroll

- Performance estimates include exit louvers at zero degree vector angle
- Non-acoustic fans do not include any added rotor-stator spacing for low noise generation
- Non-acoustic fans have two stator stiffening rings and two rotor mid-span dampers
- Acoustic fans include stator lean and two chords spacing
- Moderate noise treatment includes two acoustic splitters similar to the LF460 system
- Heavy acoustic treatment includes four acoustic splitters similar to the LF467 and LF468 systems.
- Fan designs considered are either a constant hub radius ratio of 0.454 or a constant tip speed of 1125 feet per second.

The results of this study are presented for three types of lift units as identified by the numbers on the figures where appropriate:

1) A non-acoustic type fan system
2) A moderate suppressed low noise lift fan system
3) A heavily suppressed low noise lift fan

The results of this study are presented in the following figures:

Figure 69 - Fan thrust, both nominal (1835°R, single engine flow) and maximum (2060°R with cross flow of about 9 percent).

Figure 70 - Fan sizing data relating fan maximum thrust and fan diameter as a function of design pressure ratio.

Figure 71 - Fan thrust to weight variation with pressure for the three levels of fan suppression.

Figure 72 - The variation of fan radius ratio and tip speed for the cases where the other parameter is held fixed and hub loading is maintained at a constant level.

Figures 73 and 74 - Critical installation, dimensions (length, depth and width) for the range of pressure ratios. Depth is the only parameter influenced by levels of exhaust suppression.

Figure 75 - Correction factors for use with the thrust levels in Figure 69 to correct for non-standard day operation or design for flat rating. The curve for design point fans produces a flat rated system and affects the fan size. The other two curves

reflect off-design performance for a given standard day size fan as obtained using Figures 69 and 70.

Figure 76 - The levels of fan nozzle pressure ratio, reflecting the losses of the splitters and suppression, are presented as a function of design pressure ratio

Figure 77 - The effects of design variables on fan alone response for instantaneous changes of fan inlet gas conditions and for small changes of new design speed.

NOMENCLATURE

SYMBOL	DEFINITION	UNITS
A_B	Centerbody base area	ft^2
A_n	Nozzle annulus area	ft^2
C_D	Centerbody drag coefficient	---
C_F	Flow coefficient	---
C_{FF}	Fan Stream flow coefficient	---
C_{FT}	Turbine stream flow coefficient	---
C_P	Centerbody pressure coefficient	---
C_V	Velocity coefficient	---
C_{VF}	Fan stream velocity coefficient	---
C_{VT}	Turbine stream velocity coefficient	---
D_H	Centerbody on hub diameter	ft
D_T	Fan tip diameter	ft
F_D	Centerbody drag	pounds
F_N	Exhaust stream net thrust	pounds
H	Ground plane height	ft
H_H	Higher critical ground plane height	ft
H_L	Lower critical ground plane height	ft
m	Jet mass flow	lb-sec/ft
P_1	Hub base pressure	lb/ft^2
P_o	Ambient pressure	lb/ft^2
q_{511}	Connecting duct velocity head pressure	lb/ft^2
q_{512}	Cross duct velocity head pressure	lb/ft^2
q_F	Fan stream velocity head pressure	lb/ft^2
q_o	Free stream velocity head pressure	lb/ft^2
T_{54}	Fan turbine inlet temperature	$^\circ R$
U_T	Fan tip speed	ft/sec
V_1	Jet exit velocity in ground effect	ft/sec
V_o	Ideal jet velocity for expansion to ambient pressure	ft/sec

NOMENCLATURE

SYMBOL	DEFINITION	UNITS
W_{511}	Connecting duct flow	lb/sec
W_b	Cross-duct bleed flow	lb/sec
X	Wing surface geometric parameter	ft
α	Wing angle of attack	deg
β	Exit jet flow angularity	deg
β_1	Odd louver vector angle	deg
β_2	Even louver vector angle	deg
ρ	Flow density	lb/ft^3
ρ_b	Bleed flow density	lb/ft^3

LIST OF REFERENCES

1. LF460 Detail Design. General Electric Company, NASA CR-120787, 1971

2. LF460/YJ97-GE-100, Instruction Manual for Electronic Data Processing Deck for IBM360 Computer, General Electric Company, R71AEG277, 1971

3. LF460/YJ97-GE-100, Instruction Manual for Electronic Data Processing Deck for CDC6400 Computer, General Electric Company, R71AEG278, 1971

4. LF467 Concept Definition, General Electric Company, NASA CR-120909, 1972

5. LF468 Concept Definition, General Electric Company, R71AEG362, 1971

APPENDIX A - Instructions for Expanded Customer Deck Capability

Instructions are contained for increased customer utilization of the LF460/YJ97-GE-100 performance deck. The instructions cover the following items:

1. Increased high pressure turbine temperature limit during normal operation.

2. Lift fan system sizing with customer bleed and/or horsepower extraction.

3. Using the furnished representative nozzle with the customer supplying the performance input values.

4. Using the furnished representative connecting duct with the customer supplying the performance input values.

The increased customer utilization employs using expanded input (up to 16 parameters) and permanent input. This additional capability consists of the use of constants and curve inputs. The constants may be input through expanded input (value of input can change from data case to data case or are carried over unless overridden) or through permanent input (value of input cannot be changed from data case to data case). Curve input is available only through the permanent input feature and cannot be changed on a given data run.

A description of expanded input utilization is contained in the Instruction Manual. A description of permanent input utilization is contained in Paragraph 5 of this document.

The reference to figure numbers in this document refers to those contained in the Instruction Manual.

1. Turbine Temperature Limit

The present high pressure turbine limiting temperature of 1835°R during normal system operation may be replaced through the use of expanded

input by the use of the parameter - T51J3. Temperature values of 1870°R or less may be used and deck system operation will limit the turbojet to this input value during normal engine operation. The turbine temperature limit of 2060°R will still be in force during non-normal engine operation.

2. System Sizing with Customer Bleed and/or Horsepower Extraction

The LF460/YJ97-GE-100 system may be sized with customer bleed and/or horsepower extraction by using the appropriate value from Table I for the input parameter - Z2CRSN.

TABLE I

HPX	WBQWH	Z2CRSN
0	0	0.7084
	0.005	0.7013
	0.010	0.6942
	0.015	0.6871
	0.020	0.6799
	0.025	0.6729
	0.030	0.6657
	0.035	0.6586
	0.040	0.6515
25	0	0.7087
	0.005	0.7015
	0.010	0.6944
	0.015	0.6873
	0.020	0.6802
	0.025	0.6731
	0.030	0.6659
	0.035	0.6588
	0.040	0.6517

The above tabulated values are applicable only with a power setting of 0.7 and are based on a turbine temperature limit of 1835°R at the sizing condition. For off design system operation, the turbine temperature limit will be that established through input with the parameter T51J3. All other comments in Paragraph 3.1.12 of the Instruction Manual still apply.

3. Nozzle Performance Inputs

The furnished representative nozzle performance can be replaced by either using constants as inputs for each parameter for each data case or by a combination of constants and curves as input.

3.1 Constants as Input

The following parameters may be used to replace the built in constants and/or curves for the furnished representative nozzles:

*SCF28 Scaler applied to the Figure 7 and 10 curve value for the fan duct nozzle flow coefficient when on the separated flowpath - equate to 0.

ACF28 Input parameter for user's fan duct nozzle flow coefficient for the separated flowpath - equate to desired value.

*SCF8 Scaler applied to the Figure 7, 9 and 10 curve value for the nozzle flow coefficient when on the confluent flowpath or the low pressure turbine nozzle flow coefficient for the separated flowpath - equate to 0.

ACF8 Input parameter for user's nozzle flow coefficient for the confluent flowpath or the low pressure turbine nozzle flow coefficient for the separated flowpath - equate to desired value.

---

* These parameters and other parameters which are to remain at a constant value during a data run, can be input as permanent input to conserve the number of expanded input to available size.

*SCV29 Scaler on the Figure 8 fan duct nozzle exit velocity - equate to 0.

ACV29 Input parameter for user's fan duct flow stream velocity coefficient - equate to desired value.

*SCV9 Scaler on the Figure 8 low pressure turbine nozzle exit velocity - equate to 0.

ACV9 Input parameter for user's low pressure turbine flow stream velocity coefficient - equate to desired value.

ACFGD Input incremental parameter for user's fan duct flow stream gross thrust coefficient - equate to desired value minus 1 (negative increment).

ACFG Input incremental parameter for user's low pressure turbine flow stream gross thrust coefficient - equate to desired value minus 1 (negative increment).

A28S Input parameter for the fan duct physical nozzle throat area for the separated flowpath - equate to desired value in square inches.

*SA8 Scaler on the scheduled nozzle physical throat area for the confluent flowpath and the scheduled low pressure turbine nozzle physical area for the separated flowpath - equate to 0.

AA8 Input parameter for the desired nozzle physical throat area when using the confluent flowpath and the low pressure turbine nozzle area when on the separated flowpath - equate to desired area in square inches.

*CDH,CDMB and CDS Drag Coefficients used in the base drag calculation and can be equated to 0 when the base drag is not applicable.

---

* These parameters and other parameters which are to remain at a constant value during a data run, can be input as permanent input to conserve the number of expanded input to available size.

*XL26 Input pressure loss coefficient ($\Delta P/q$) referenced to the Station 26 velocity head and can be used to represent internal fan duct nozzle losses with the cruise installation - equate to desired value.

*XL26PR Same as XL26 except used with the wing installation.

*XL58 Input pressure loss coefficient ($\Delta P/q$) referenced to the Station 58 velocity head and can be used to represent internal low pressure turbine nozzle losses with the cruise installation - equate to desired value.

*XL58PR Same as XL58 except used with the wing installation.

AP2726 Input incremental fan duct nozzle pressure loss in addition to or in place of the XL26 and XL26PR input - equate to desired value minus 1 (negative increment).

AP6Q59 Input incremental low pressure turbine nozzle pressure loss in addition to or in place of the XL58 and XL58PR input - equate to desired value minus 1 (negative increment).

3.2 Constants and Curves as Input

The following curves may be input to provide variable values as a function of cycle parameters during a data run:

Curve Name	Function of	Output Parameter	Louvers	Flow
CF8CGG	P8QP0	CF8	No	Confluent
BMF8CG	BETAS	BETAMX	Yes	Confluent
CF8C1G	BETAT & BETAS	CF8	Yes	Confluent

* These parameters and other parameters which are to remain at a constant value during a data run, can be input as permanent input to conserve the number of expanded input to available size.

Curve Name	Function of	Output Parameter	Louvers	Flow
CF8GGG	P8QPO	CF8	No	Separate
BMXF8G	BETAS	BMXCF8	Yes	Separate
CF81GG	BMXF8T & BETAS	CF8	Yes	Separate
CFGN1G	P8QPO	CV9	No	Both
BMXV9G	BETAS	BMXCV9	Yes	Both
CV91GG	BMXV9T & BETAS	CV9	Yes	Both
CF28GG	P28QPO	CF28	No	Separate
BMF28G	BETAS	BMCF28	Yes	Separate
CF281G	BMF28T & BETAS	CF28	Yes	Separate
CFGDMG	P28QPO	CV29	No	Both
BMV29G	BETAS	BMCV29	Yes	Both
CV291G	BMV29T & BETAS	CV29	Yes	Both

The curves named CF8C1G, CF81GG, CV91GG, CF281G and CV291G are transformed curve fits of Figures 8, 9 and 10. The minimum values for the transformed curve fits are 0 (thrust angle, BETAB = 0) and the maximum values are those corresponding to the end points of the BETAS (spoiler angle) curves in Figures 8, 9 and 10. These maximum values are contained in curves BMF8CG, BMXF8G, BMXV9G, BMF28G and BMV29G and are divided into the input BETAB value to enter the transformed curves with the parameter names of BETAT, BMXF8T, BMXV9T, BMF28T and BMV29T.

When using the above curves as input, the following parameters are established in the cycle deck with the shown values and should be reinitialized to these values if they were replaced on previous points:

SCF28 = 1	SCV29 = 1
ACF28 = 0	ACV29 = 0
SCF8 = 1	SCV9 = 1
ACF8 = 0	ACV9 = 0

The rest of the parameters contained in Paragraph 3.1 may be used as desired.

4. Connecting Duct Inputs

The furnished representative connecting duct consists of a diffuser, throttling valve and cross-duct sections. The following parameter inputs, by section, will permit replacing the furnished performance.

4.1 Diffuser Section

XL511 Input pressure loss coefficient ($\Delta P/q$) referenced to the gas generator turbine exit velocity head - equate to desired value.

AP51Q5 Input incremental diffuser pressure loss in addition to or in place of the XL511 input - equate to desired value minus 1 (negative increment).

AE511 Input parameter for the diffuser exit area - equate to desired area in square inches.

4.2 Throttling Valve Section

SP5351 Scaler on the Figure 4 throttling valve pressure loss - equate to 0 for eliminating the Figure 4 data; this parameter input capability is already provided with the name TVSCL.

AP5351 Input incremental throttling valve pressure loss in addition to the cycle calculated pressure loss (SP5351 or TVSCL = 1) - equate to desired value minus 1 (negative increment) or use as the total pressure ratio across the throttling valve (SP5351 or TVSCL = 0) - equate to desired pressure loss ratio.

AE513 Input parameter for specifying the inlet area for the throttling valve section - equate to desired area in square inches. (This area and AE511 must be equal.)

The Figure 4 curve may be replaced with a new curve by the name of DP513G and as a function of the cross-duct bleed flow to the gas generator exit flow ratio.

4.3 Cross-Duct Section

4.3.1 Bleed Out

A pressure loss is applied to account for the port losses and the 90 degree turn required for the bleed flow.

SP512 Scaler on the Figure 2 pressure loss - equate to 0 for eliminating the Figure 2 data.

AP512 Input incremental turning pressure loss in addition to the cycle calculated pressure loss (SP512 = 1) - equate to desired value minus 1 (negative increment) or use as the total pressure ratio loss (SP512 = 0) - equate to desired value.

The Figure 2 curve may be replaced with a new curve having the name DPQ51G and is a function of the cross-duct bleed flow to the gas generator exit flow ratio. The pressure loss coefficient is referenced to the velocity head at Station 511.

In addition to the flow turning pressure loss, a pressure loss is applied for the duct length connecting the two lift fan systems. This loss can be replaced as follows:

AEHØLE Input cross-duct area, equate to desired value in square inches.

XL515 Input pressure loss coefficient ($\Delta P/q$) parameter referenced to the AEHØLE velocity head - equate to desired value.

AP515 Input incremental cross-duct pressure loss in addition to or in place of the XL515 input - equate to desired value minus 1 (negative increment).

The resulting pressure is that which is available at the bleed port inlet at the bleed in lift fan system.

4.3.2 Bleed In

A pressure loss is applied to the bleed in to account for the port losses and turning 90 degrees.

SP511 Scaler on the Figure 3 pressure loss - equate to 0 for eliminating the Figure 2 data.

AP511 Input incremental turning pressure loss in addition to the cycle calculated pressure loss (SP511 = 1) - equate to desired value minus 1 (negative increment) or use as the total pressure ratio loss (SP511 = 0) - equate to desired value.

The Figure 3 curve may be replaced with a new curve having the name DPQ52G and is a function of the volumetric bleed flow to the volumetric gas generator exit flow ratio (WBRATIØ).

Where $WBRATI\emptyset = \frac{WB512}{PS512}(R512)(T512)/\frac{W51}{PS511}(R51)(T51)$

The pressure loss coefficient is referenced to the velocity head occurring with the AEHØLE area.

During engine-out and bleed-in operation, the Figure 3 pressure loss coefficient is replaced by the following parameter:

ACONST Input pressure loss coefficient referenced to the AEHØLE velocity head and can be overridden or implemented by the parameters SP511 and AP511 - equate to desired value.

5. Permanent Input Description

The permanent input follows the THEEND⑧999 card of the expanded input/output section in the permanent input section. (Paragraph 4.3 in the Instruction Manual)

The constant format for input is given below:

Columns 2-7 and 29-34	One to six character name and is left adjusted
13 and 40	Equal sign
14-27 and 41-54	Value of input and must include a decimal point - is right adjusted
28 and 55	Comma

The above cards are preceded by a card with REAL punched in columns 2-5 and followed by a card with THEEND punched in columns 2-7.

The curve input format is as follows:

First Card

Columns 4-7	Must be T = 6H
8-13	Six character curve name
14	Comma
15-17	The number of X values - an integer and is right adjusted
18	Comma
19-21	The number of Y values - an integer and is right adjusted
22	Comma

Subsequent Cards

Columns 4-5	X = which is first card containing X values Y = which is first card containing Y values Z = which is first card containing Z values For univariate curves, the X= or Y= card is omitted - for a constant value curve, the Z= card is all that is necessary
6-7	Must be blank
8-21 24-37 40-53 56-69	Values of X, Y or Z ordinates and must contain a decimal point - is right adjusted

Subsequent Cards (continued)

Columns 22, 38, 54, 70	Comma
23, 39, 55	Must be blank

The curve input cards must be preceded by a card with CURVE punched in Columns 2-6 and followed by a card with THEEND punched in Columns 2-7.

The permanent input section is followed by a card with NOMORE punched in Columns 2-7 and is required whether permanent input is used or not.

TABLE I, INTERCONNECT DUCTING LOSSES

- Refer to Figure 9 for Station Designations

- Diffuser (Station 51 to 511)

  A_{e51} = 161.94 sq. in.

  $\Delta P/q_{51}$ = 0.15

- Bleed-out (Station 511 to 512)

  A_{e511} = 232.4 sq. in.

  $\Delta P/q_{511}$ = See Figure 10

- Cross-duct (Station 512 to 515)

  A_{e512} = 116.2 sq. in.

  $\Delta P/q_{512}$ = 1.4

- Bleed-in (Station 512 to 511P)

  A_{e512} = 116.2 sq. in.

  $\Delta P/q_{512}$ = See Figure 11

- Scroll Inlet (Station 513 to 53)

  A_{e513} = 232.4 sq. in.

  $\Delta P/q_{513}$ = 0.05

TABLE II - RESEARCH AIRCRAFT NOISE CONTOUR RESULTS

	Company	No. Engines	Thrust/Engine	Flight Path	Installation Suppression[2]	PNdB on 500' S.L.	95 PNdB Acreage
1.	McDonnell	6	12,216[1] lbs	Steep	No	106	240
2.	McDonnell	6	12,216 lbs	Steep	Type 1	103.5	120
3.	McDonnell	6	12,216 lbs	Short Run, Low Altitude Transistion	Type 1	103	140
4.	North American	6	10,500 lbs	Steep	No	105	170
5.	North American	4	12,216 lbs	Steep	No	105.5	216
		2	5,000 lbs				
6.	North American	6	10,500 lbs	Steep	Type 1	102.5	78
7.	Boeing	4	12,216 lbs	Steep	No	105	I78
8.	McDonnell	6	12,216 lbs	Steep	Type 2	101	114
9.	McDonnell	6	12,216 lbs	steep	Type 3	100	81

(1) Noise Rating Point

(2)	Type 1	Type 2	Type 3
L/C Fan Inlet	-5 db	-5 db	No noise
L/C GG. Inlet	-5 db	No noise	No noise
All Fan Exhaust	-6 db	-6 db	-6 db

TABLE III. ENGINE DISCHARGE GAS CONDITION FOR LF4XX STUDY

	Std. Day	90°F Day
Exhaust Gas Temperature, °R	2060	2060
Engine Discharge Pressure, psia	61.5	57.35
Scroll Inlet Airflow, lb/sec	76.2	71.6
Duct Pressure Loss, percent	11	11

TABLE IV

LF464 Performance Summary

	Light Treatment (2 Splitters)		Heavy Treatment (4 Splitters)	
Design Tip Speed	1125	1108	1125	1108
Design Pressure Ratio	1.3216	1.3256	1.3216	1.3256
Radius Ratio	.4447	.454	.4447	.454
Design Hub Loading	2	2	2	2
Design Airflow	711.4	703.8	711.4	703.8
Specific Flow	40	40	40	40
η_R Gas Gen	.985	.985	.985	.985
% Bleed	.5	.5	.5	.5
HP ext.	25	25	25	25
η_R Fan	1.0	1.0	1.0	1.0

Rating	Max. Cont.	Nom.	Max. Cont.	Nom.	Max. Cont.	Nom.	Max. Cont.	Nom.
Std. Day								
% η Gas Gen	101.5	101.5	101.5	101.5	101.5	101.5	101.5	101.5
Lift	15739	12783	15658	12716	14937	12074	14831	12012
Base Drag	506	414	519	425	754	616	772	631
Ut	1125	1018	1108	1003	1125	1018	1108	1003
Pressure Ratio	1.3216	1.258	1.3256	1.262	1.3216	1.258	1.3256	1.262
WA Fan	711.4	644	703.8	637	711.4	644	703.8	637
% Duct Loss	11.2	10.78	11.2	10.78	11.2	10.78	11.2	10.78
T54	2052	1835	2052	1835	2052	1835	2052	1835
90°F Day								
%η Gas Gen	101.5	101.5	101.5	101.5	101.5	101.5	101.5	101.5
Lift	14251	11928	14177	11865	13484	11257	13415	11198
Base Drag	460	387	472	398	685	575	701	589
Ut	1100	1015	1084	1000	1100	1015	1084	1000
Pressure Ratio	1.29	1.24	1.293	1.243	1.29	1.24	1.293	1.243
WA Fan	659	605	652	598	659	605	652	598
% Duct Loss	11.2	10.78	11.2	10.78	11.2	10.78	11.2	10.78
T54	2053	1864	2053	1864	2053	1864	2053	1864

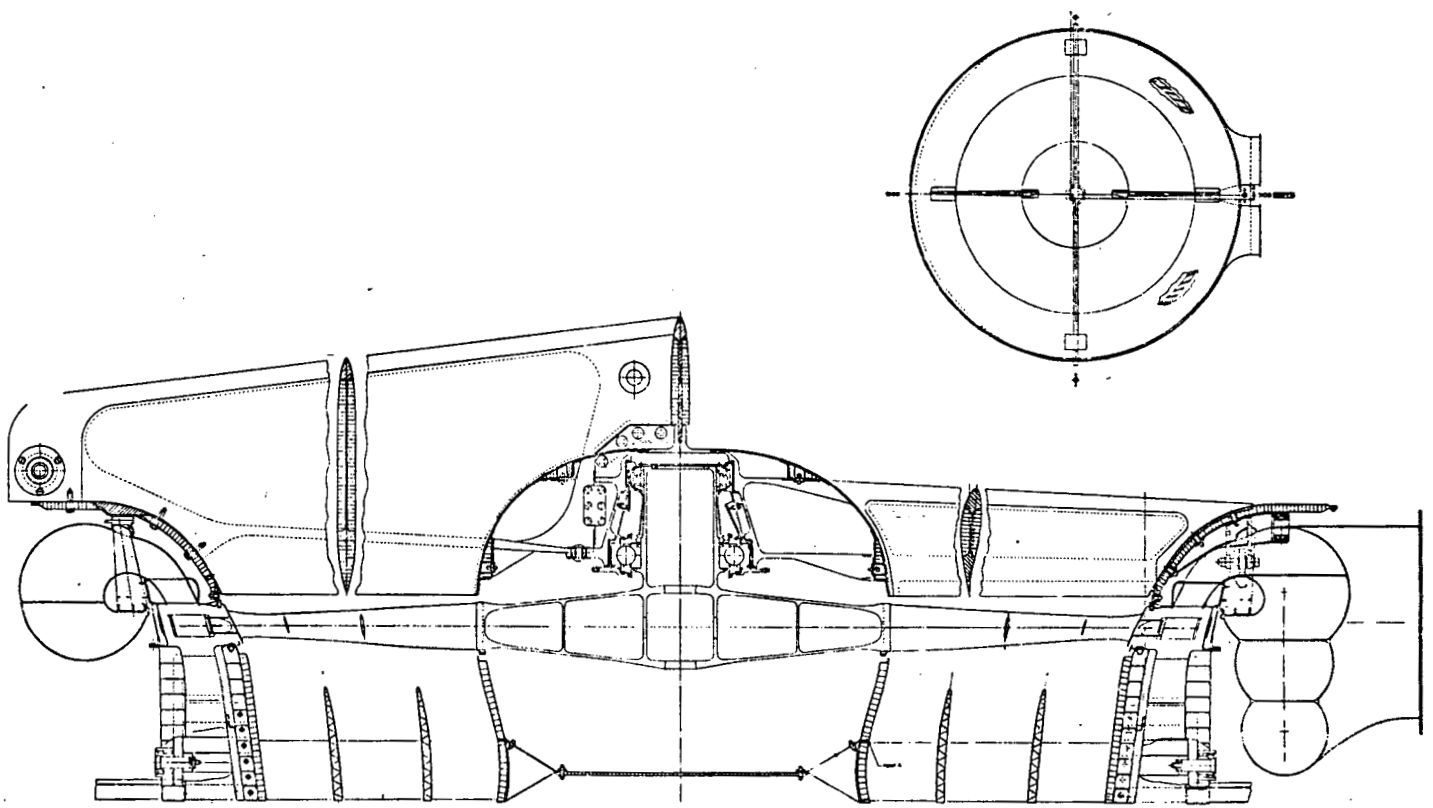

Figure 1. LF460 Lift Fan Layout

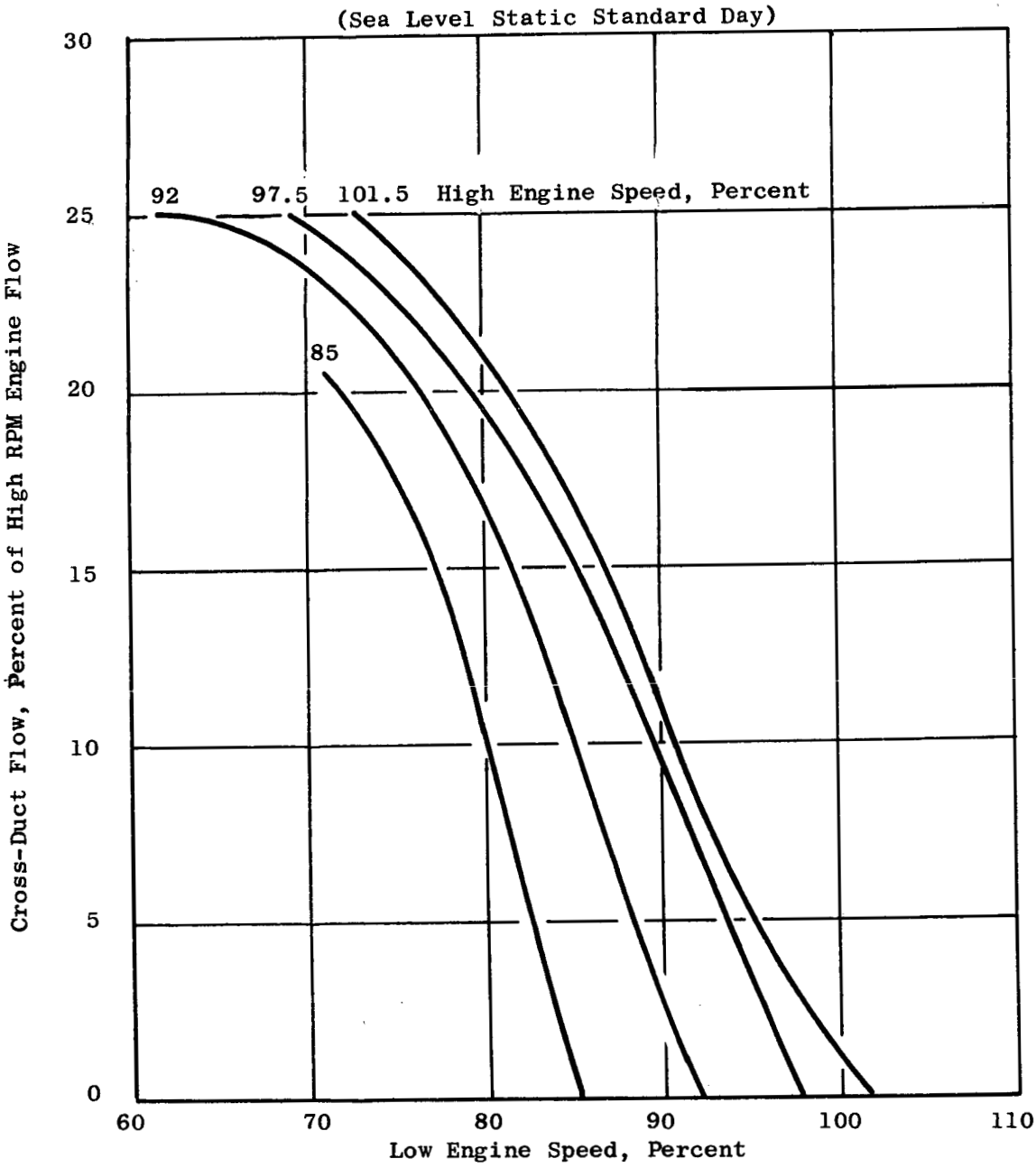

Figure 2. Effects of Engine Speed Unbalance on Cross-Duct Flow

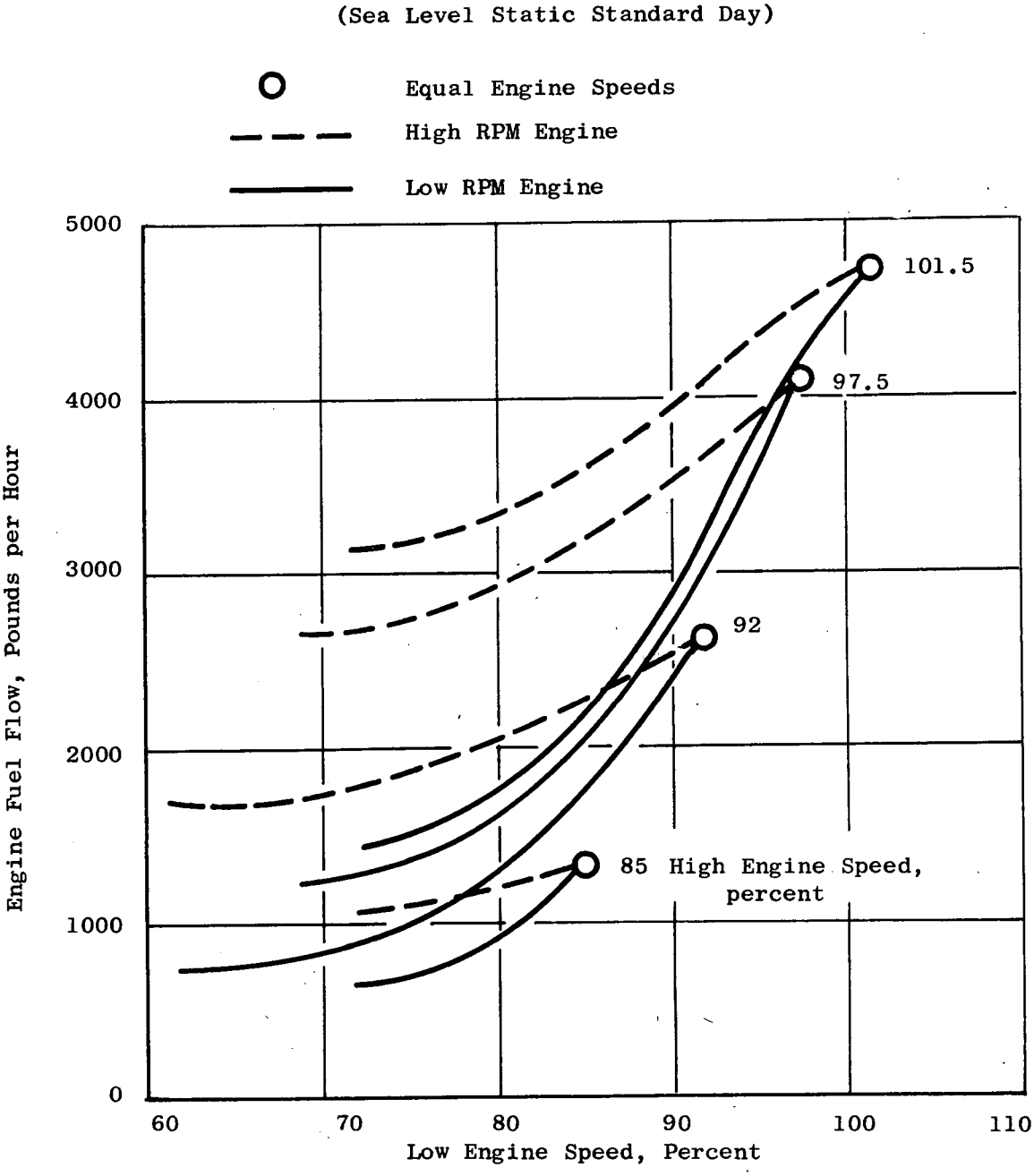

Figure 3. Effects on Engine Speed Unbalance on Engine Fuel Flow

E

(Sea Level Static Standard Day)

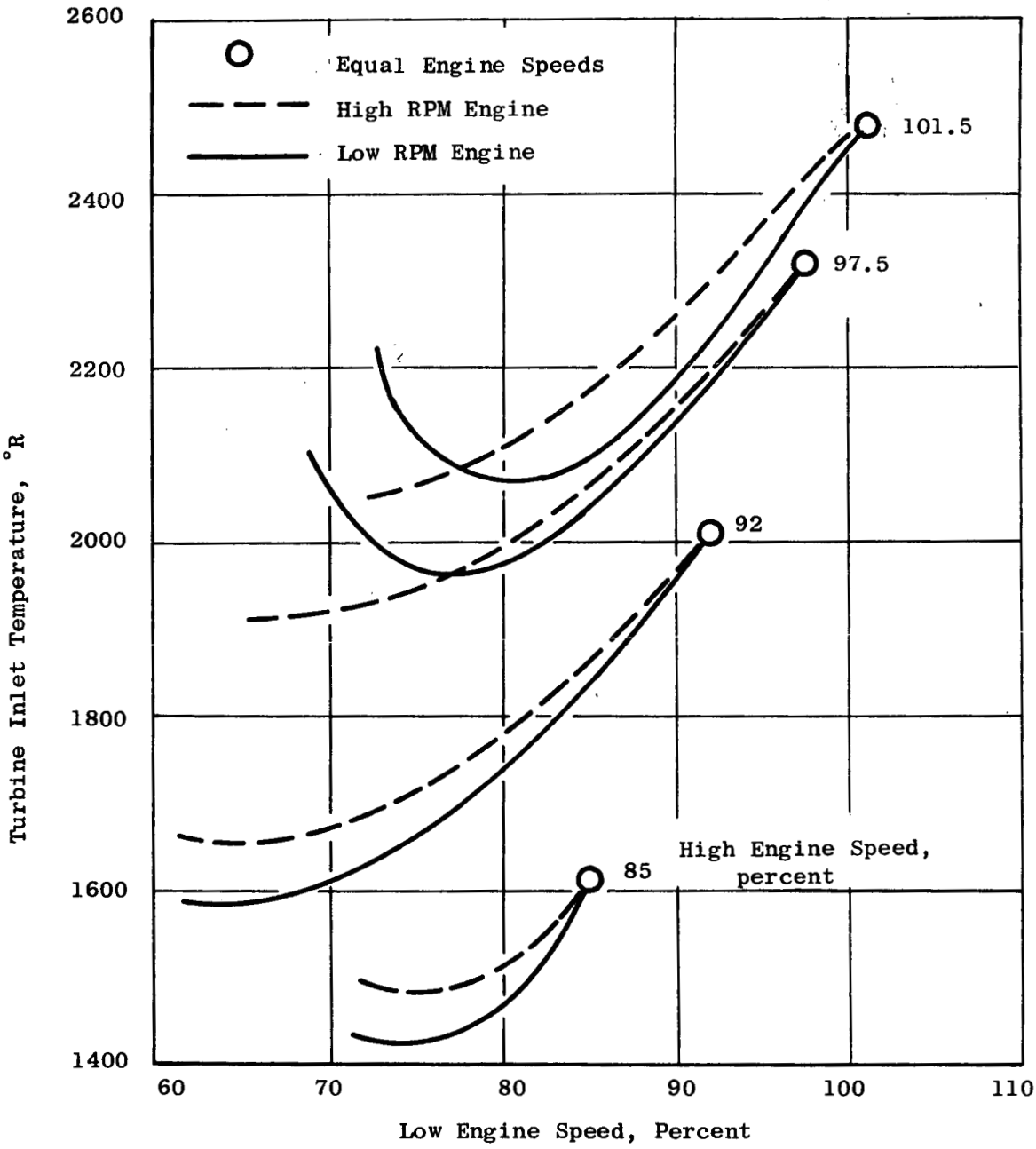

Figure 4. Effects of Engine Speed Unbalance on Turbine Inlet Temperature

(Sea Level Static Standard Day)

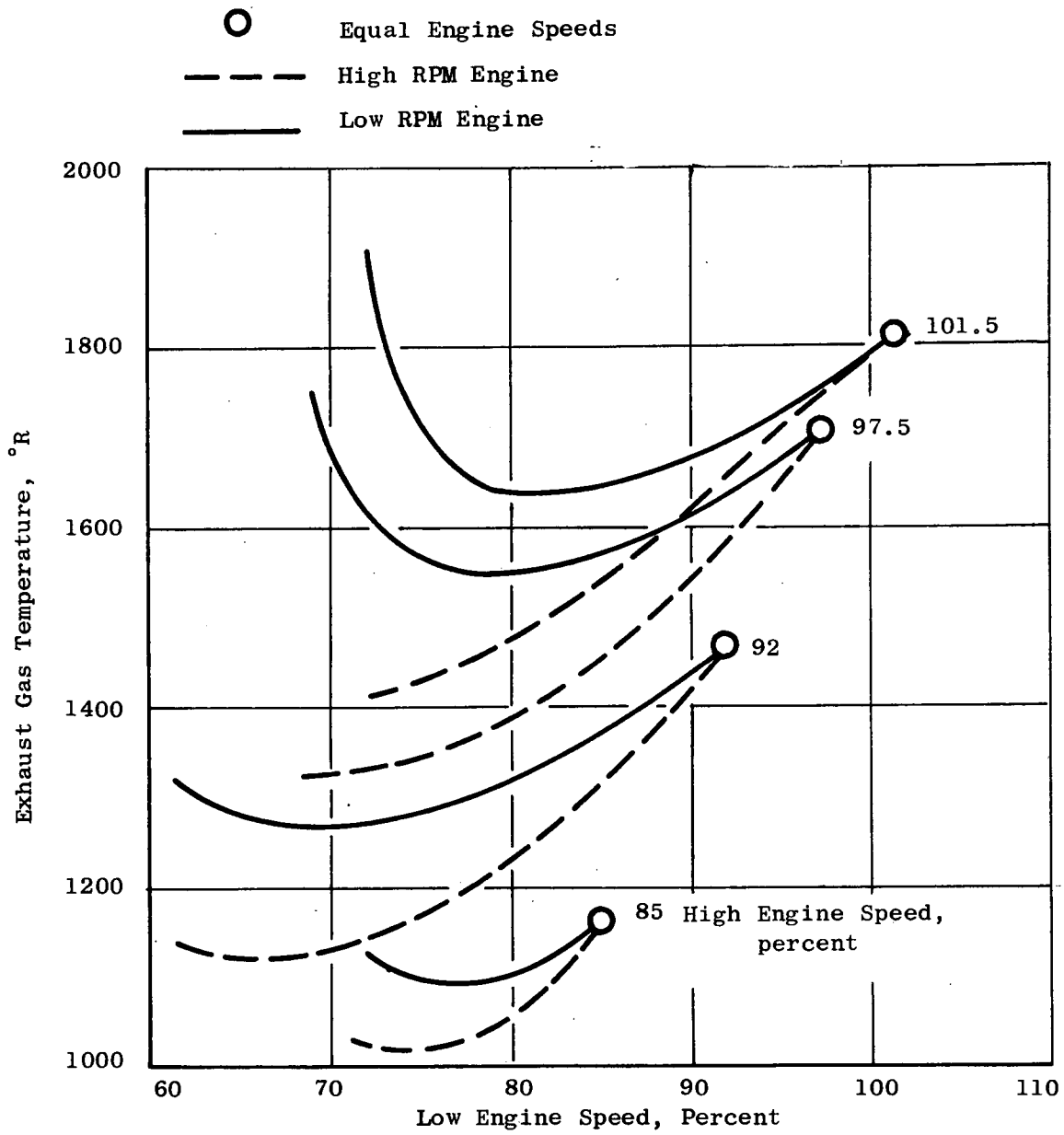

Figure 5. Effects of Engine Speed Unbalance on Exhaust Gas Temperature

(Sea Level Static Standard Day)

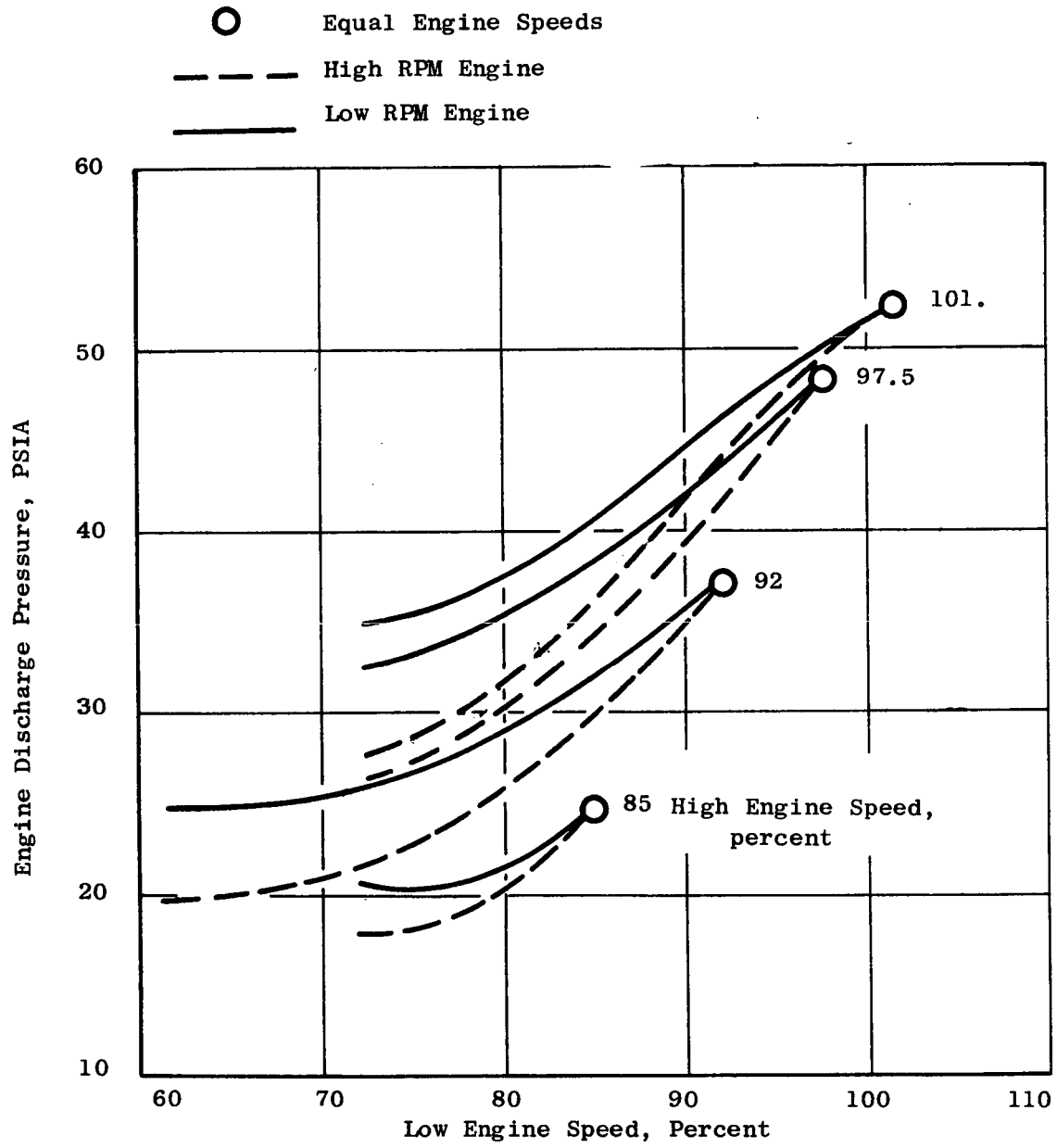

Figure 6. Effects of Engine Speed Unbalance on Engine Discharge Pressure

(Sea Level Static Standard Day)

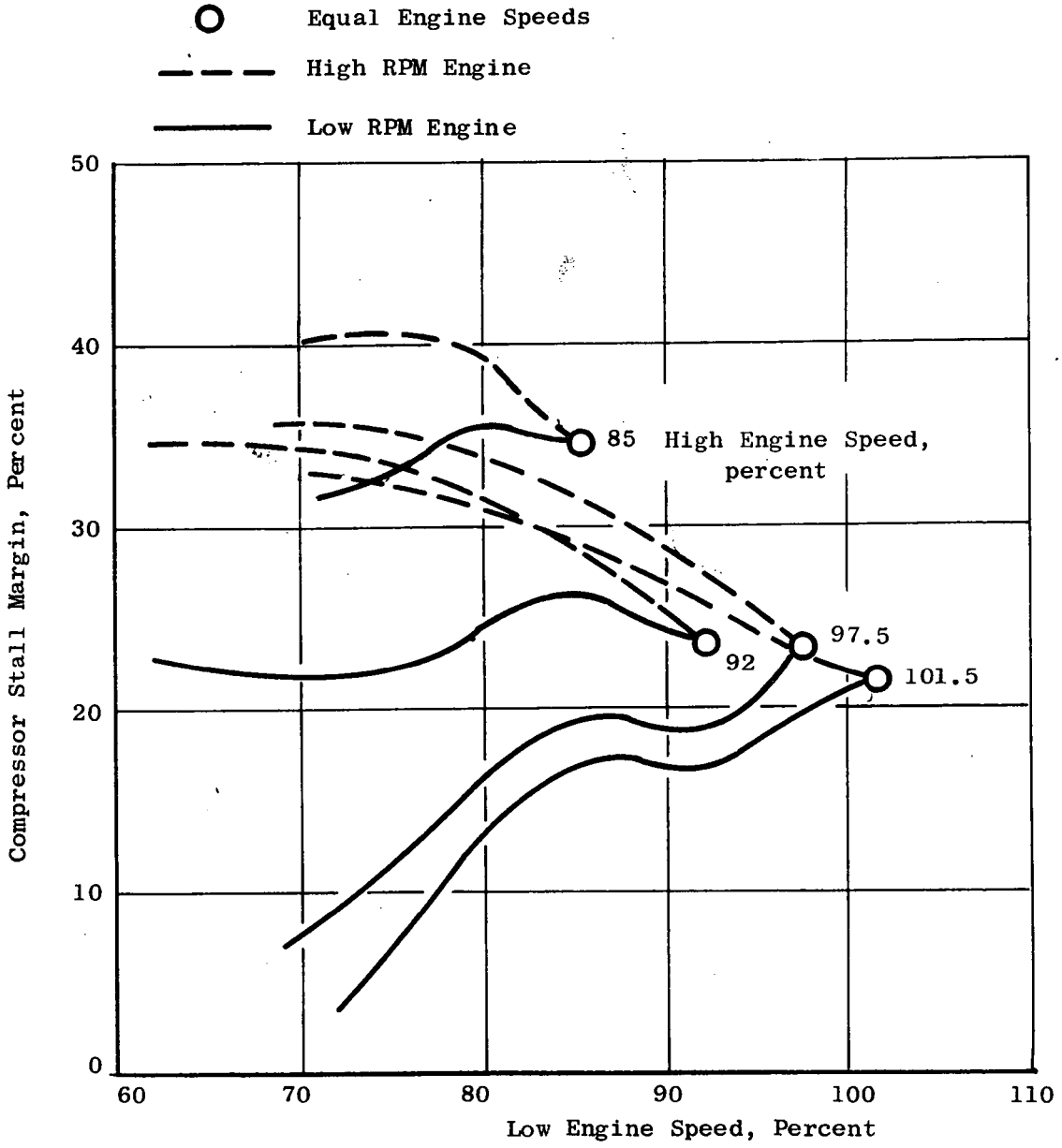

Figure 7. Effects of Engine Speed Unbalance on Compressor Stall Margin

- No Allowance for Low Side Engine Acceleration

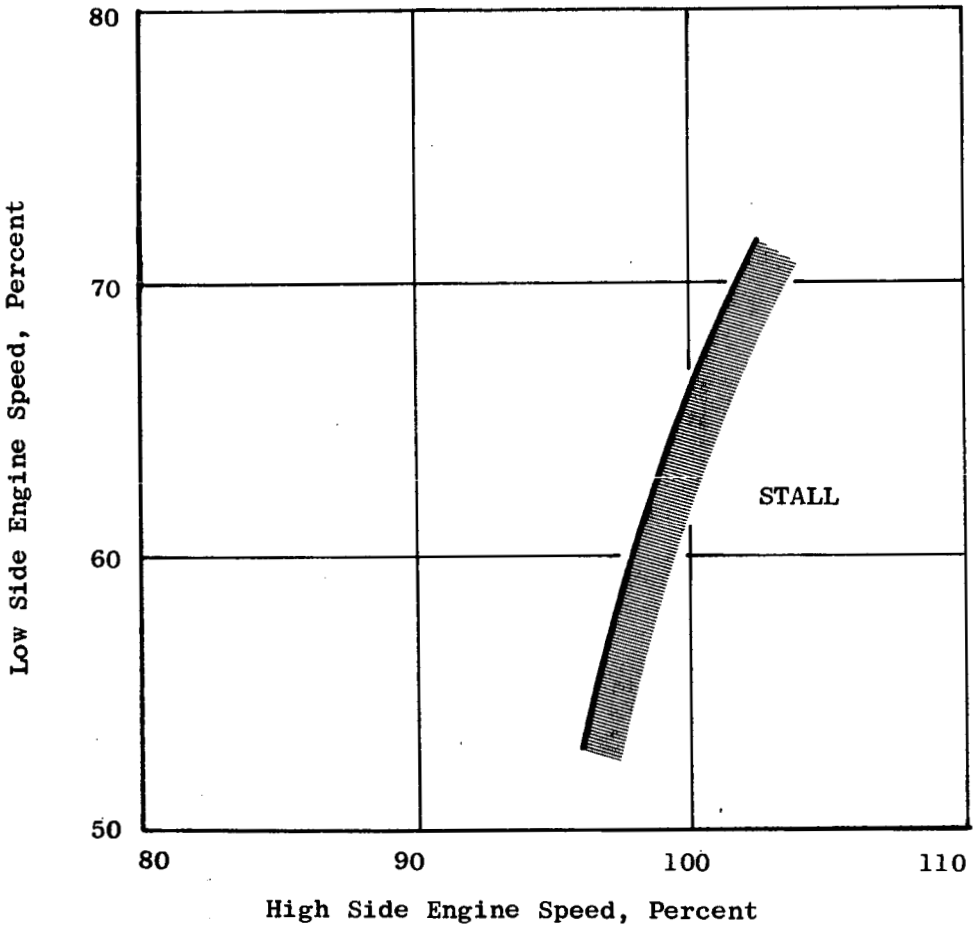

Figure 8. Engine Speed Unbalance Limitation as Established by Stall

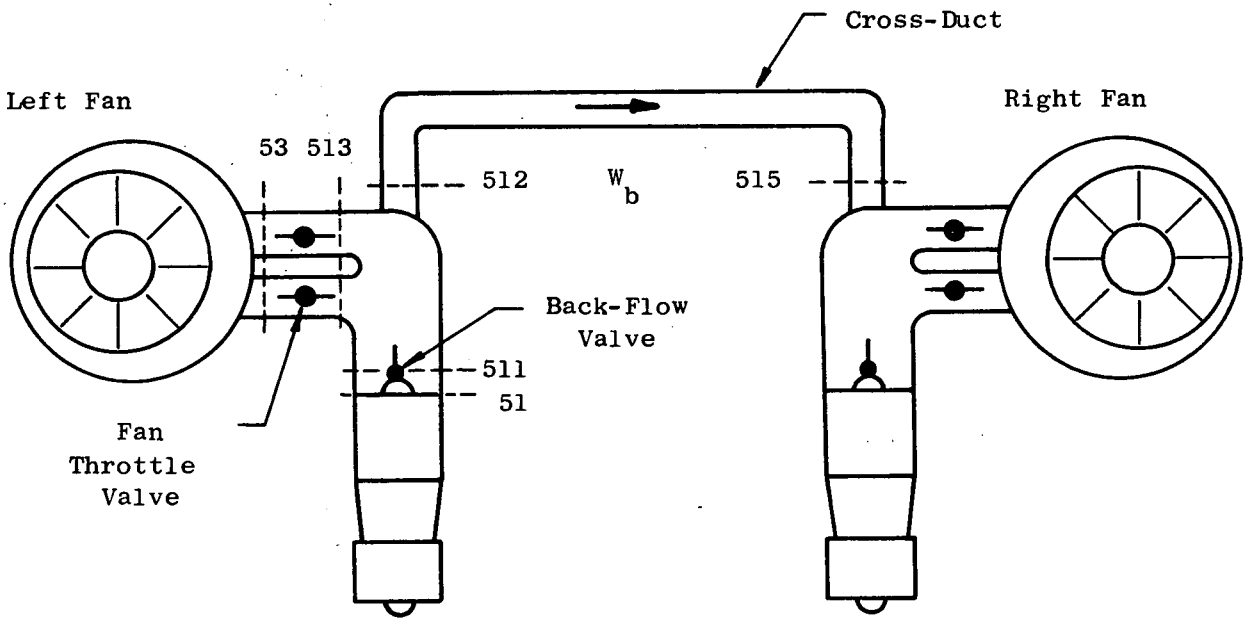

Figure 9. Schematic of Fan Interconnected Ducting System

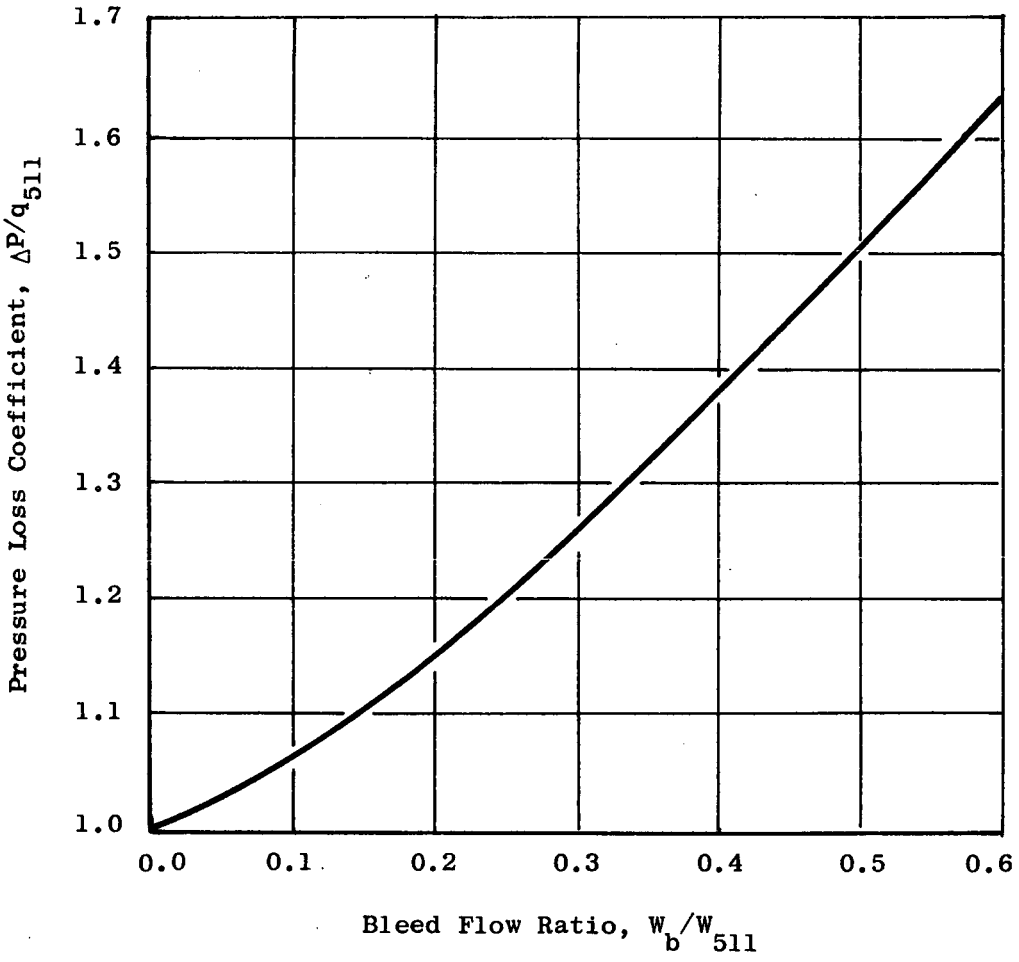

Figure 10. Interconnect Duct Pressure Loss Coefficient for Bleed Out of System

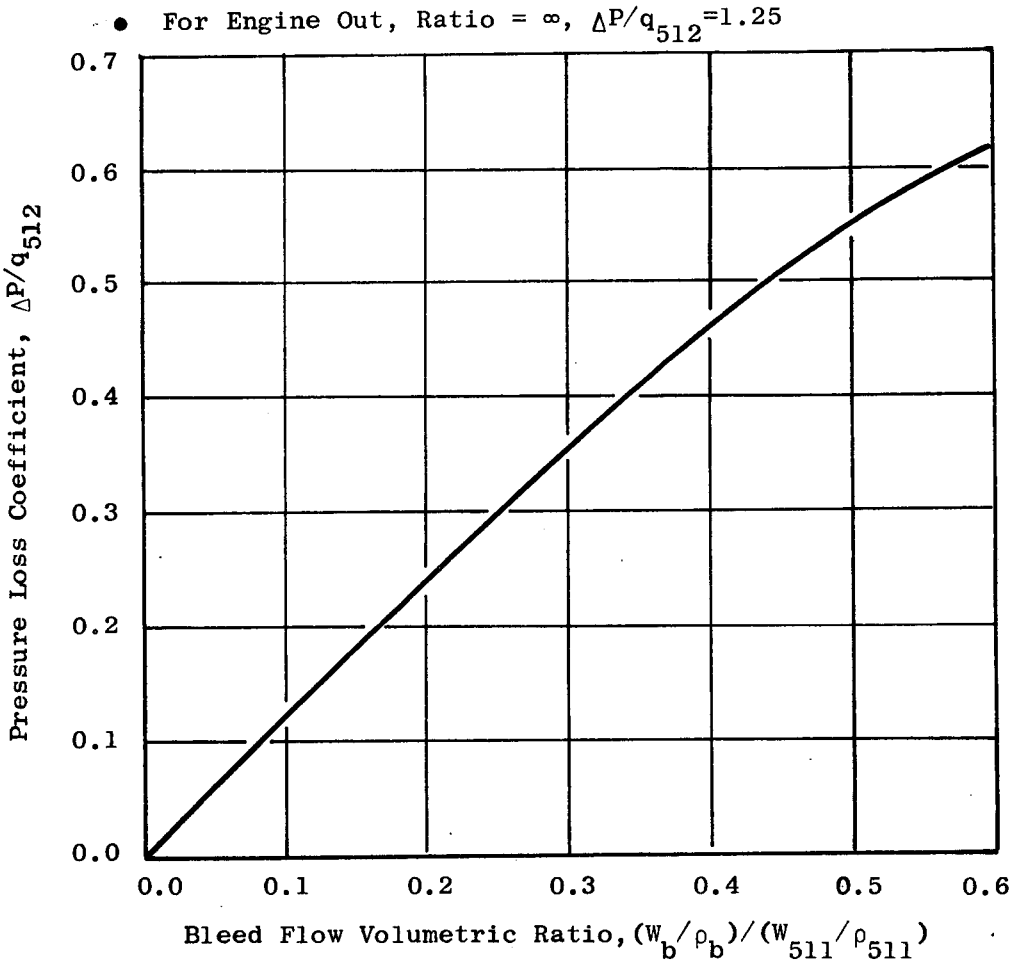

Figure 11. Interconnect Duct Pressure Loss Characteristics for Bleed into System

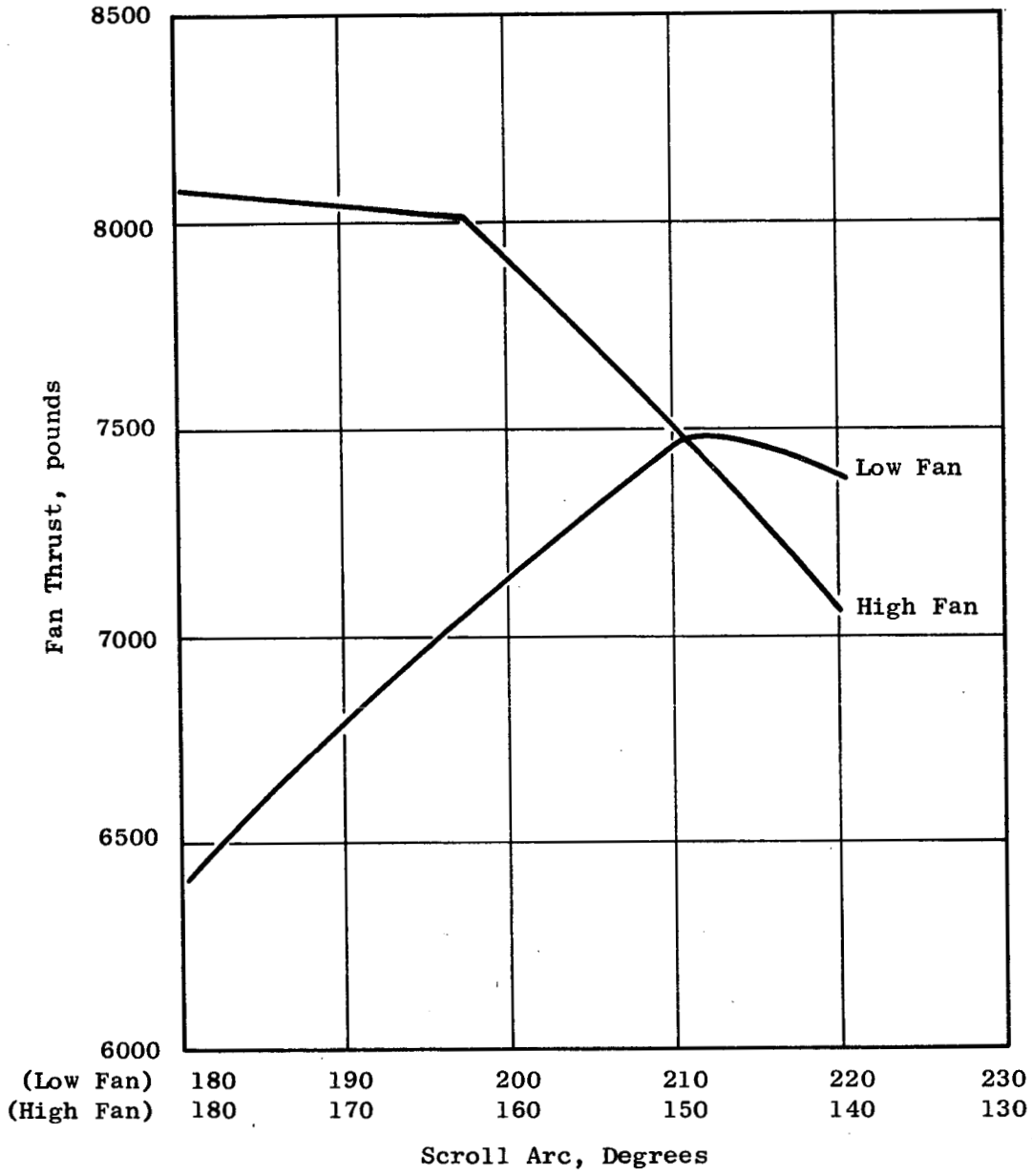

Figure 12. Fan Thrust Variation with Scroll Arc, Engine-Out Operation

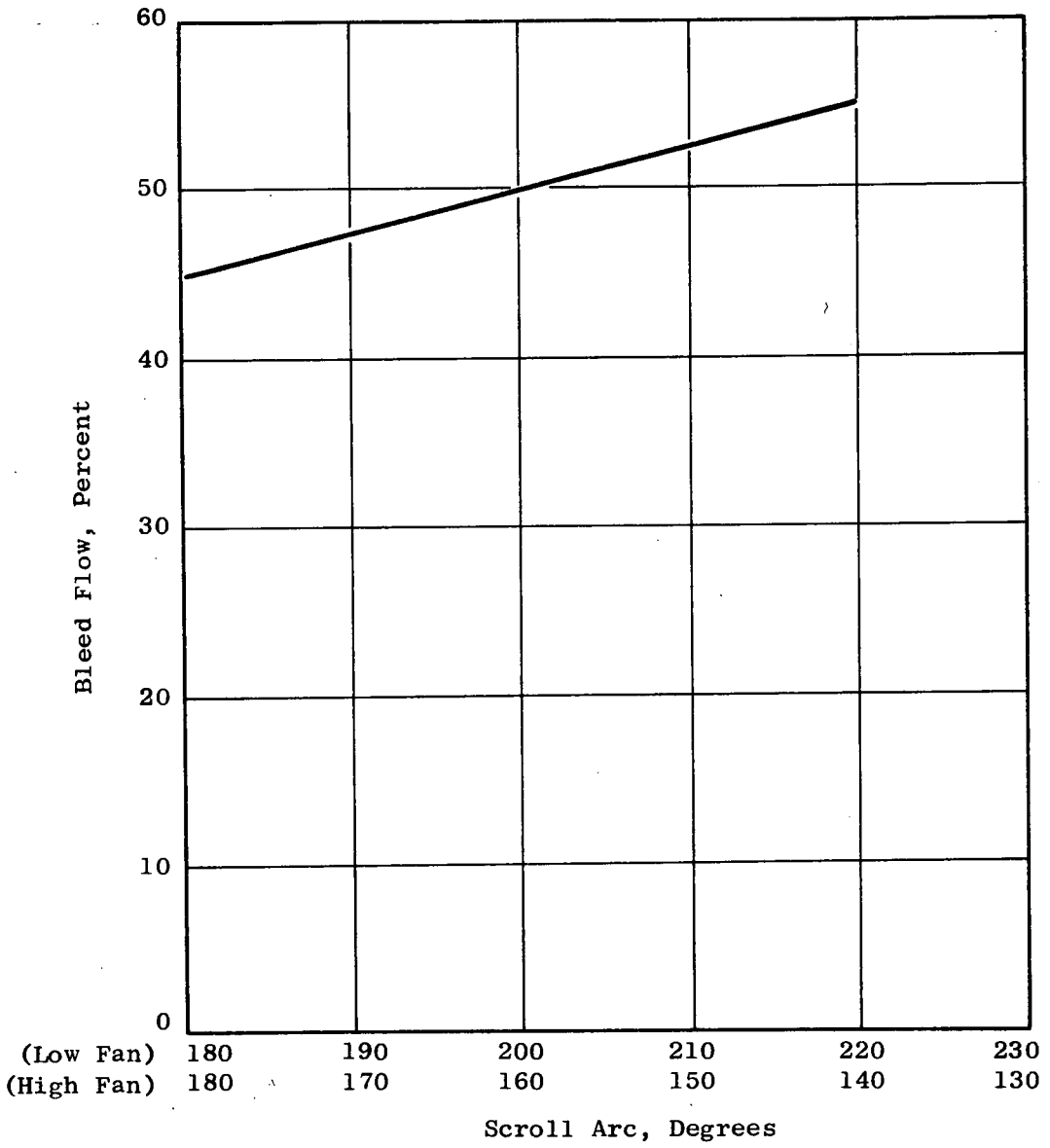

Figure 13. Interconnect Flow Variation with Scroll Arc, Engine-Out Operation

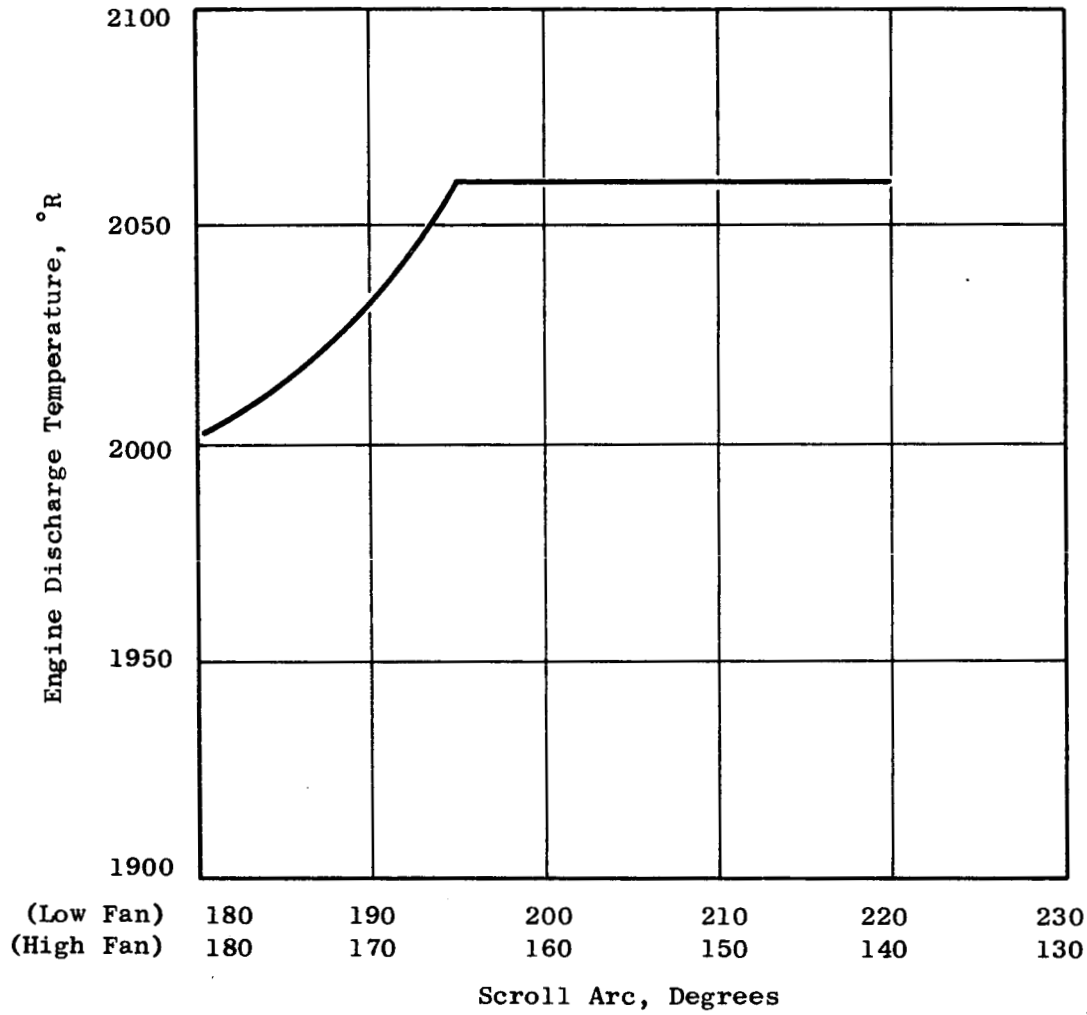

Figure 14. Engine Temperature Variation with Scroll Arc, Engine-Out Operation

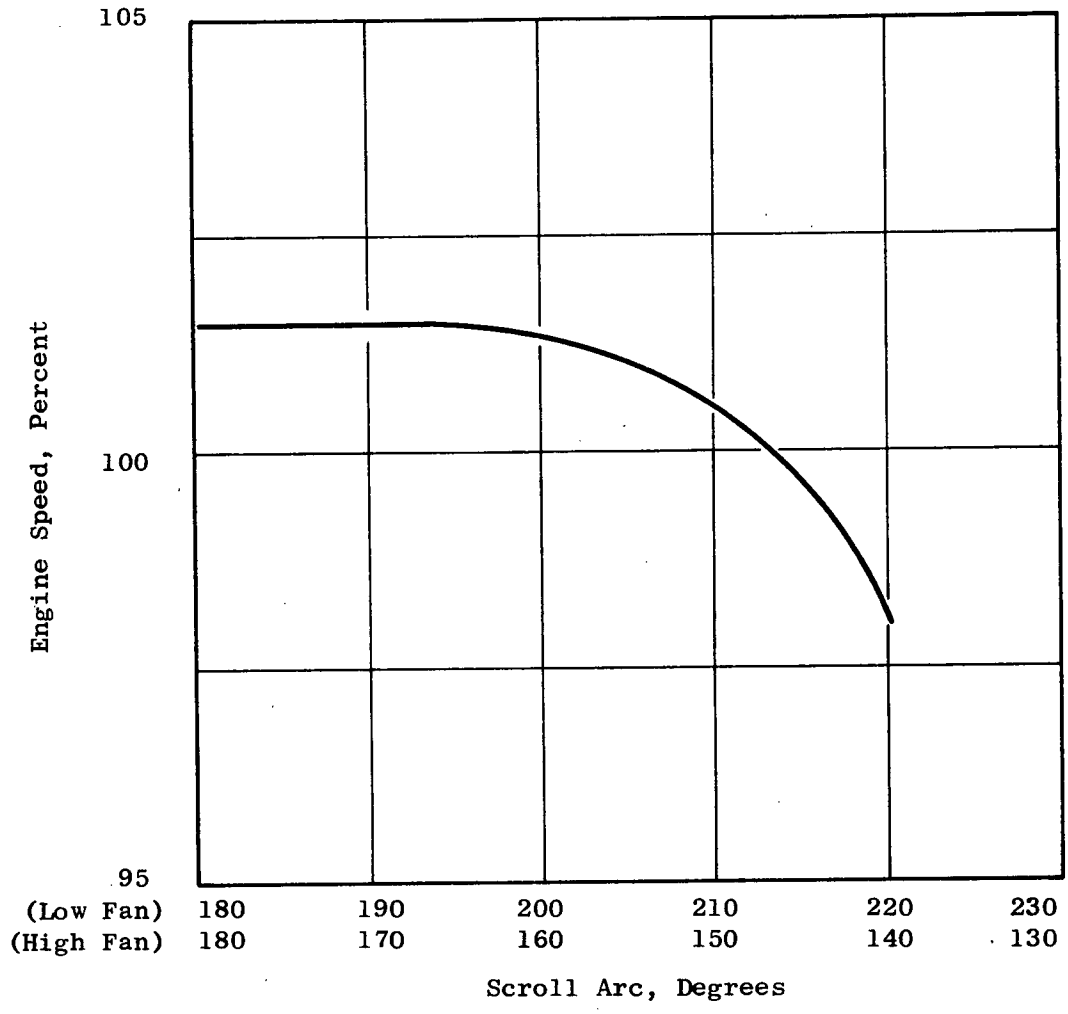

Figure 15. Engine Maximum Speed Variation with Scroll Arc, Engine-Out Operation

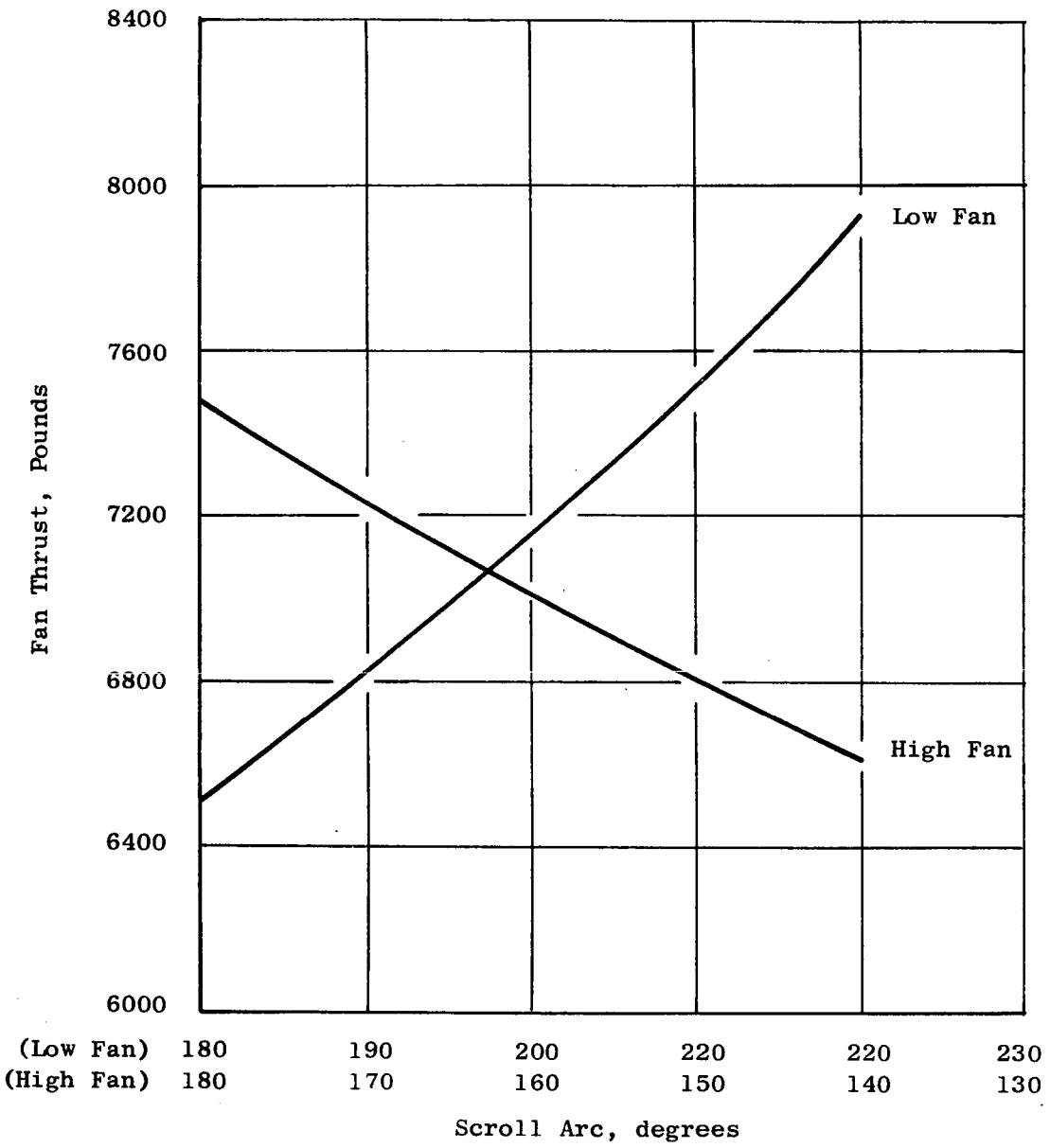

Figure 16. Fan Thrust Variation with Scroll Arc, Engine-Out Operation, 50 percent Duct Losses

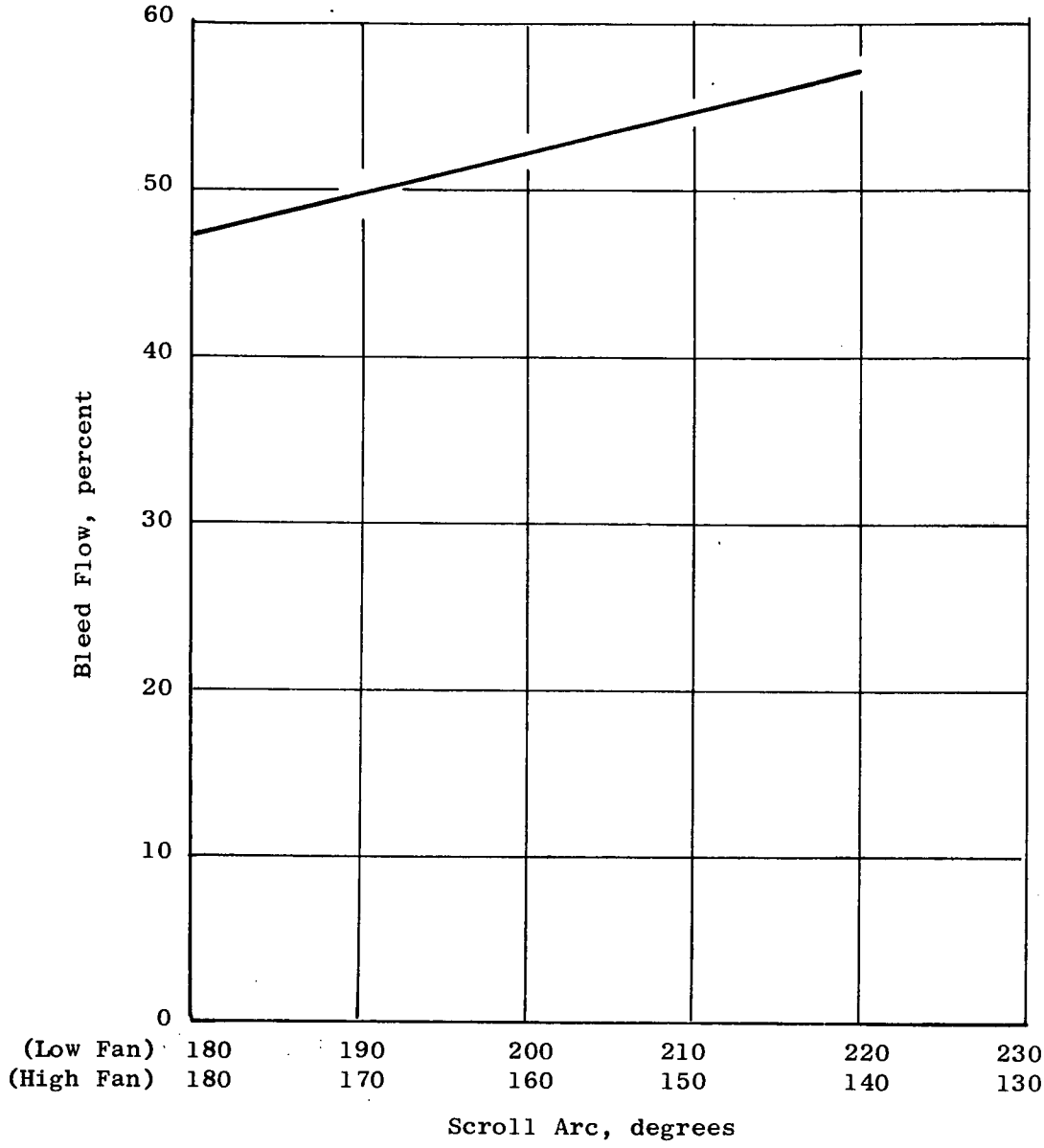

Figure 17. Interconnect Flow Variation with Scroll Arc, Engine-Out Operation, 50 percent Duct Losses

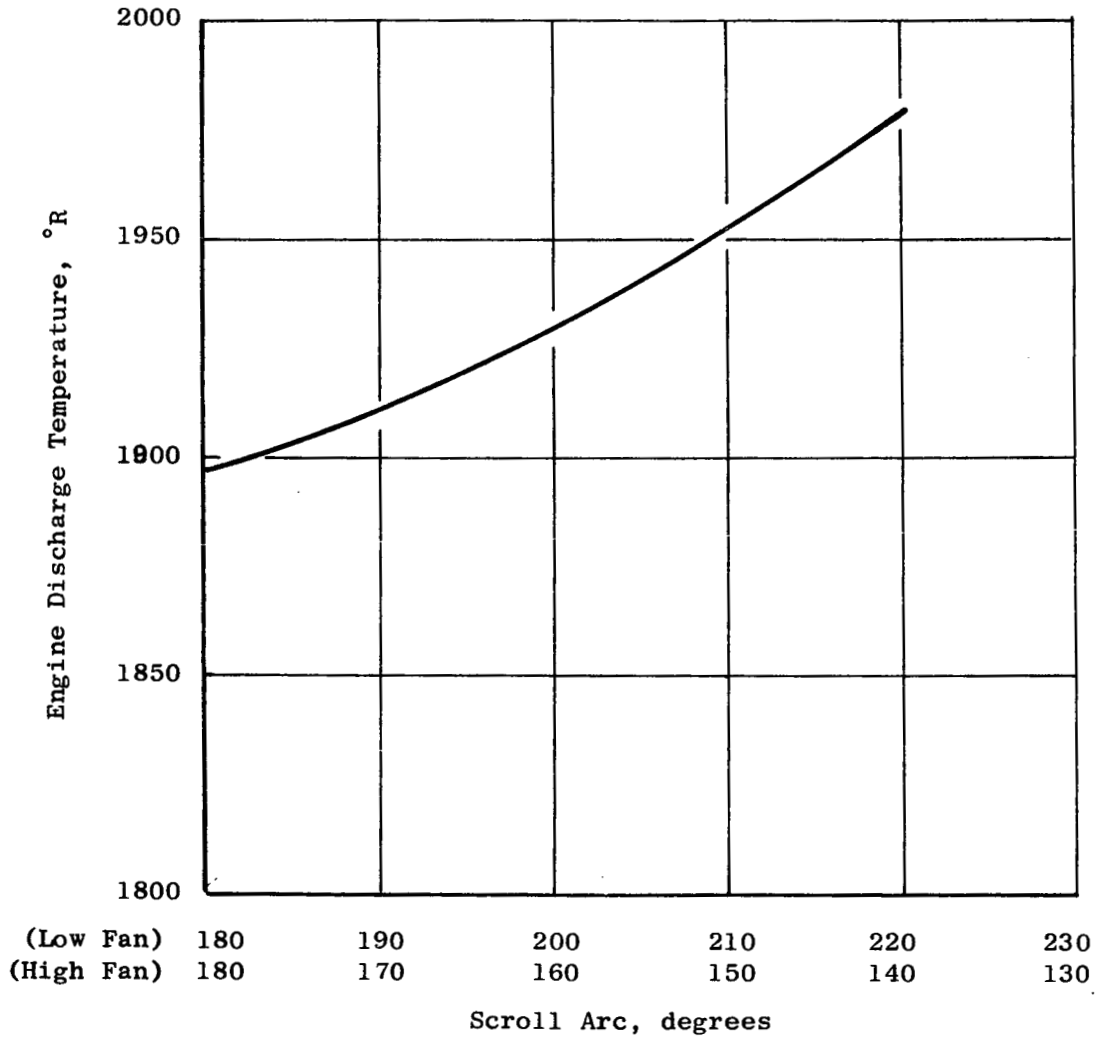

Figure 18. Engine Temperature Variation with Scroll Arc, Engine-Out Operation, 50 percent Duct Losses

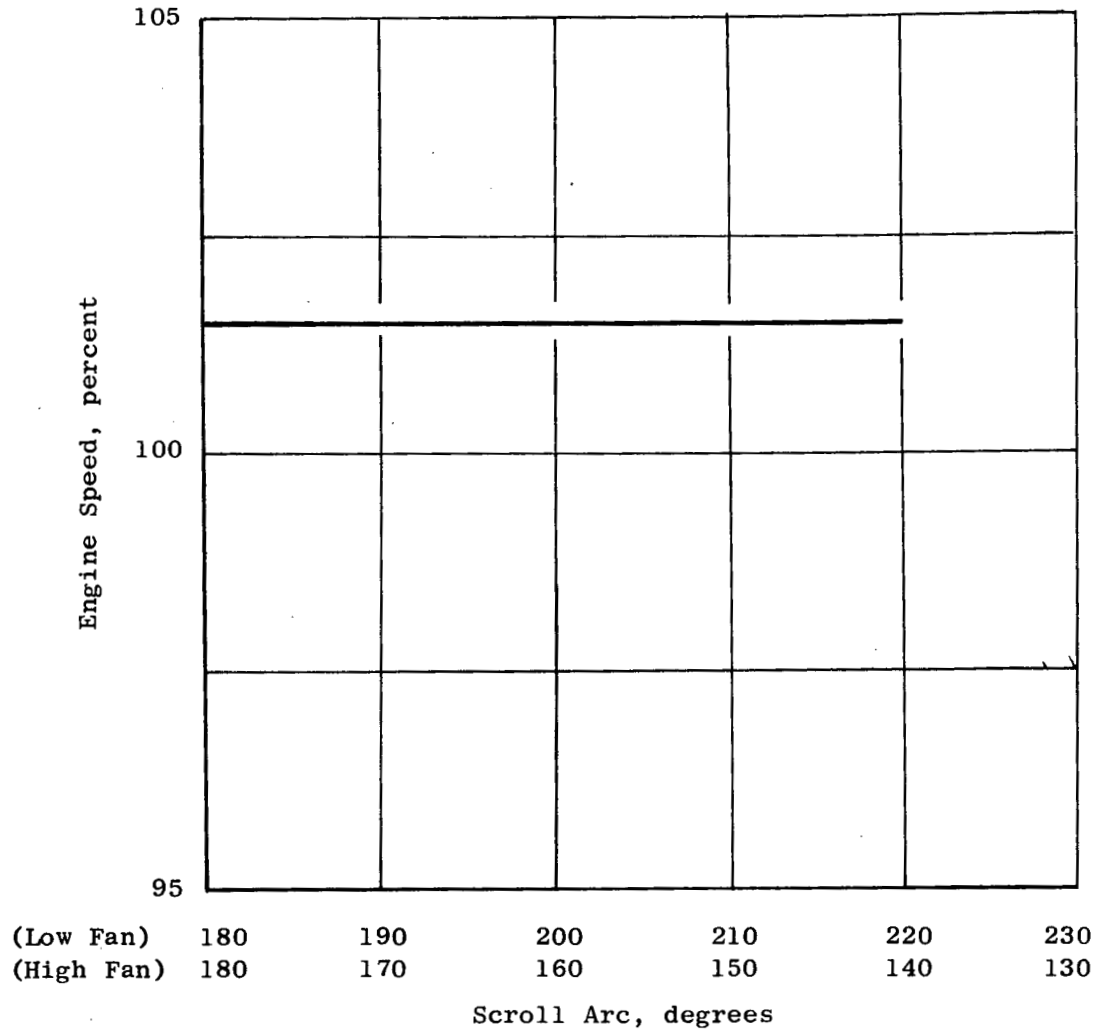

Figure 19. Engine Maximum Speed Variation with Scroll Arc, Engine-Out, 50 percent Duct Losses

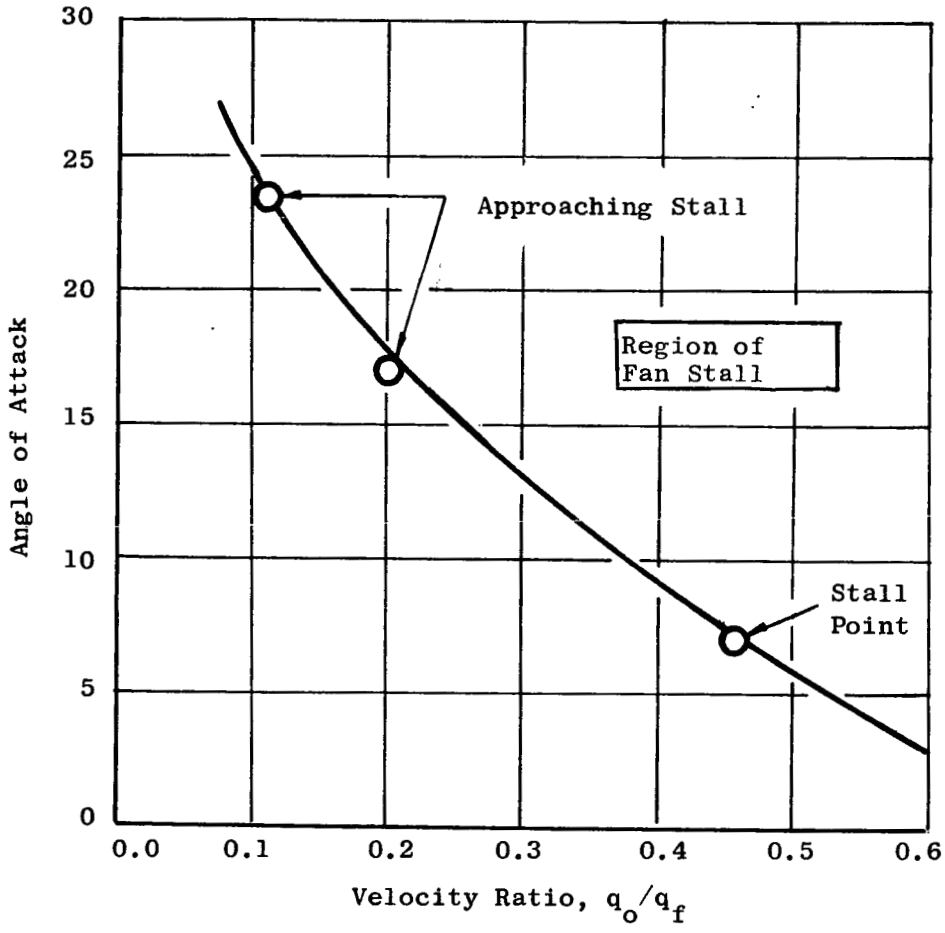

Figure 20. Stall Envelope for LF336/A as Observed During NASA Windtunnel Tests

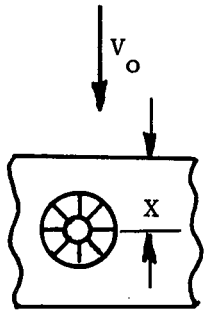

D_T = Fan Tip Diameter

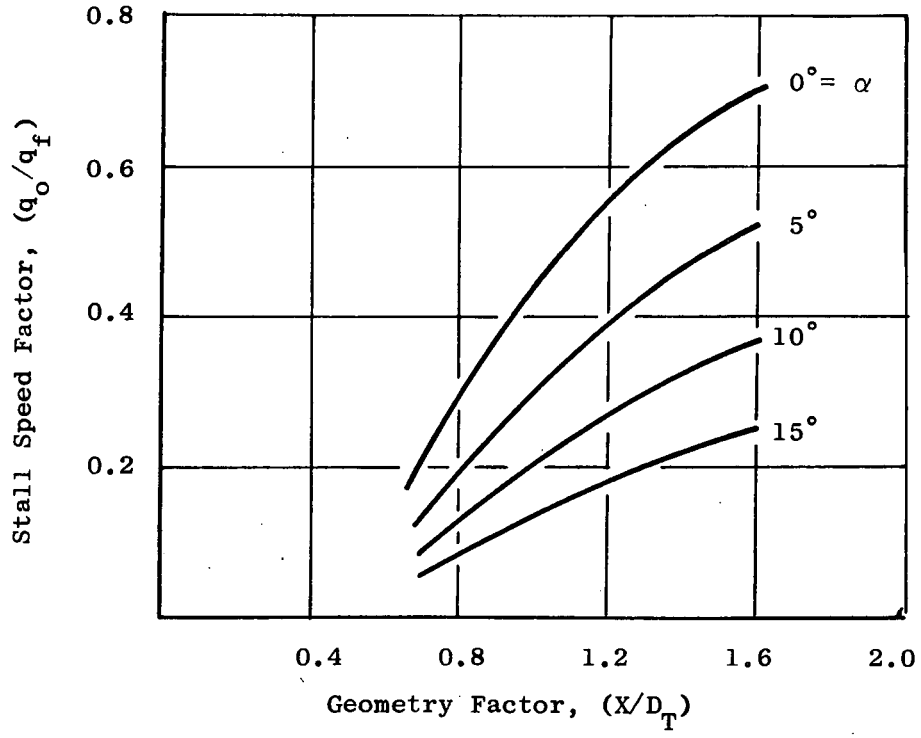

Figure 21. Estimated Stall Envelope for Horizontally Mounted Lift Fans

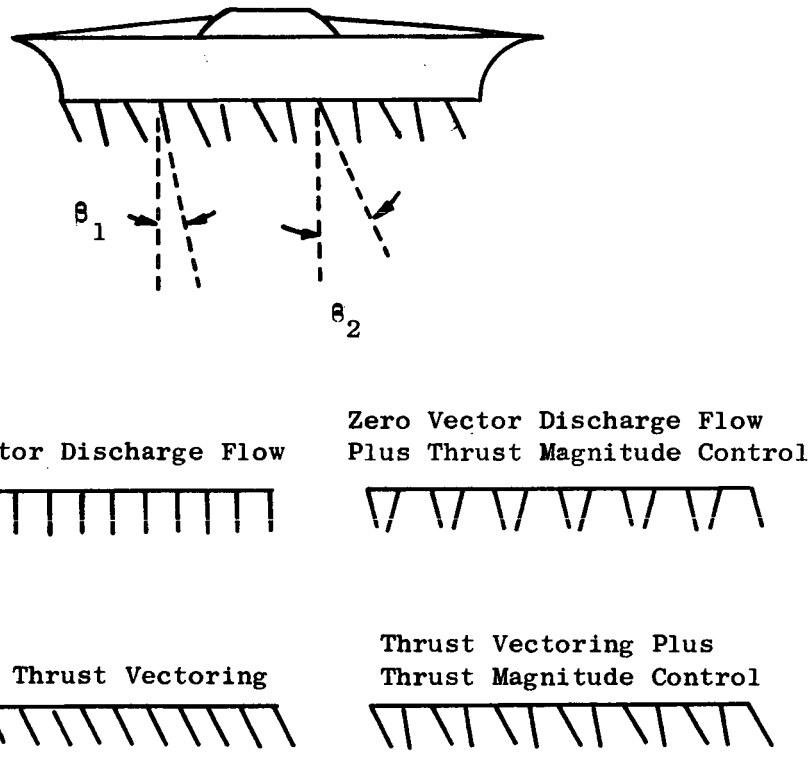

Figure 22. Schematic of Exit Louver System

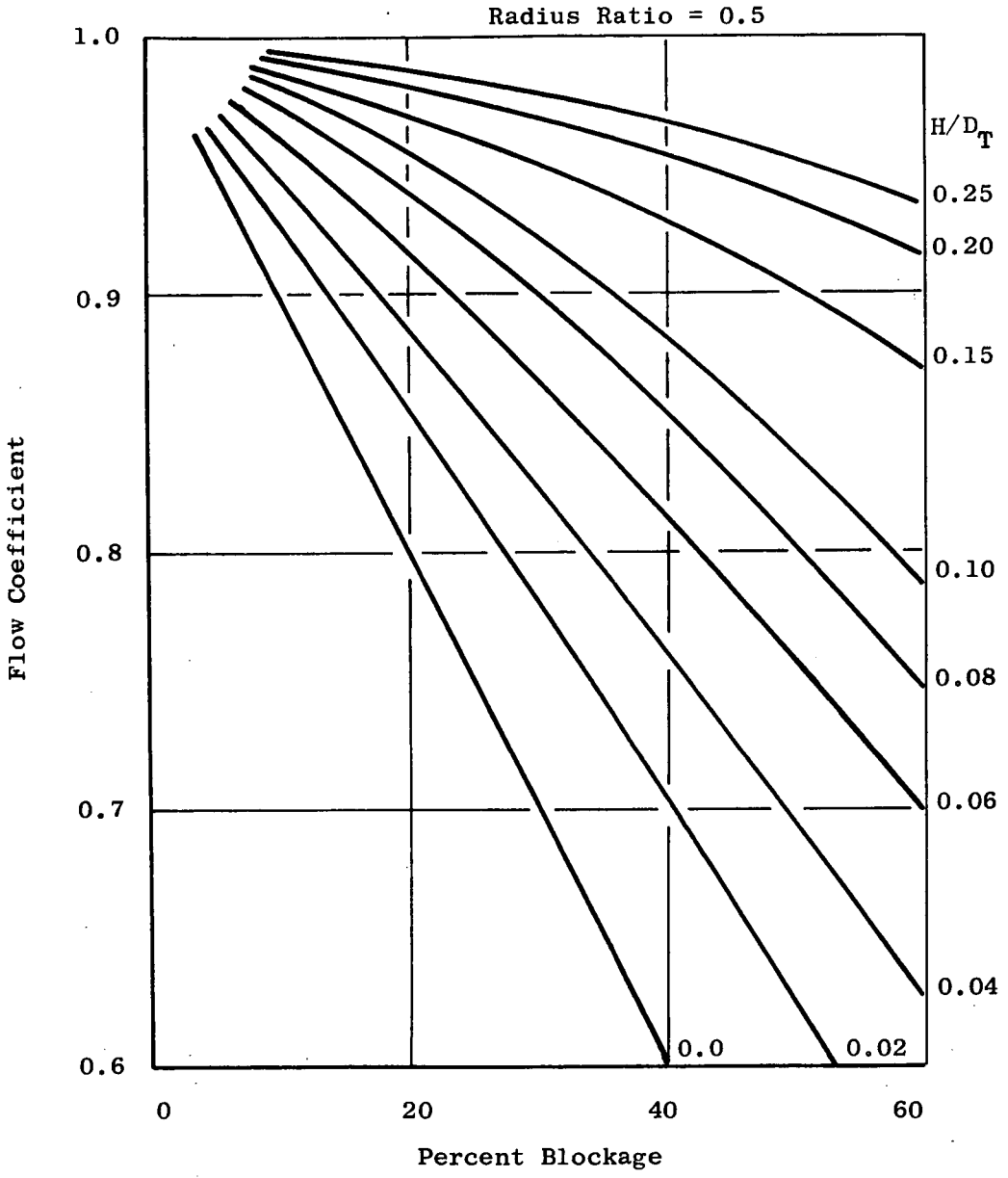

Figure 23. Throttling Characteristics of Blockage Downstream of an Annular Nozzle

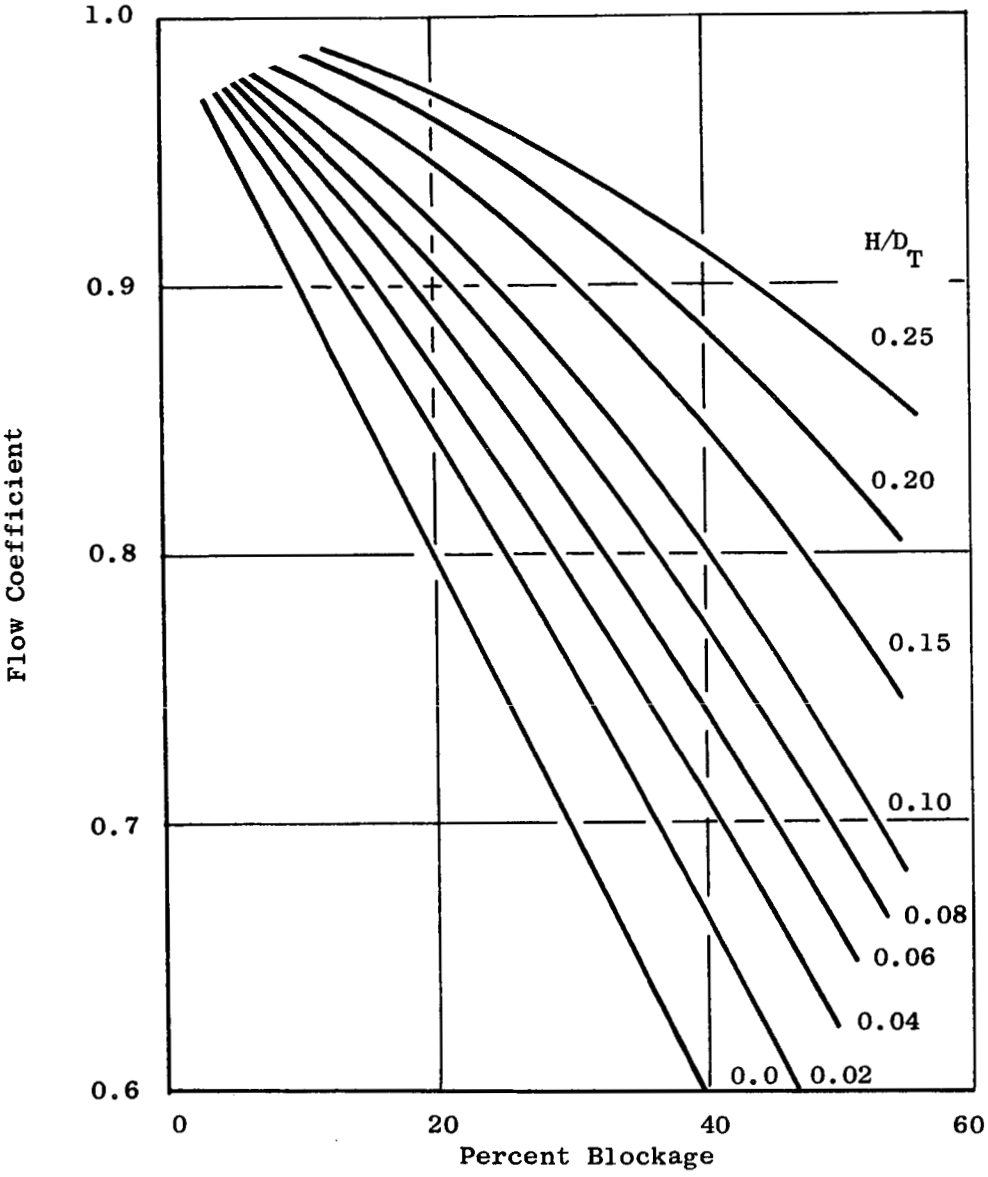

Figure 24. Throttling Characteristics of Blockage Downstream of a Round Nozzle

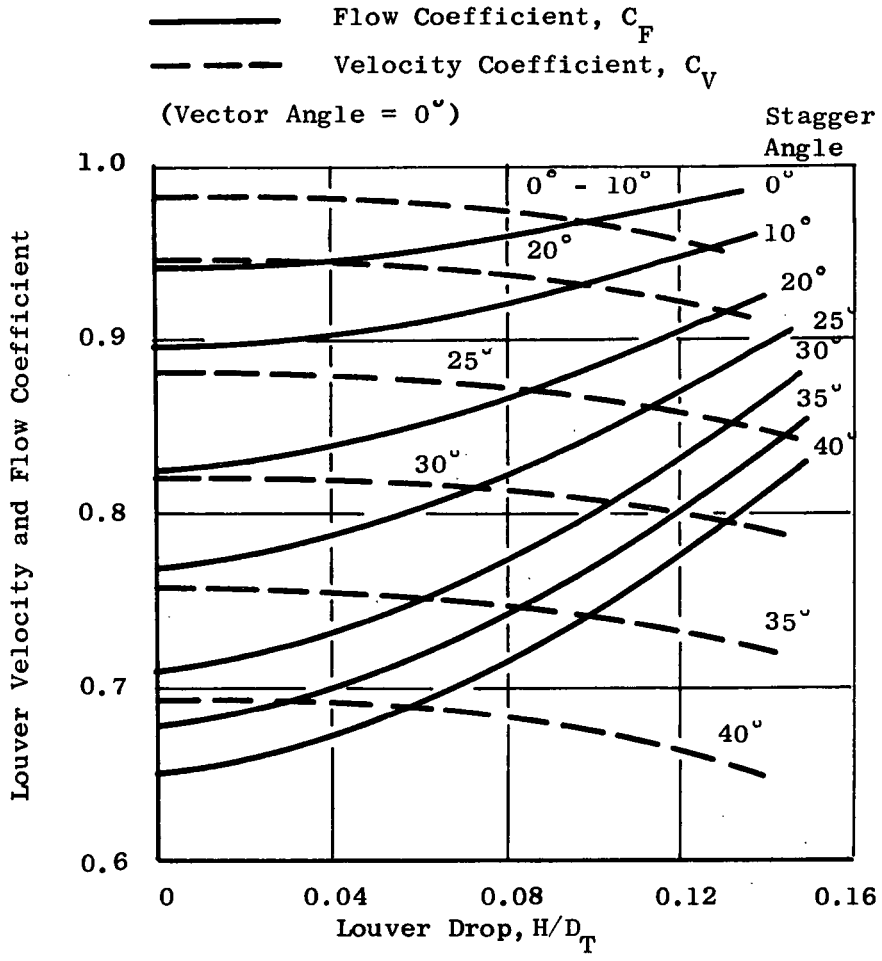

Figure 25. Estimated Performance of Louvers with Stagger at Variable Drop Height

Turbine Flow Coefficient:

$$C_{FT} = [1-(1-C_{FF}(0.5)]$$

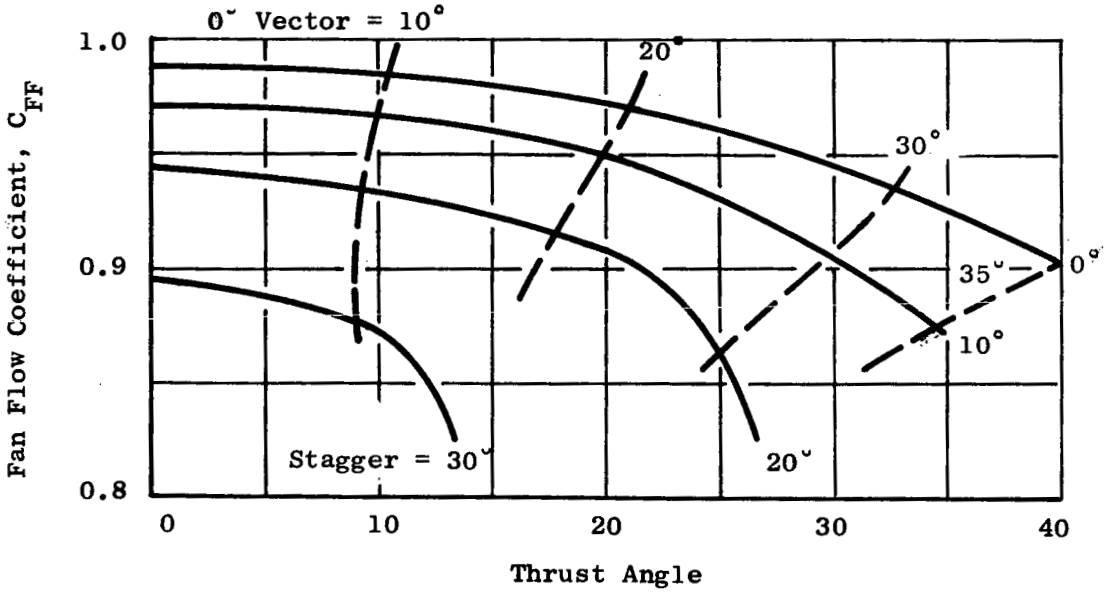

Figure 26. Estimated Louver Flow Coefficient for LF460, Drop Height = 4.5"

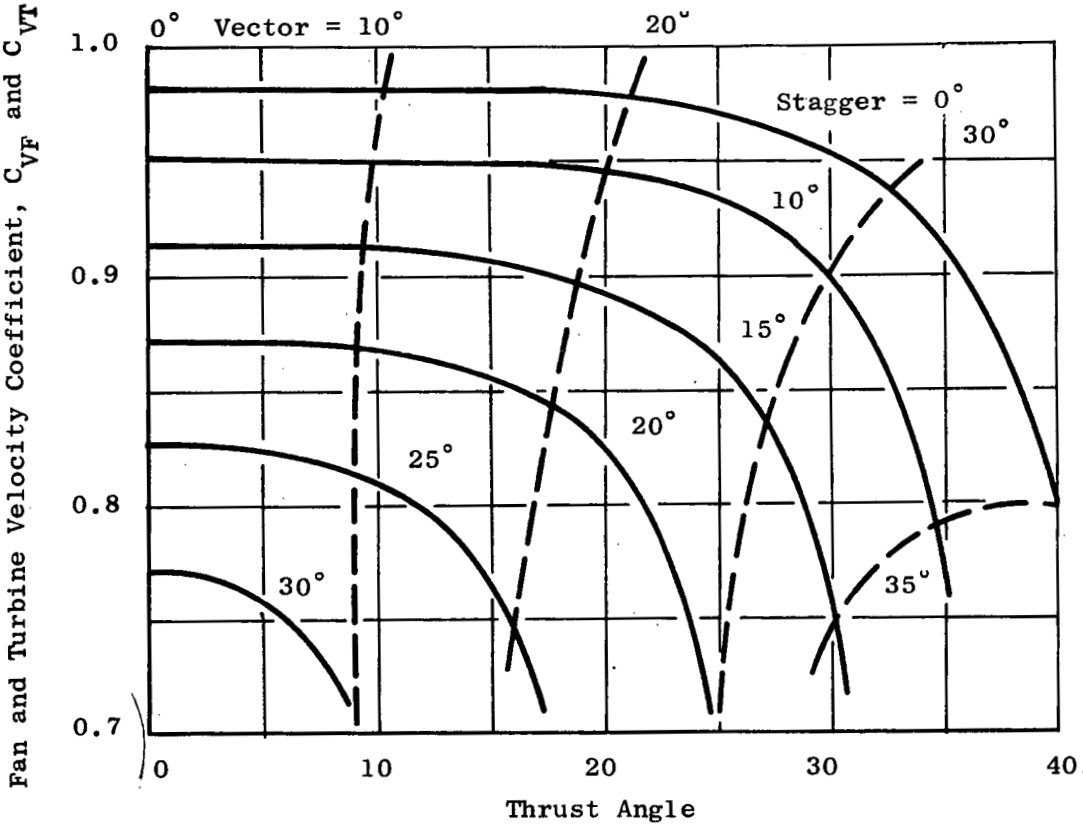

Figure 27. Estimated Louver Velocity Coefficient for LF460, Drop Height = 4.5"

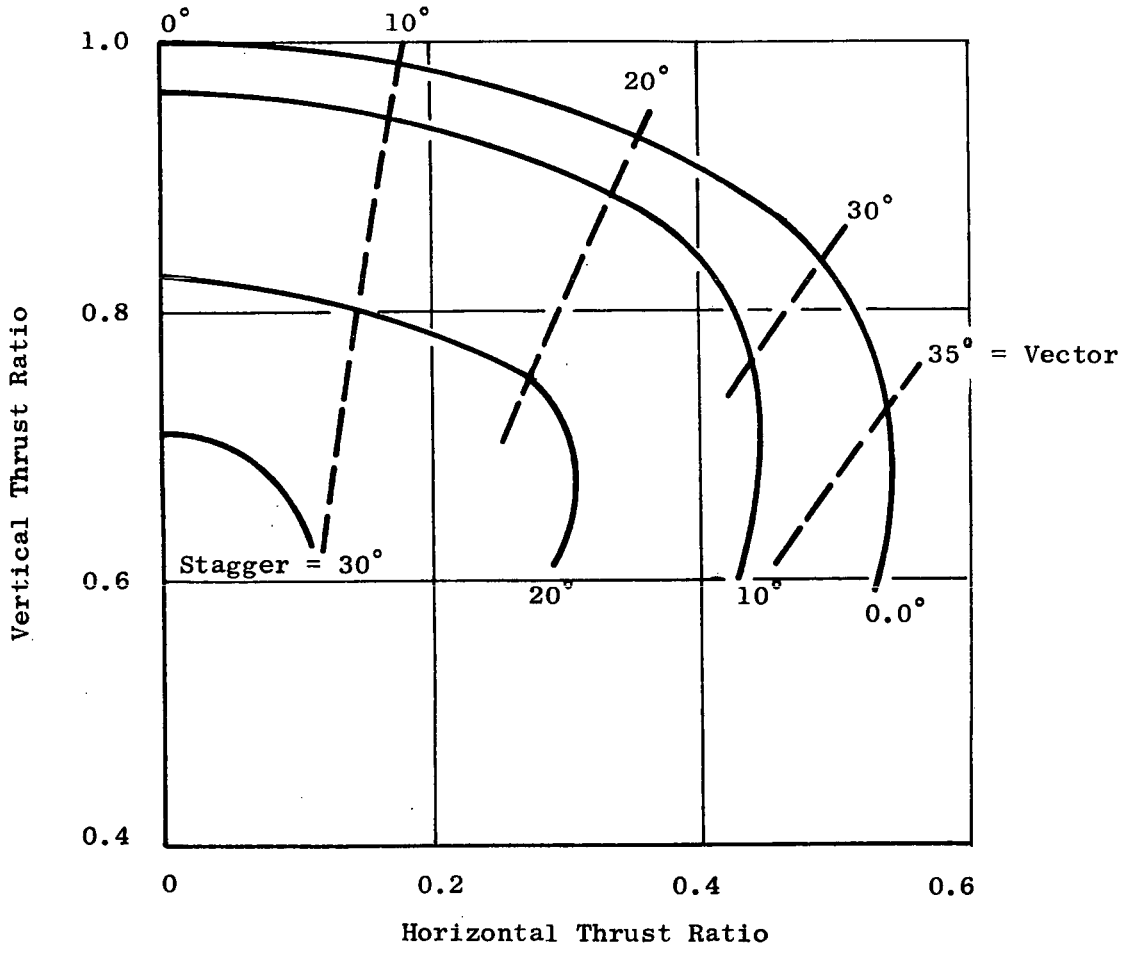

Figure 28. Estimated Thrust Characteristics of the LF460 With Louvers

Note: Assumes Negligible Losses in Flow Transfer Ducting.

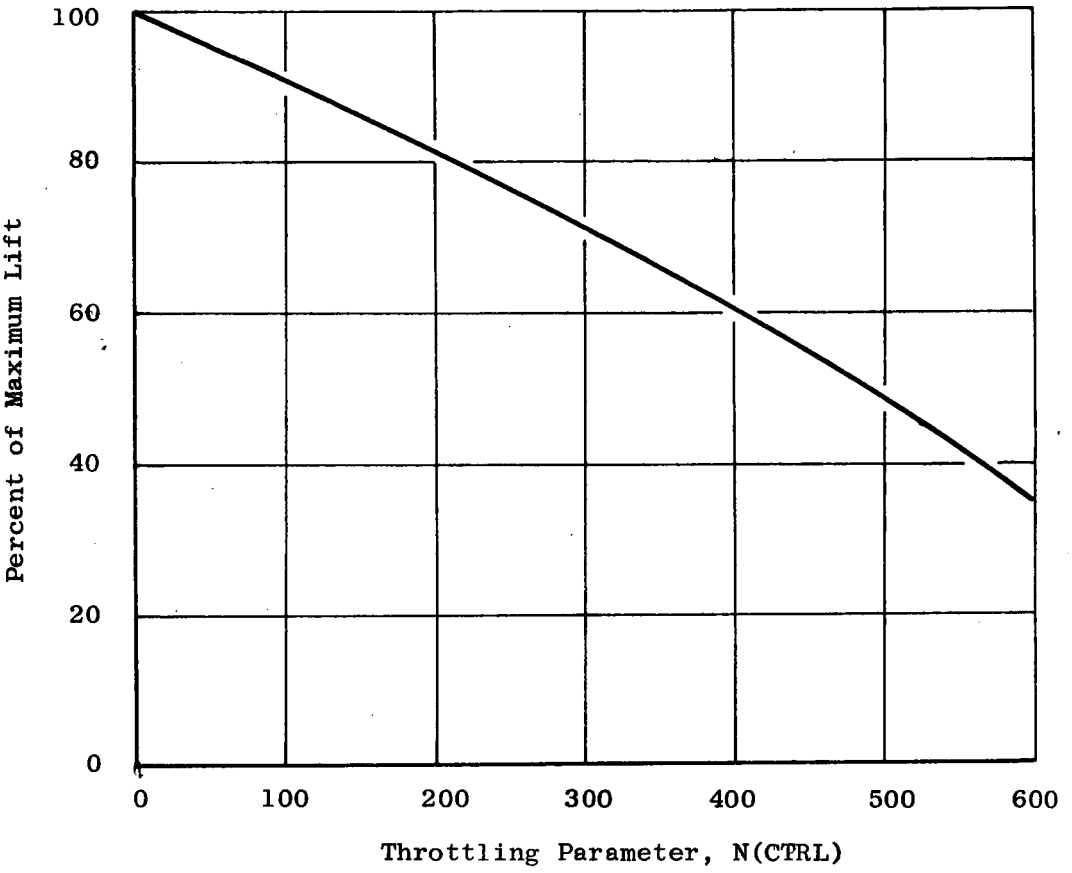

Figure 29. Nomograph for Estimating Fan Lift with Control Inputs

- Six Interconnected Systems
- Maximum Lift at Maximum Control Conditions is 15,000 Pounds
- Control Inputs are as follows:

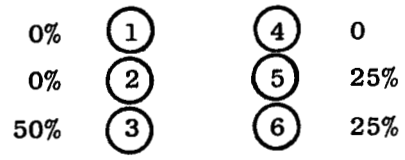

- From Figure 29 fan lift levels are as follows:

Unit No.	Percent Control	N(CTRL)	Percent Lift	Fan Lift
1	0	0	100	15,000
2	0	0	100	15,000
3	50	300	70.5	10,600
4	0	0	100	15,000
5	25	150	85.8	13,850
6	25	150	85.8	13,850

- Estimated lift levels can be used to determine control moments and total system lift levels

Figure 30. Example of Control for a Six Fan, Six Engine System

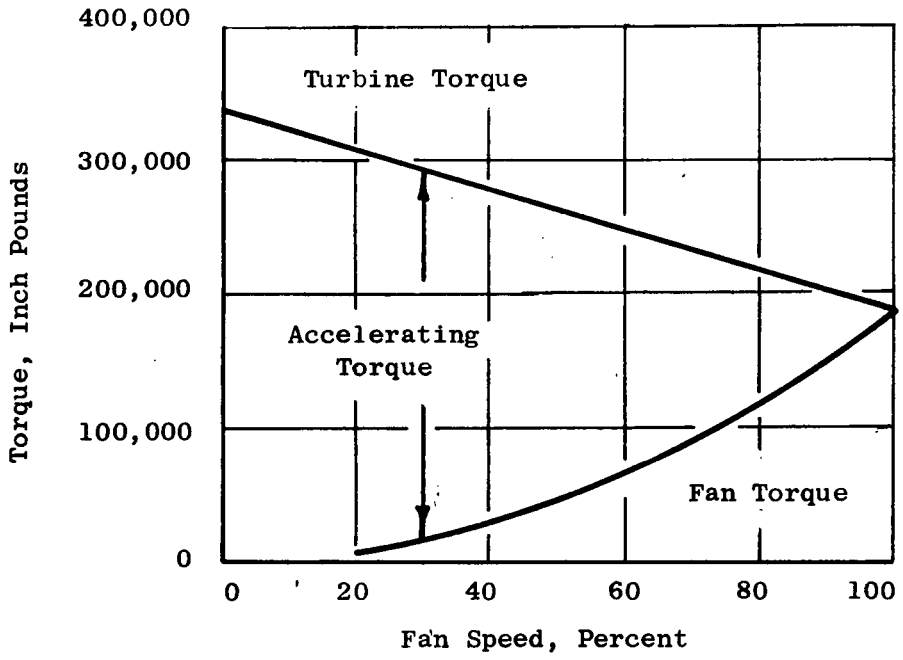

Figure 31. Estimated Torque Unbalance Variation with Speed

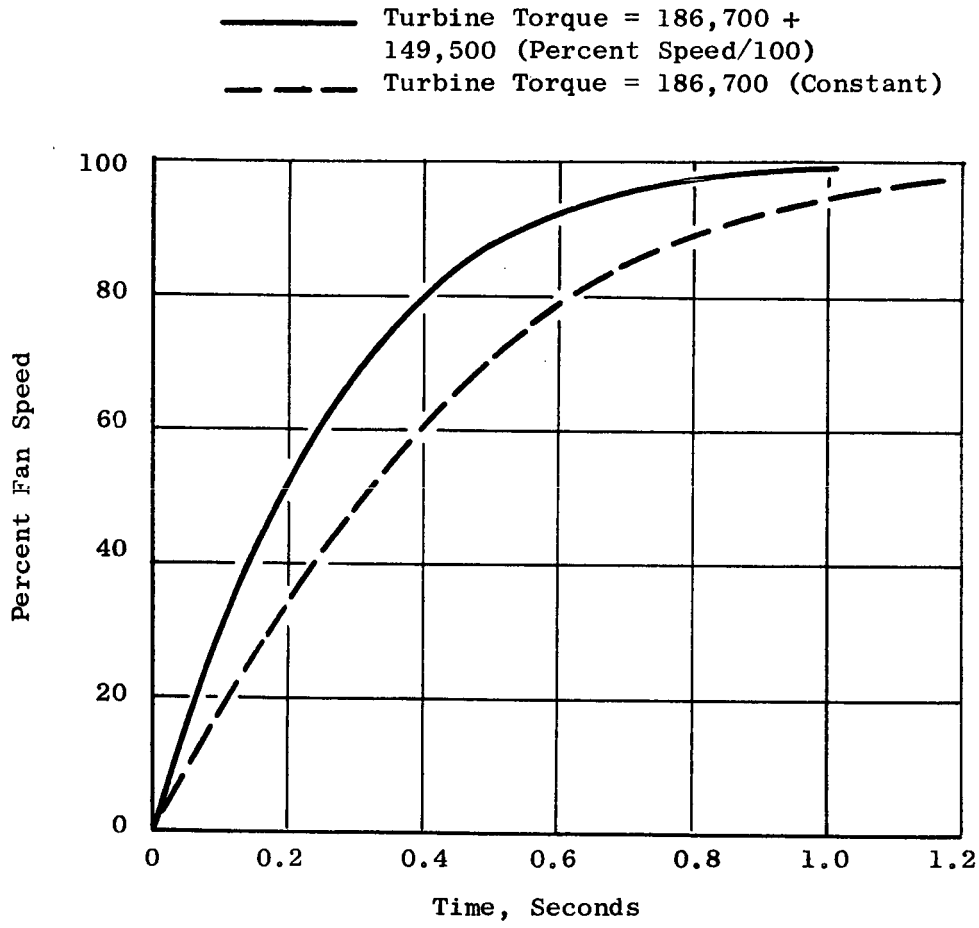

Figure 32. Estimated Acceleration Times for LF460 Lift Fan

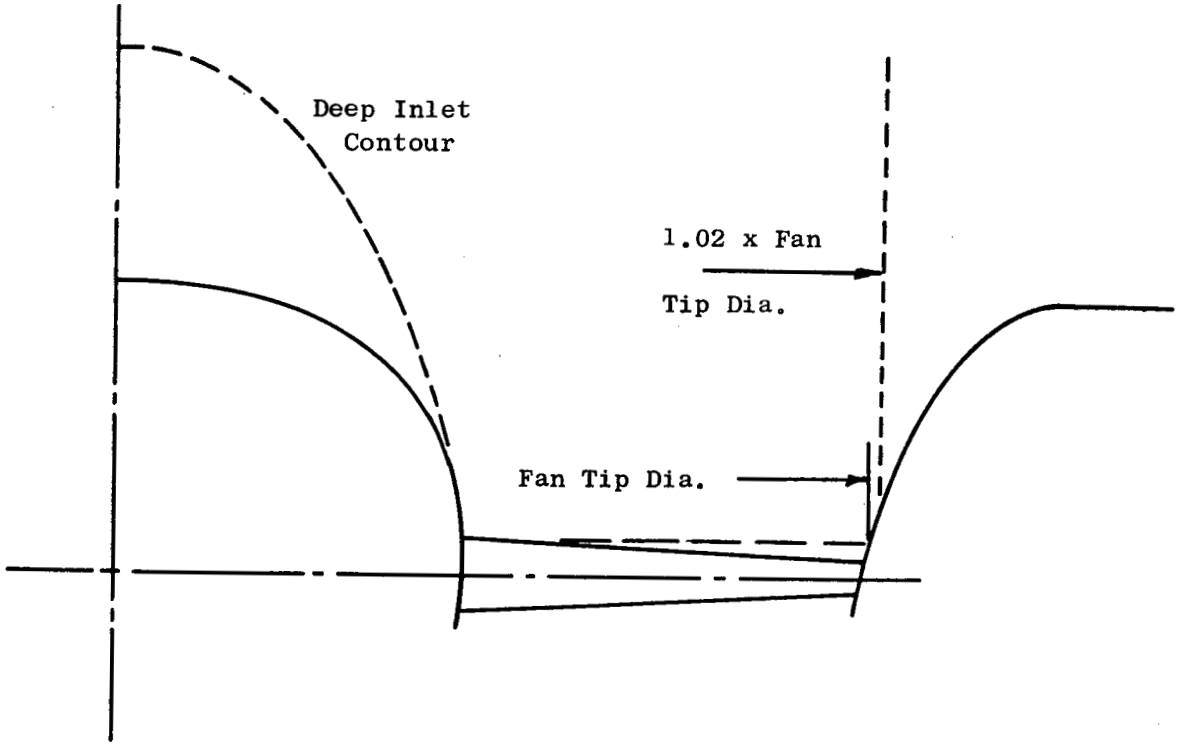

Figure 33. Typical Cruise Inlet Contour Limitation for LF4XX Design Lift Unit

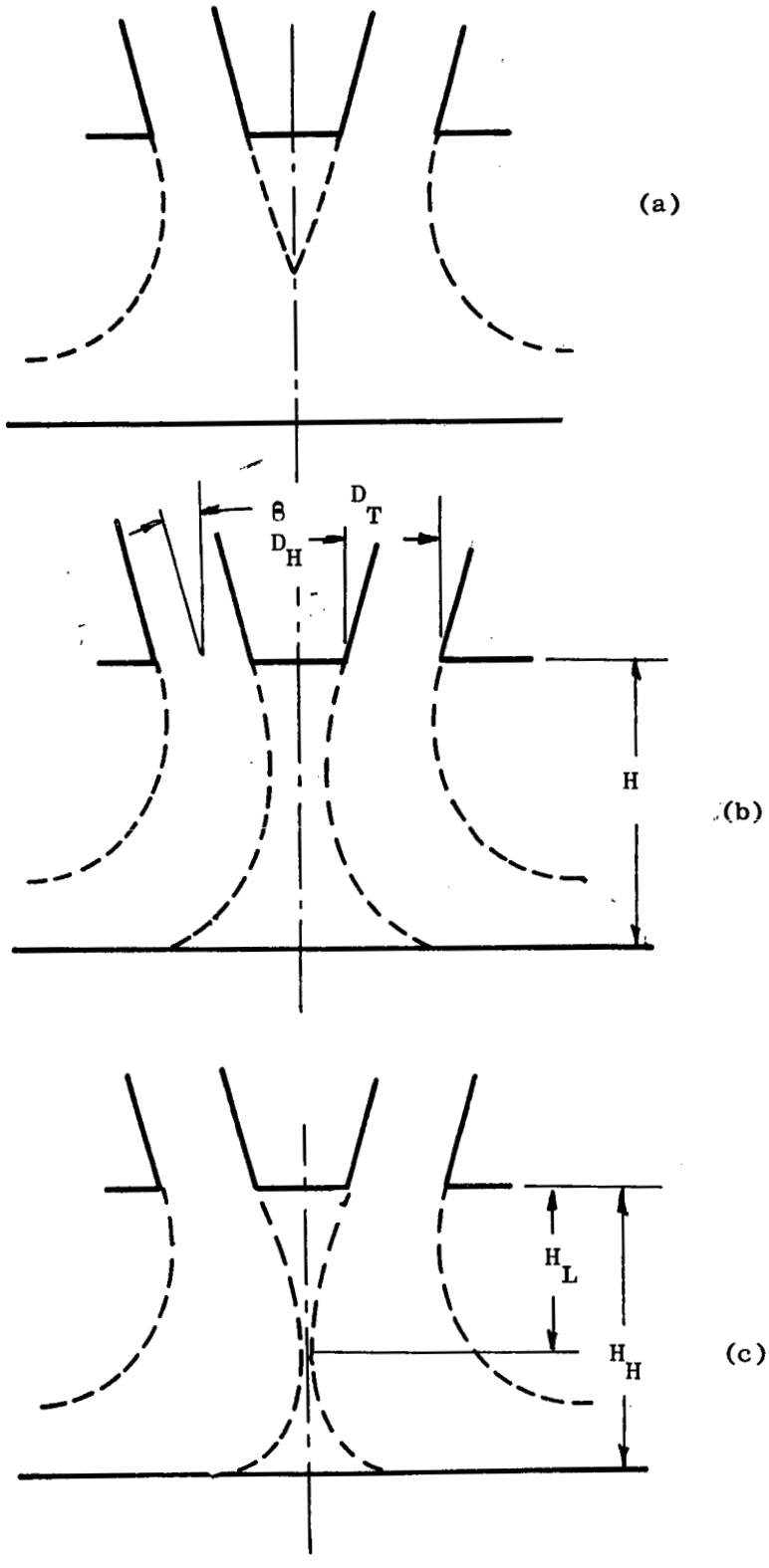

Figure 34. Annular Jet Flow Patterns in Presence of Ground Plane

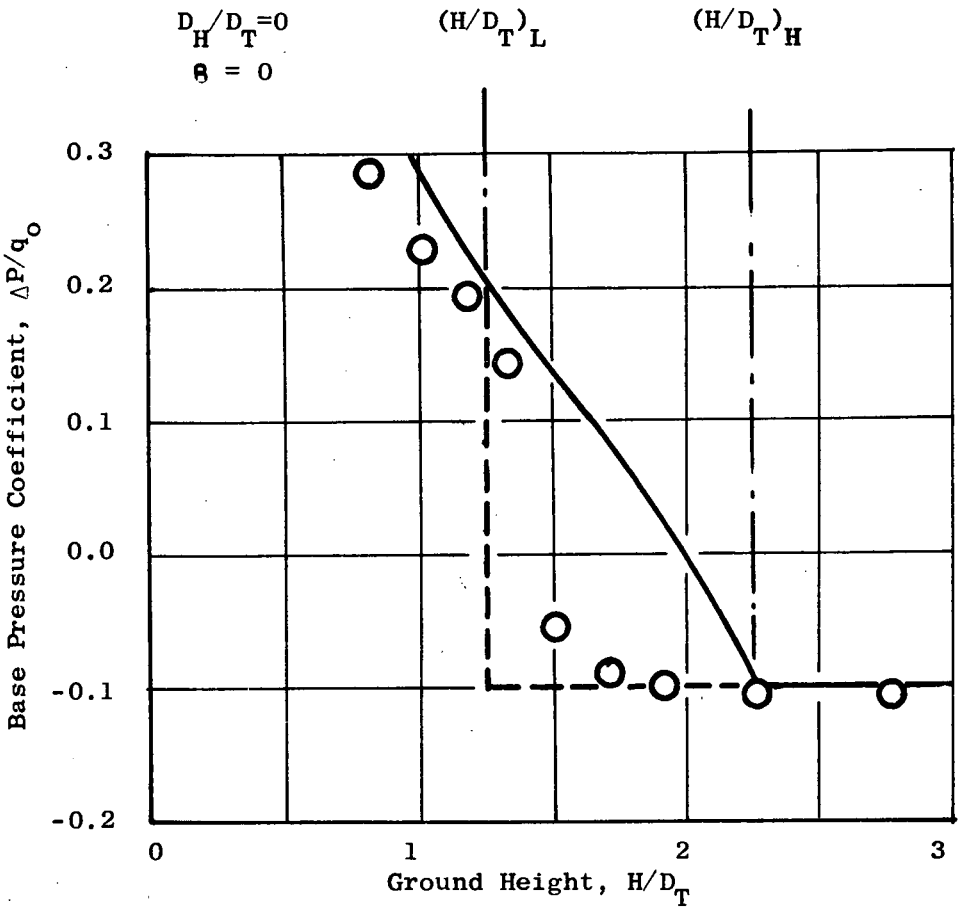

Figure 35. Comparison of Theory and Experiment for 26" Low Speed Scale Model Fan

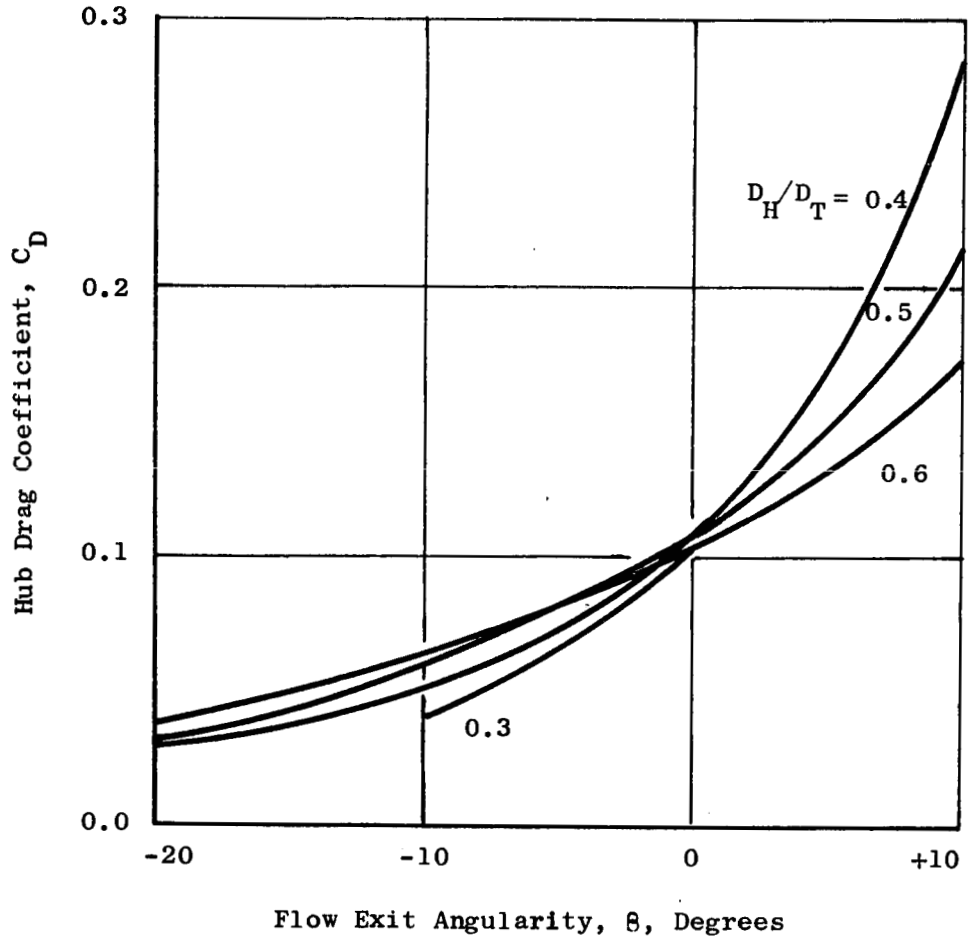

Figure 36. Hub Drag Coefficient, Out of Ground Effect

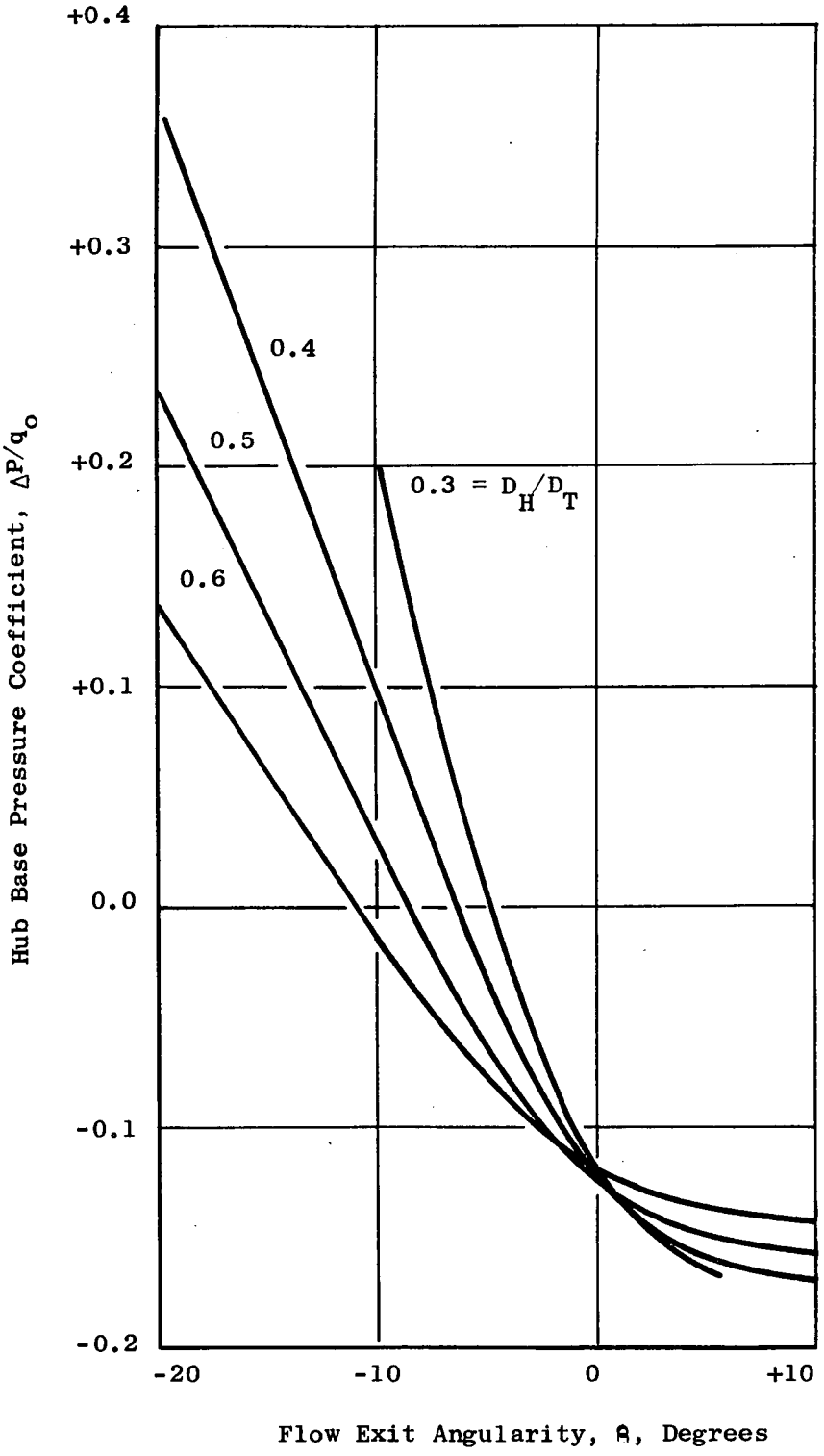

Figure 37. Hub Base Pressure Coefficient, Out of Ground Effect

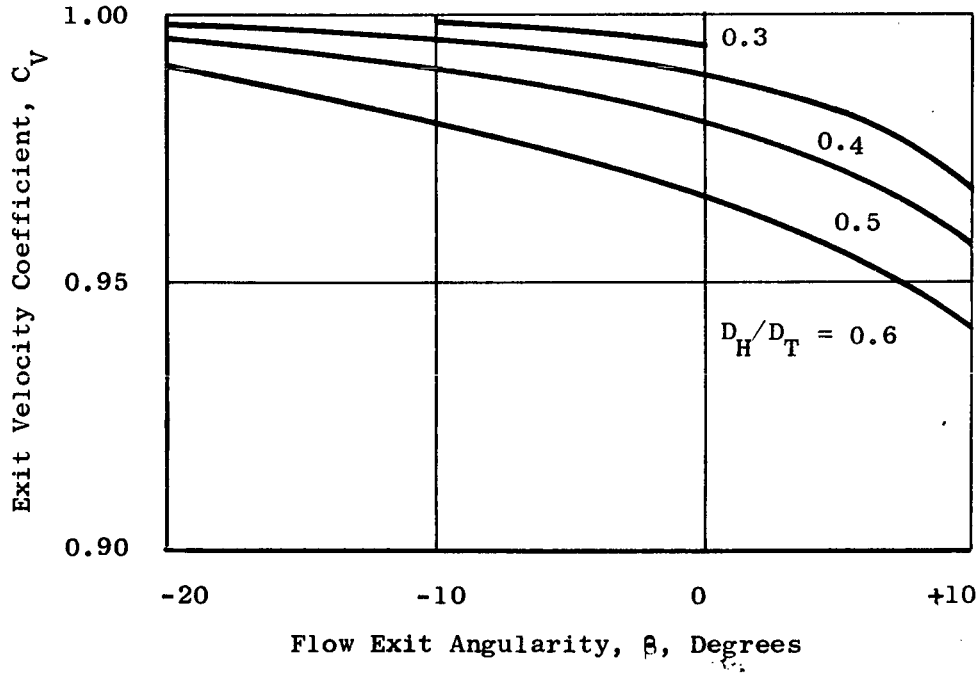

Figure 38. Exit Velocity Coefficient, Out of Ground Effect

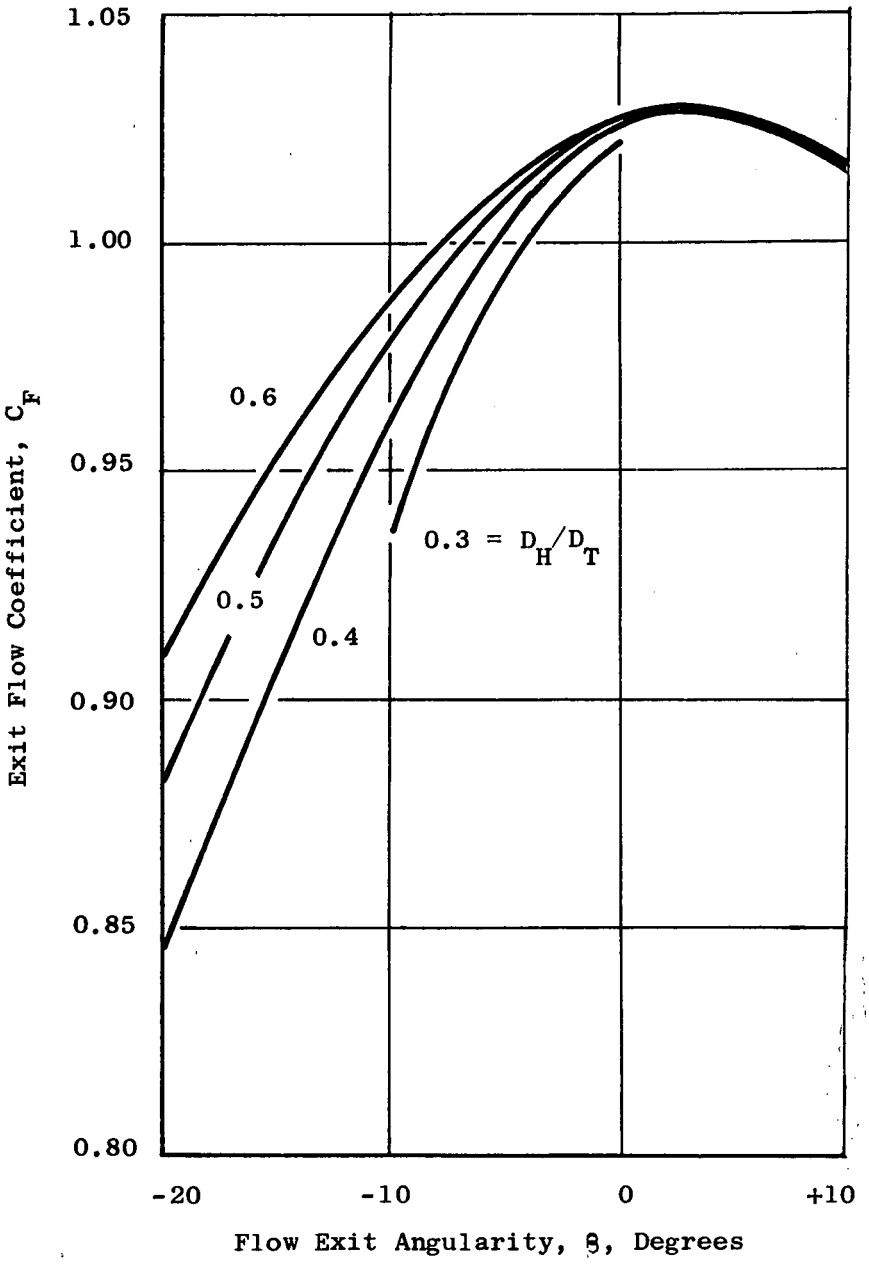

Figure 39. Exit Flow Coefficient, Out of Ground Effect

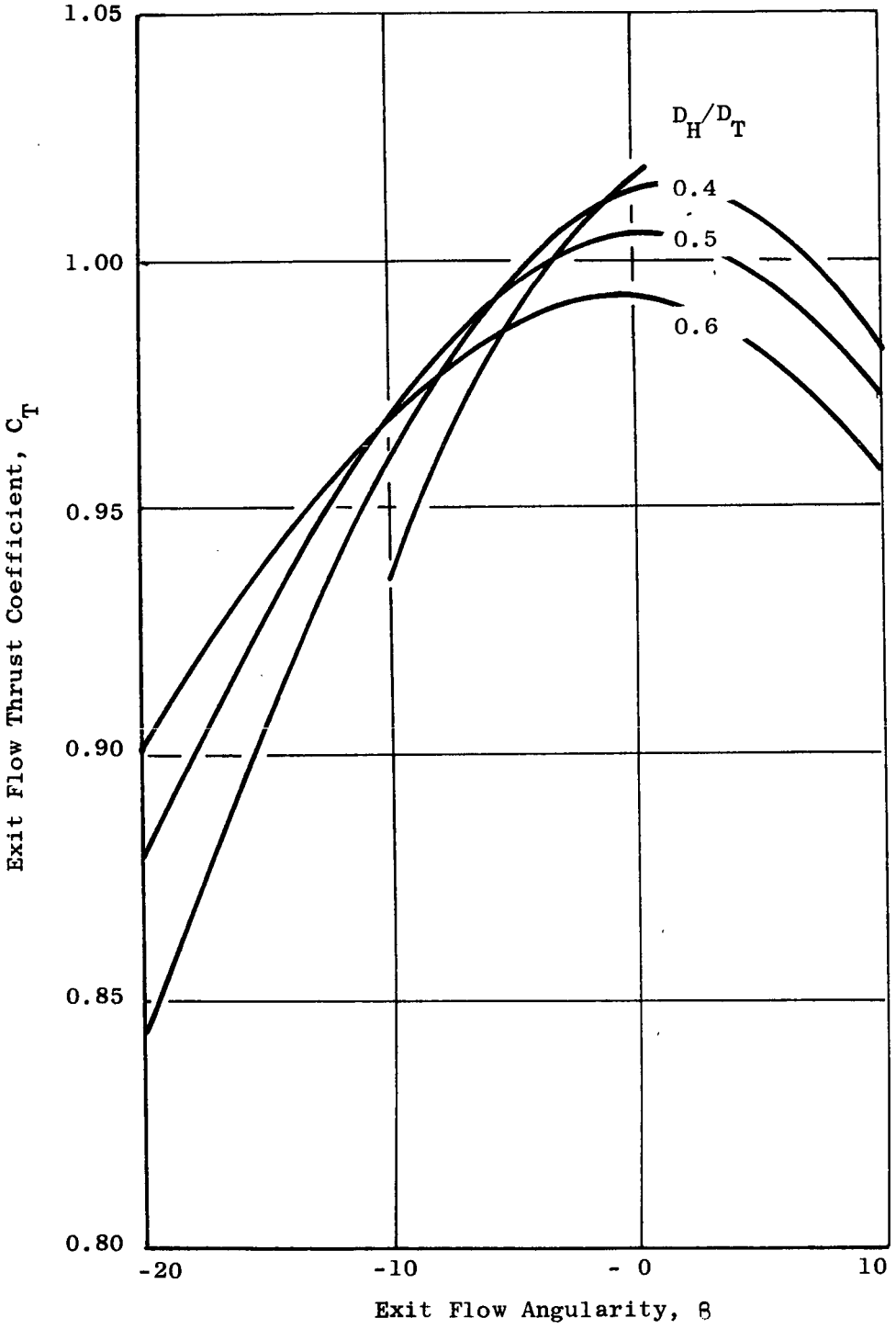

Figure 40. Exit Thrust Coefficient, Out of Ground Effect

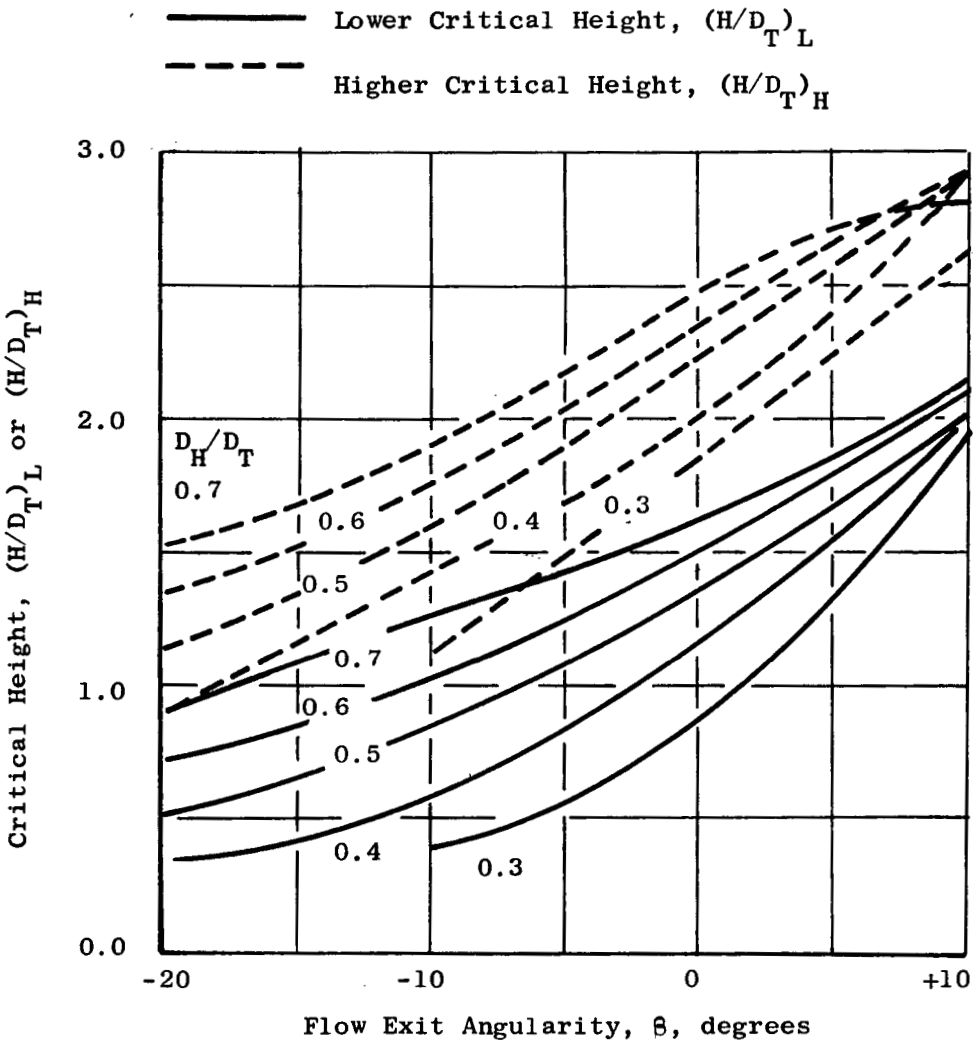

Figure 41. Critical Height Parameter, In Ground Effect

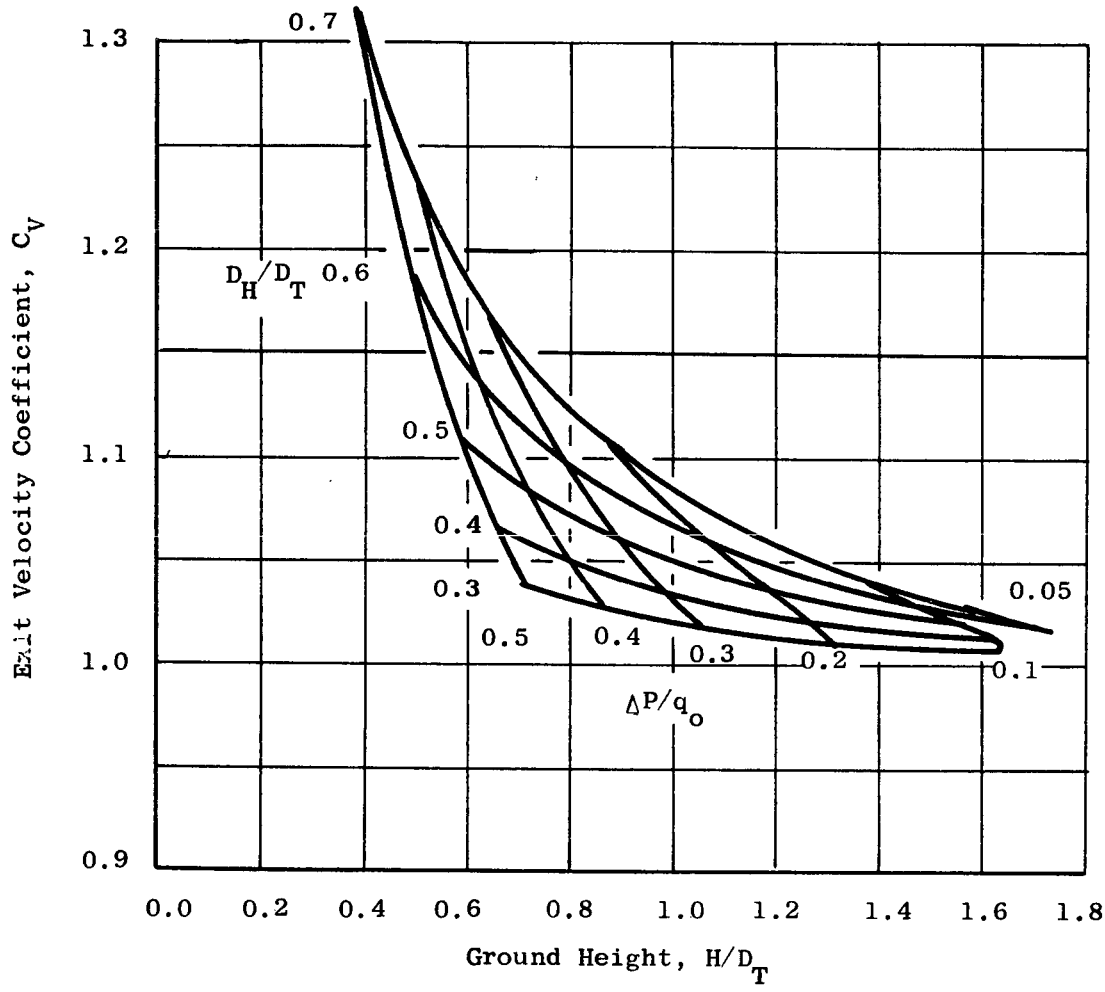

Figure 42. Exit Velocity Coefficient at Flow Exit Angularity of 0 degrees, In Ground Effect

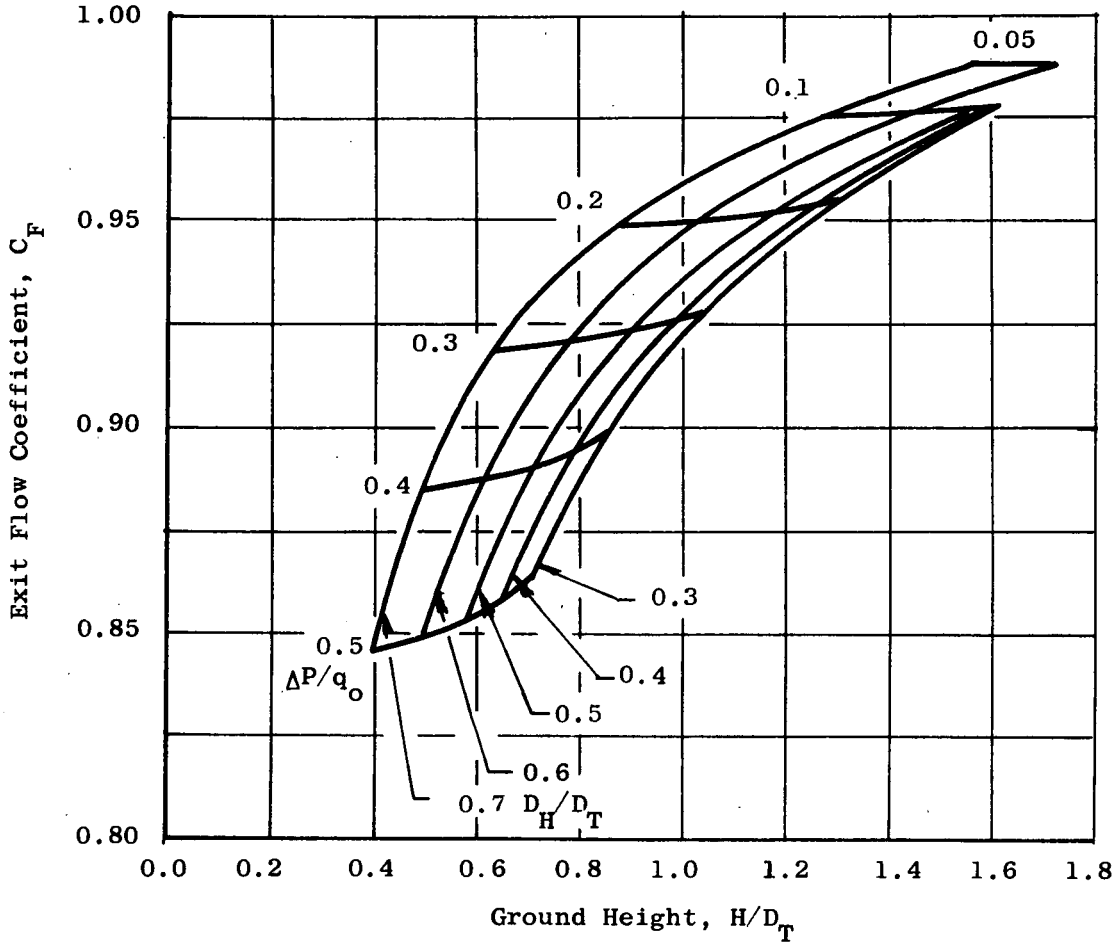

Figure 43. Exit Flow Coefficients at Flow Exit Angularity of 0 degrees, In Ground Effect

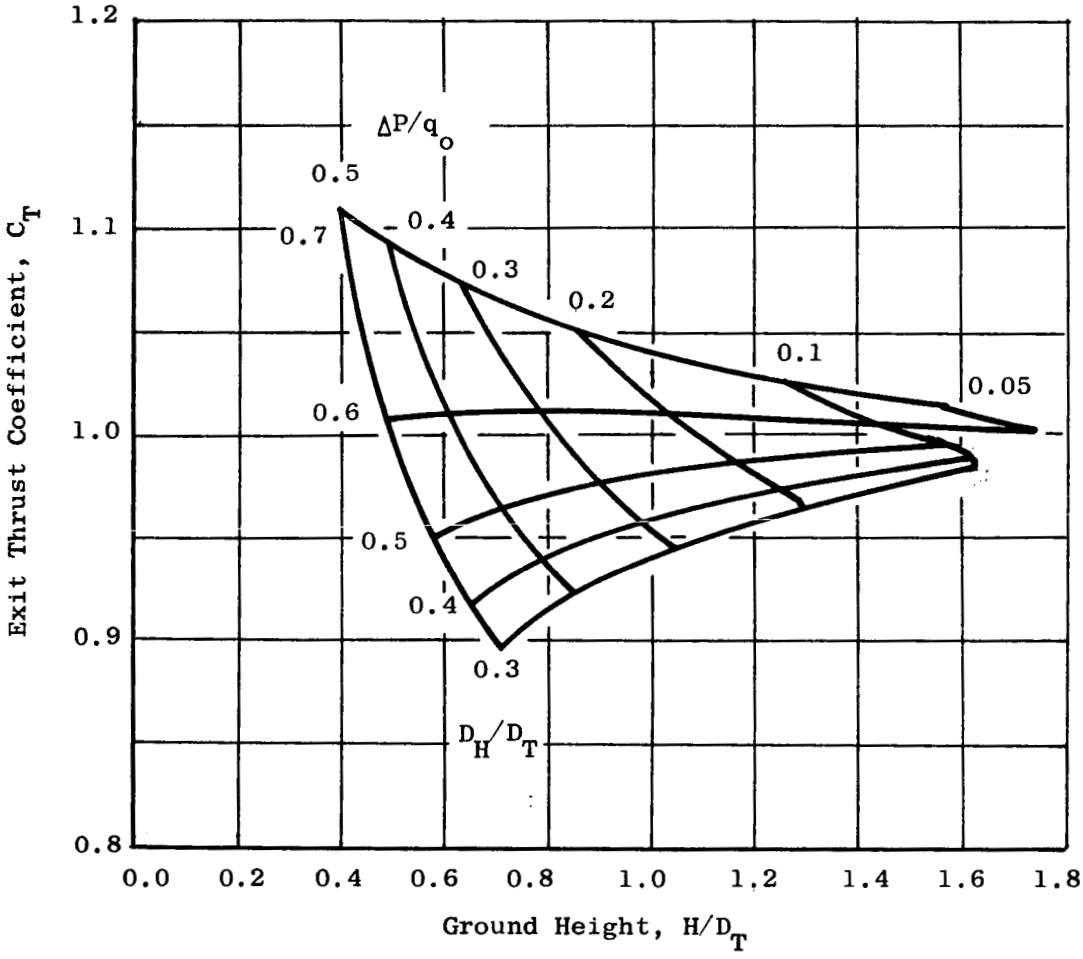

Figure 44. Exit Thrust Coefficient at Flow Exit Angularity of 0 degrees, In Ground Effect

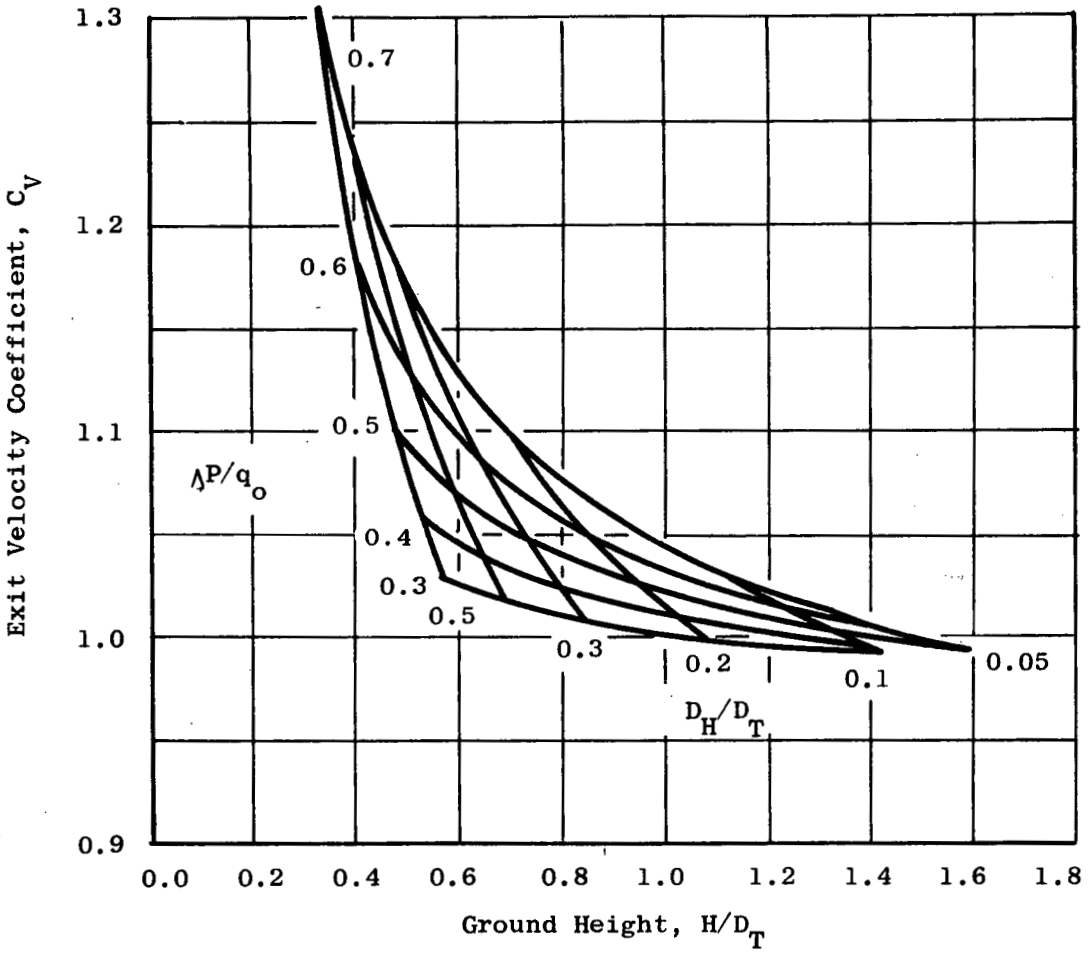

Figure 45. Exit Velocity Coefficient at Exit Flow Angularity of 10 degrees, In Ground Effect

C2

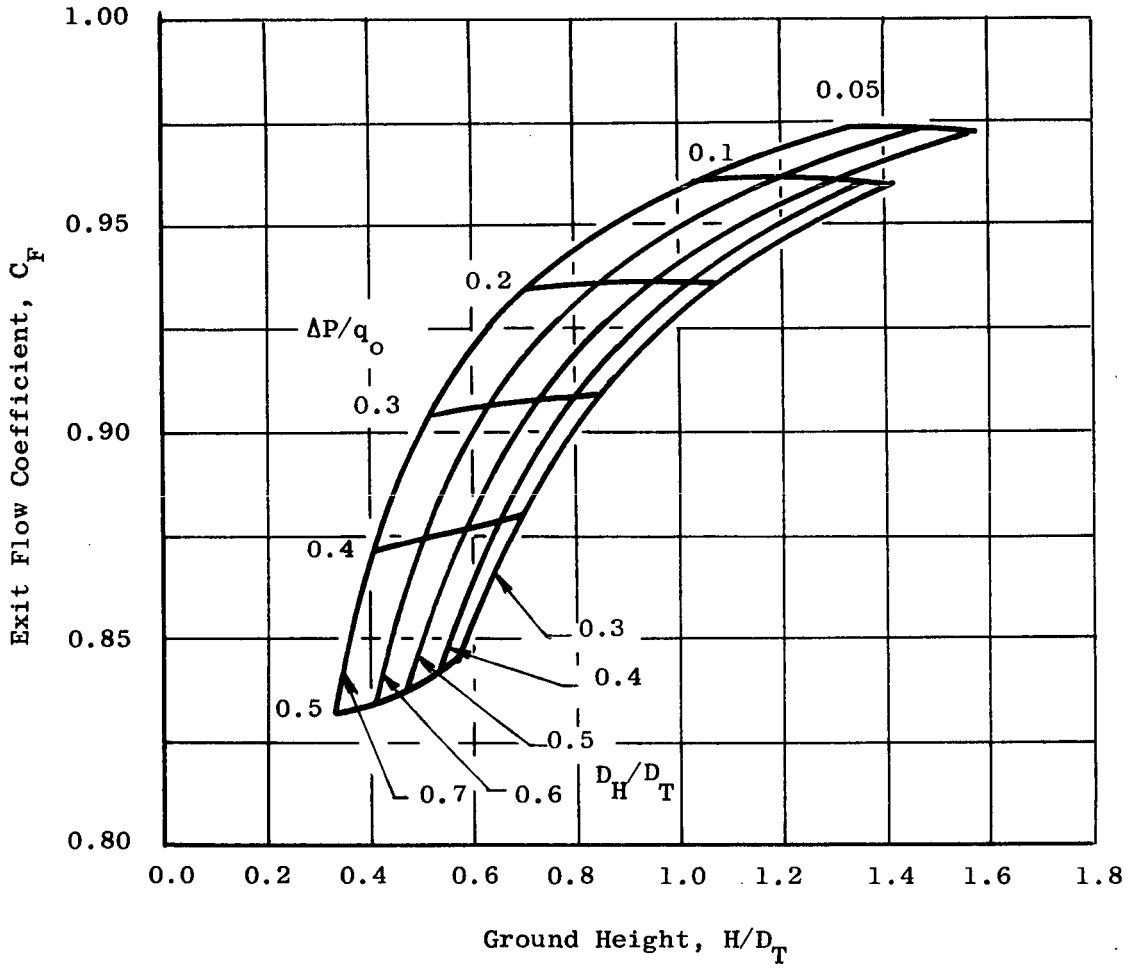

Figure 46. Exit Flow Coefficient at Exit Flow Angularity of 10 degrees, In Ground Effect

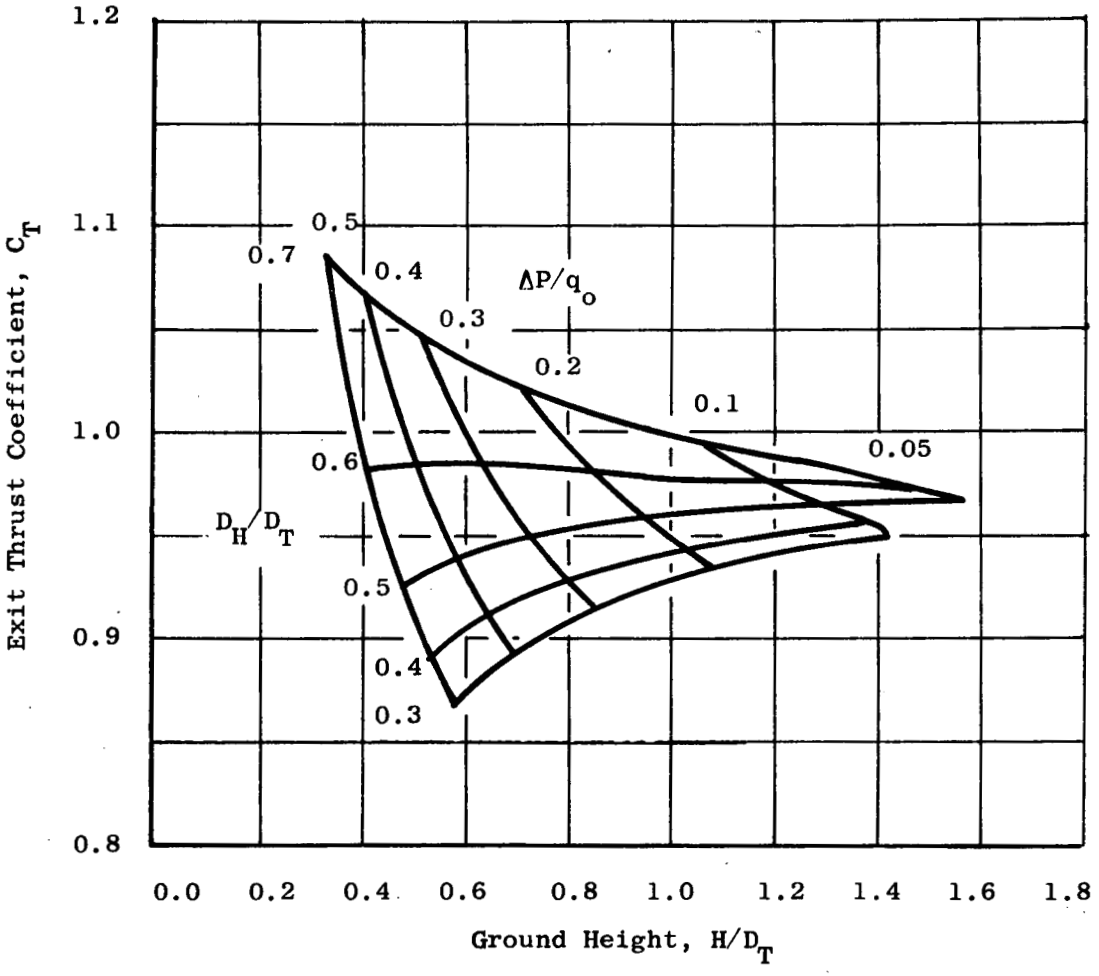

Figure 47. Exit Thrust Coefficient at Exit Flow Angularity of 10 degrees, In Ground Effect

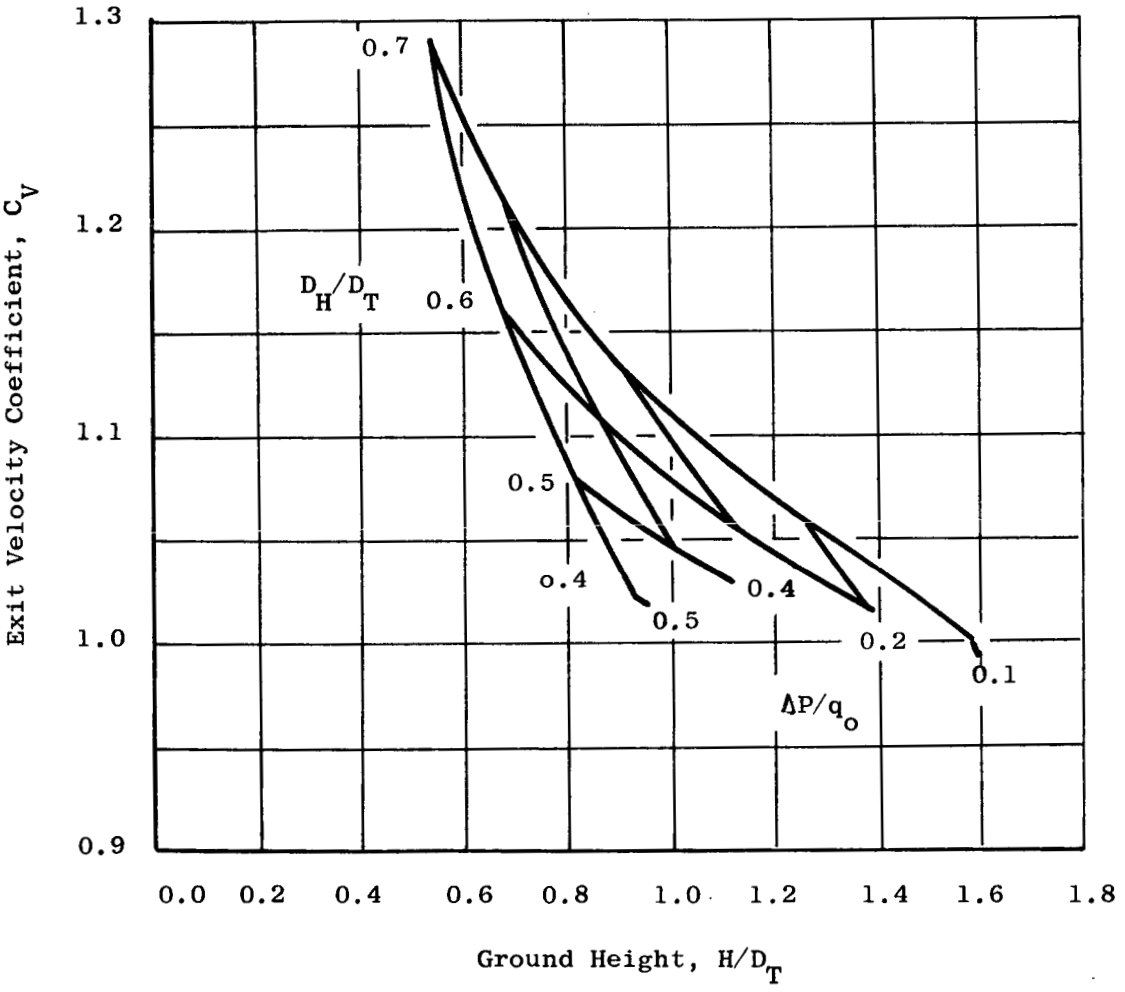

Figure 48. Exit Velocity Coefficient at Exit Flow Angularity of -20 degrees, In Ground Effect

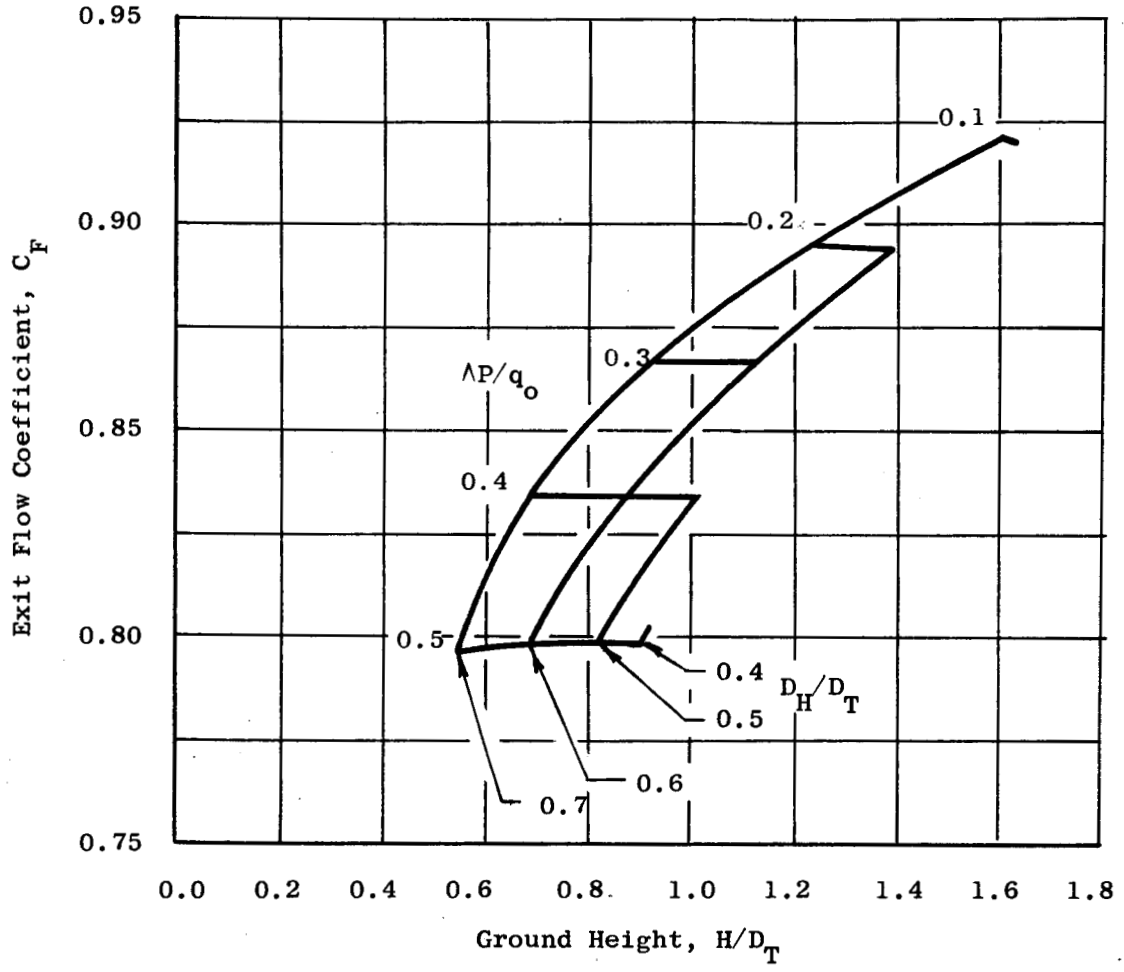

Figure 49. Exit Flow Coefficient at Exit Flow Angularity of -20 degrees, In Ground Effect

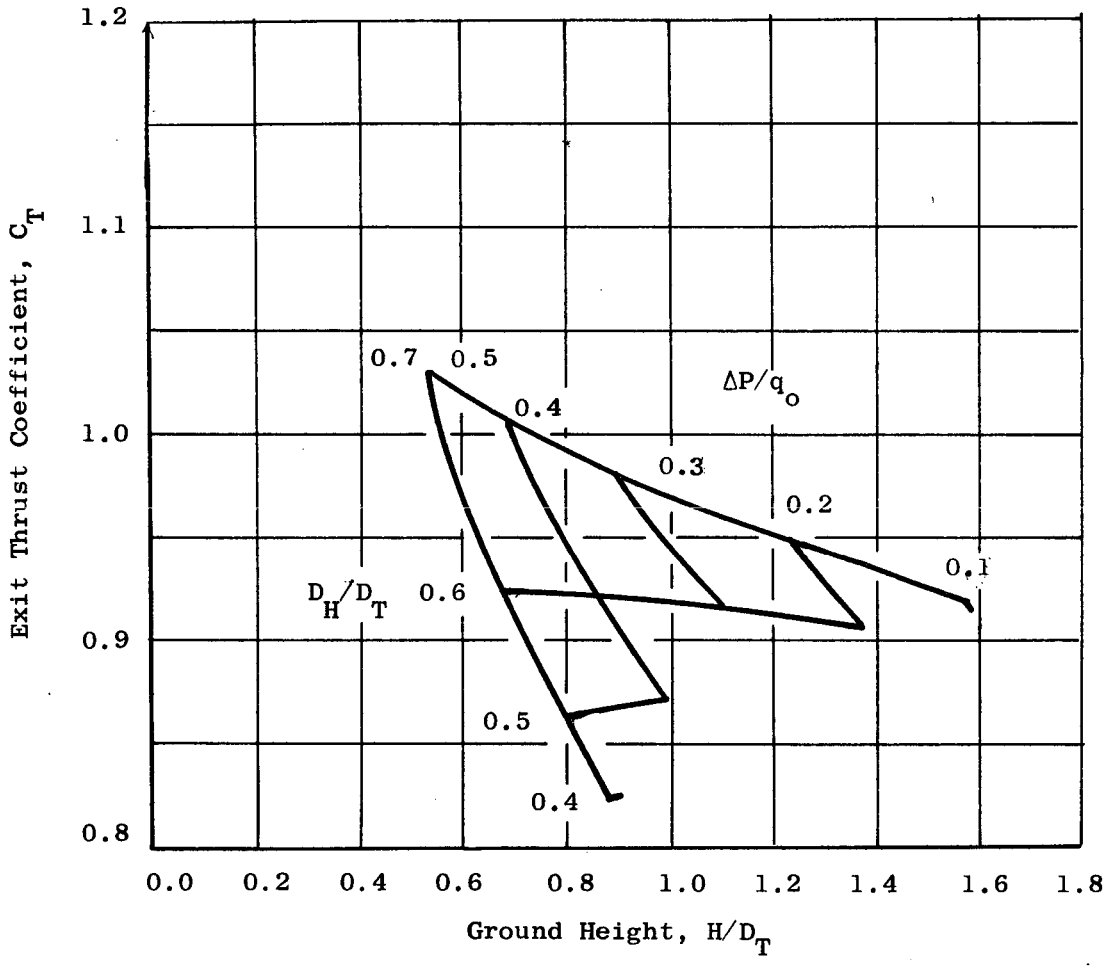

Figure 50. Exit Thrust Coefficient at Exit Flow Angularity of -20 degrees, In Ground Effect

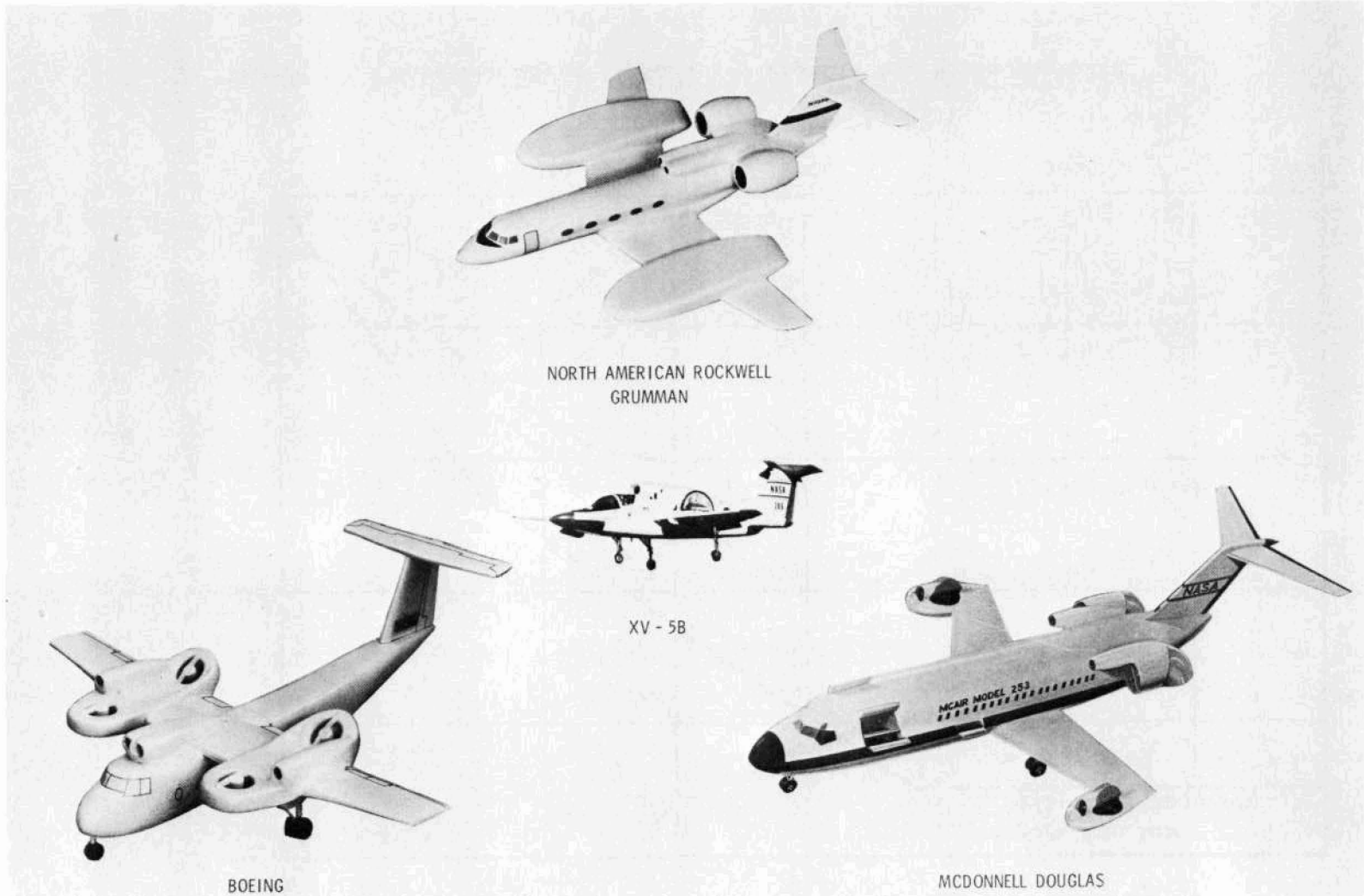

Figure 51. Photograph of Research Aircraft Models

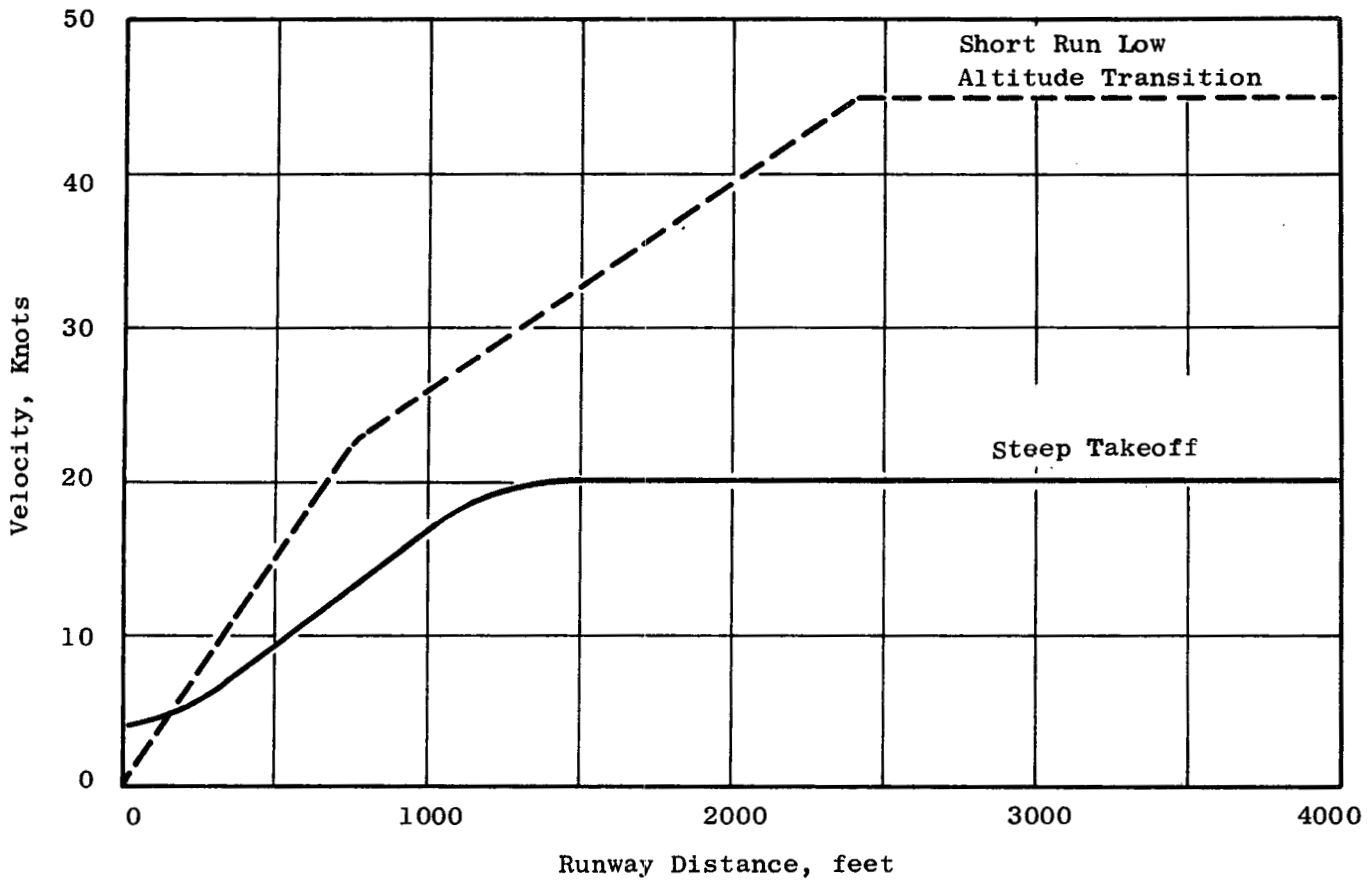

Figure 52. Research Aircraft Velocity Profile for Noise Contours

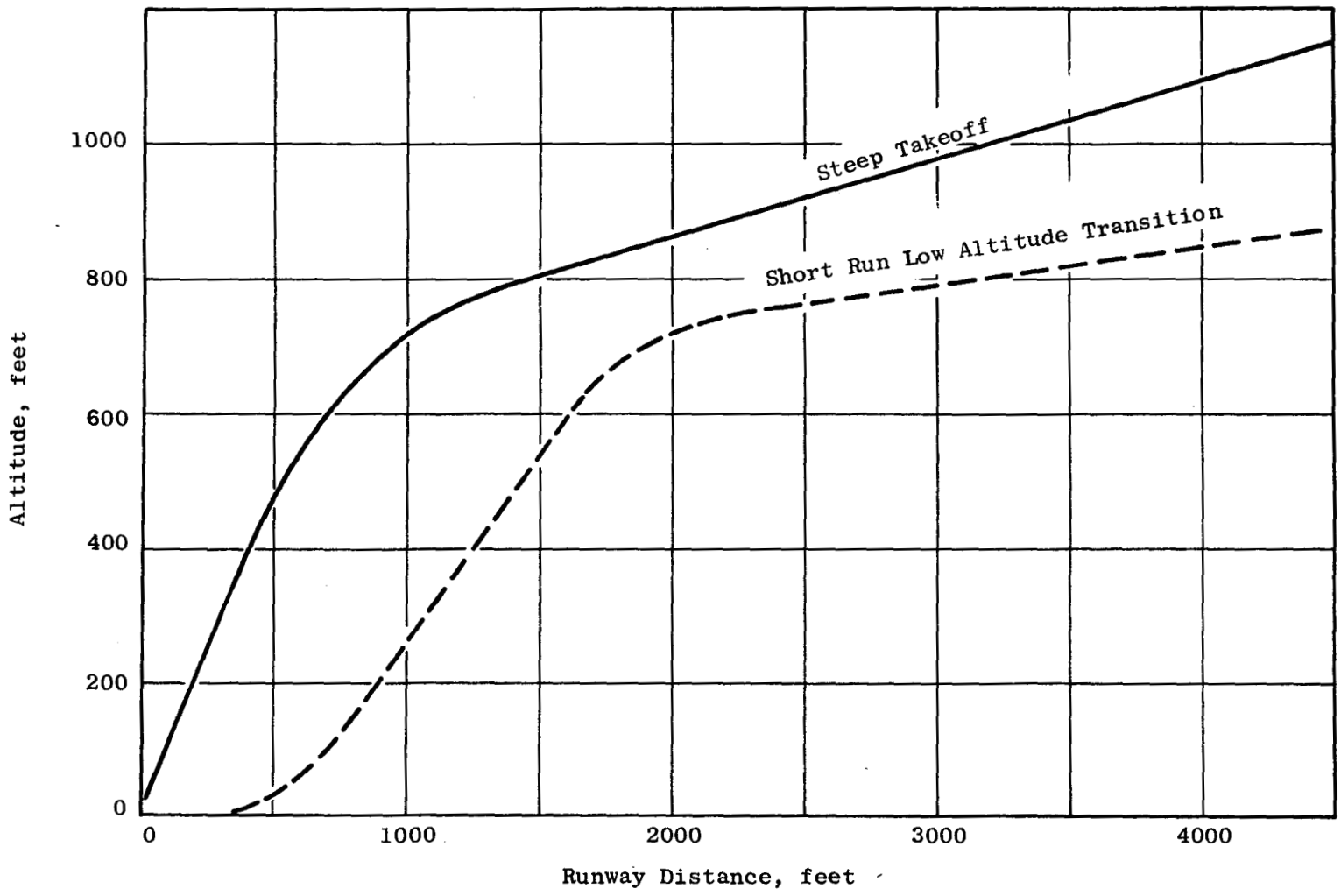

Figure 53. Research Aircraft Altitude Profile for Noise Contours

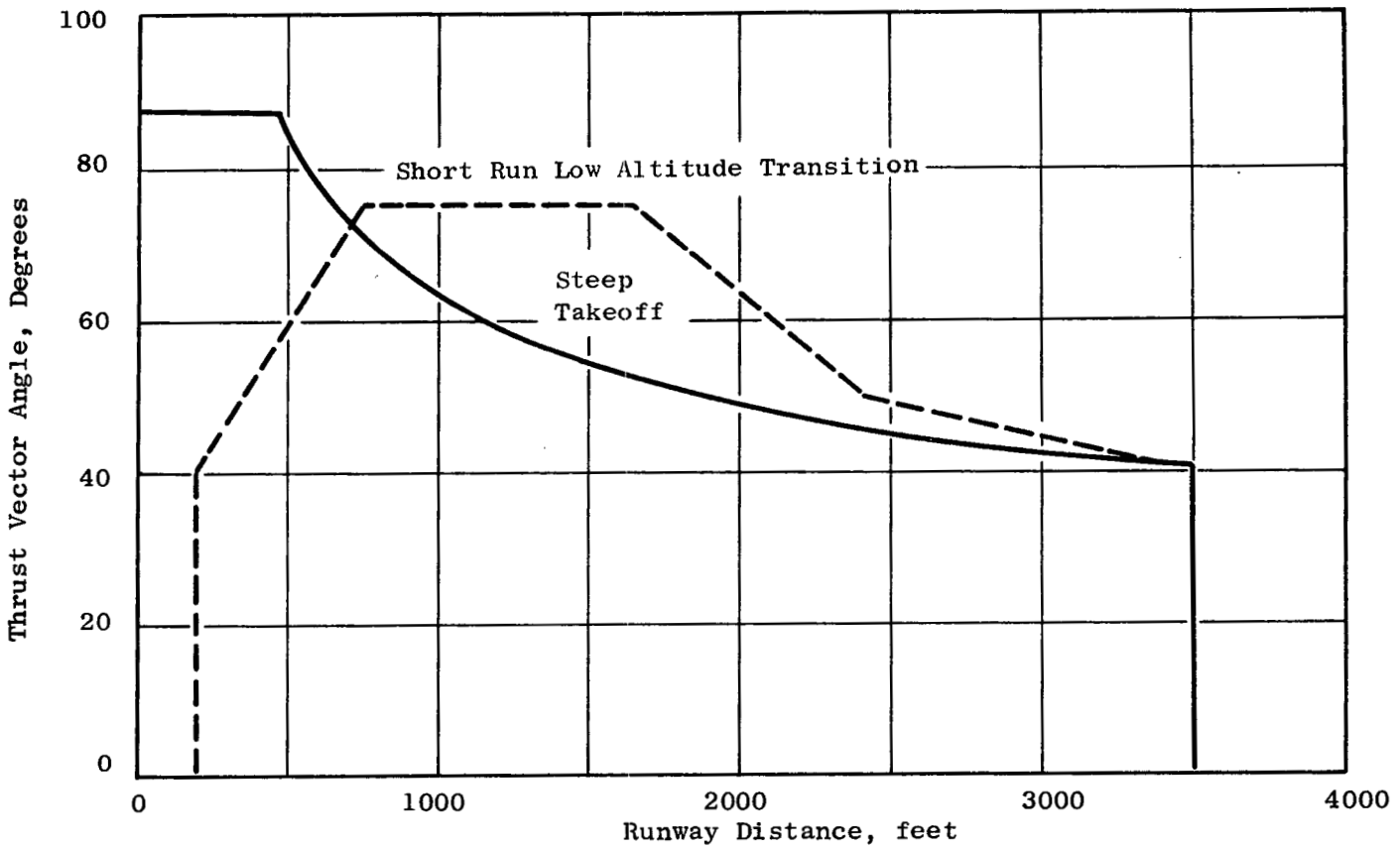

Figure 54. Research Aircraft Thrust Vector Angle Schedule for Noise Contours

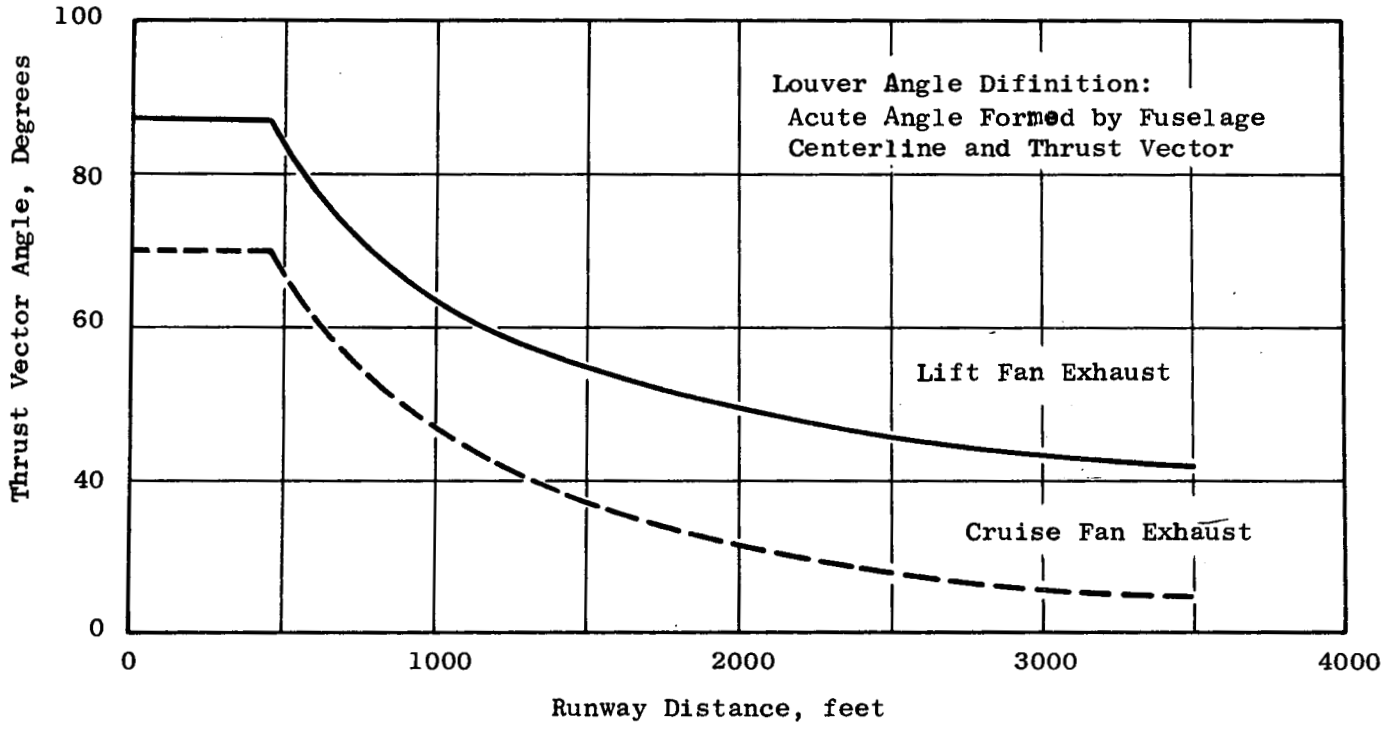

Figure 55. Boeing Research Aircraft Thrust Vector Schedule for Noise Contours

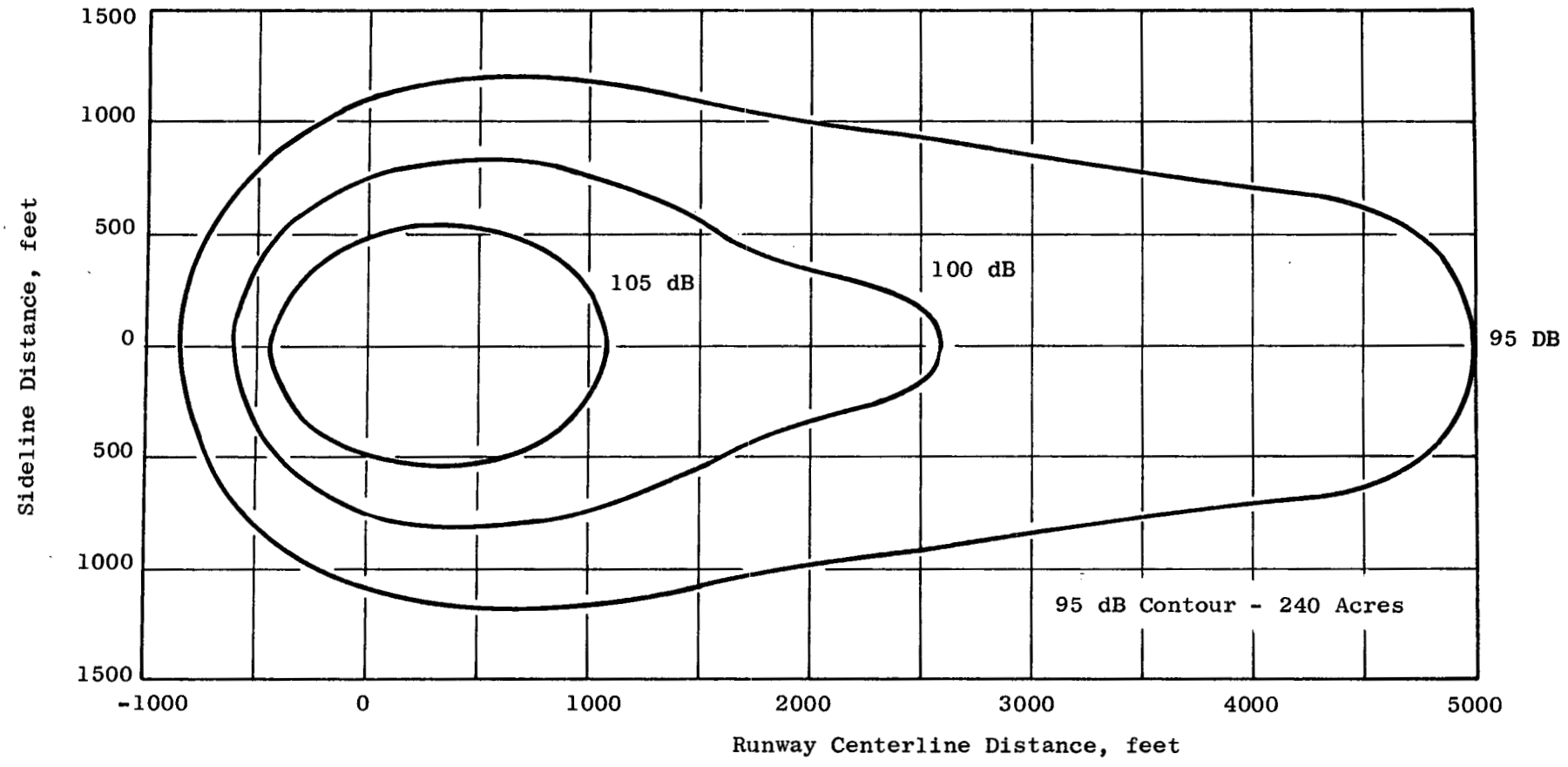

Figure 56. Noise Contour for McDonnell Research Aircraft, No Installation Suppression, Steep Takeoff Path

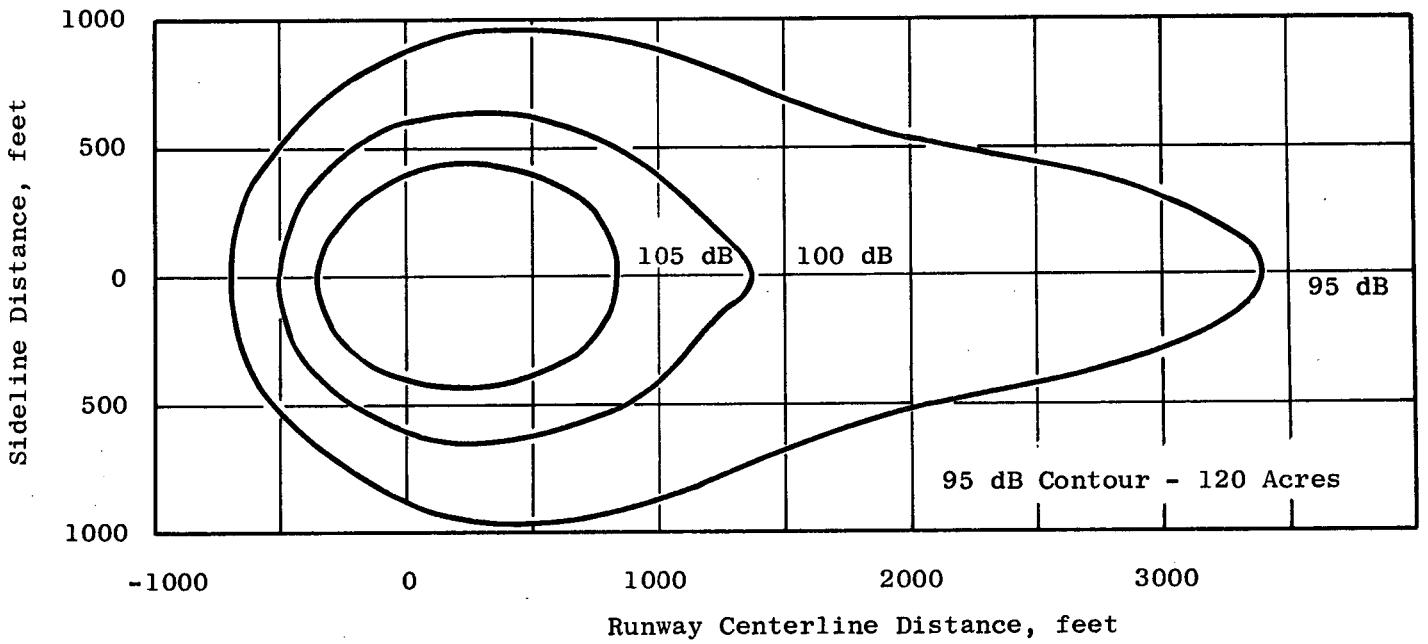

Figure 57. Noise Contour for McDonnell Research Aircraft with Suppression, Steep Takeoff Path

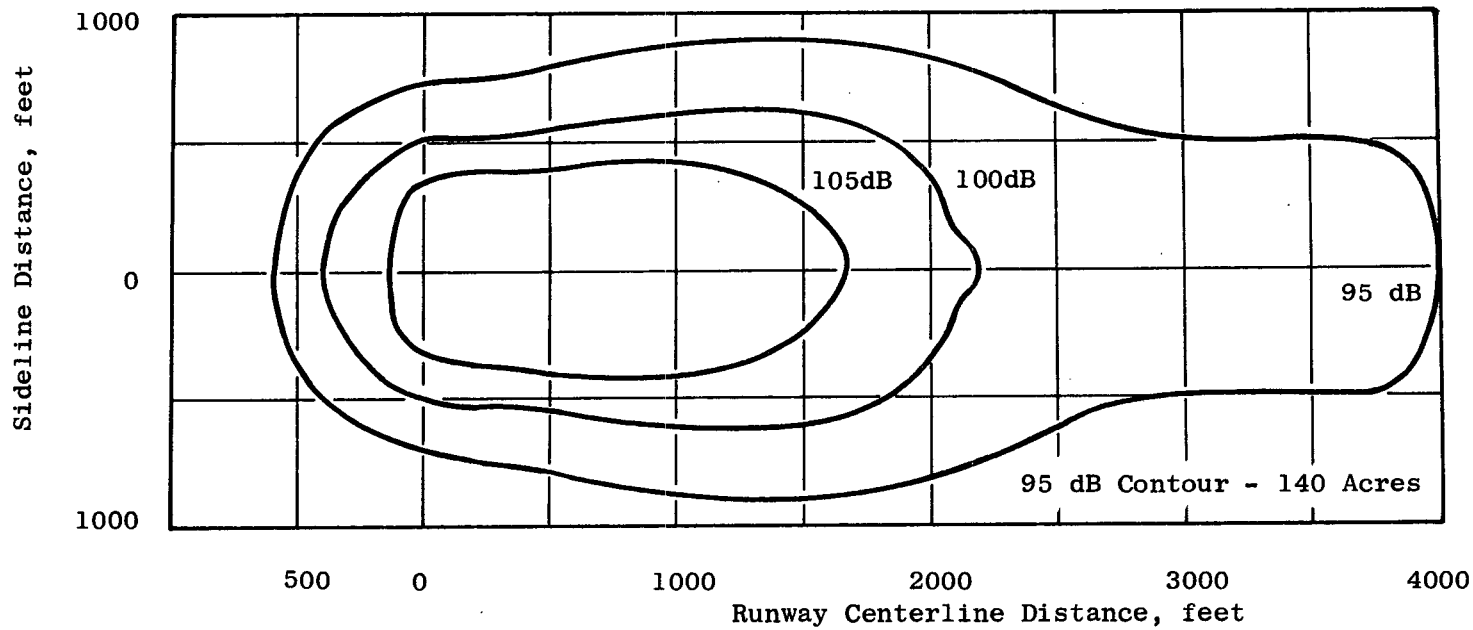

Figure 58. Noise Contour for McDonnell Research Aircraft with Suppression, Low Altitude Transition Path

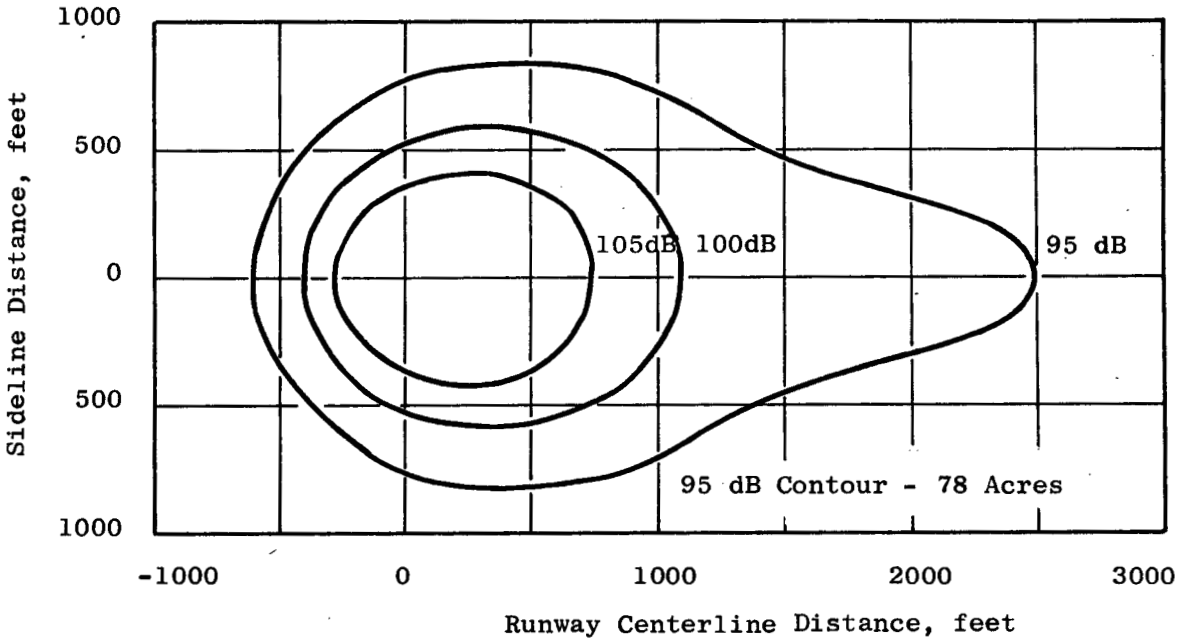

Figure 59. Noise Contour for North American Research Aircraft with Suppression, Steep Takeoff Path

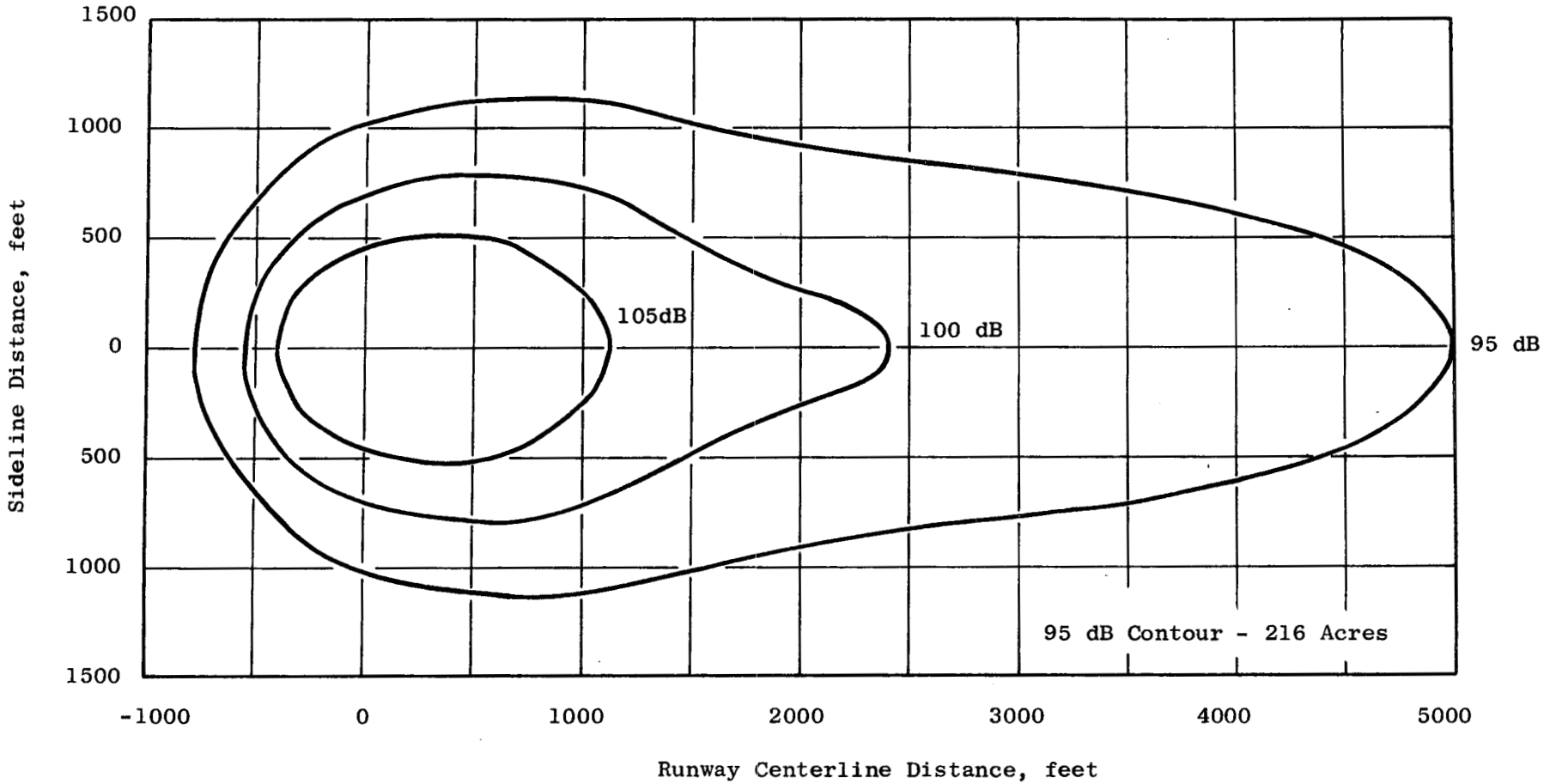

Figure 60. Noise Contour for North American Research Aircraft, No Installation Suppression, Steep Takeoff Path, Four fans at 12,216 pounds lift, Two fans at 5000 pounds lift

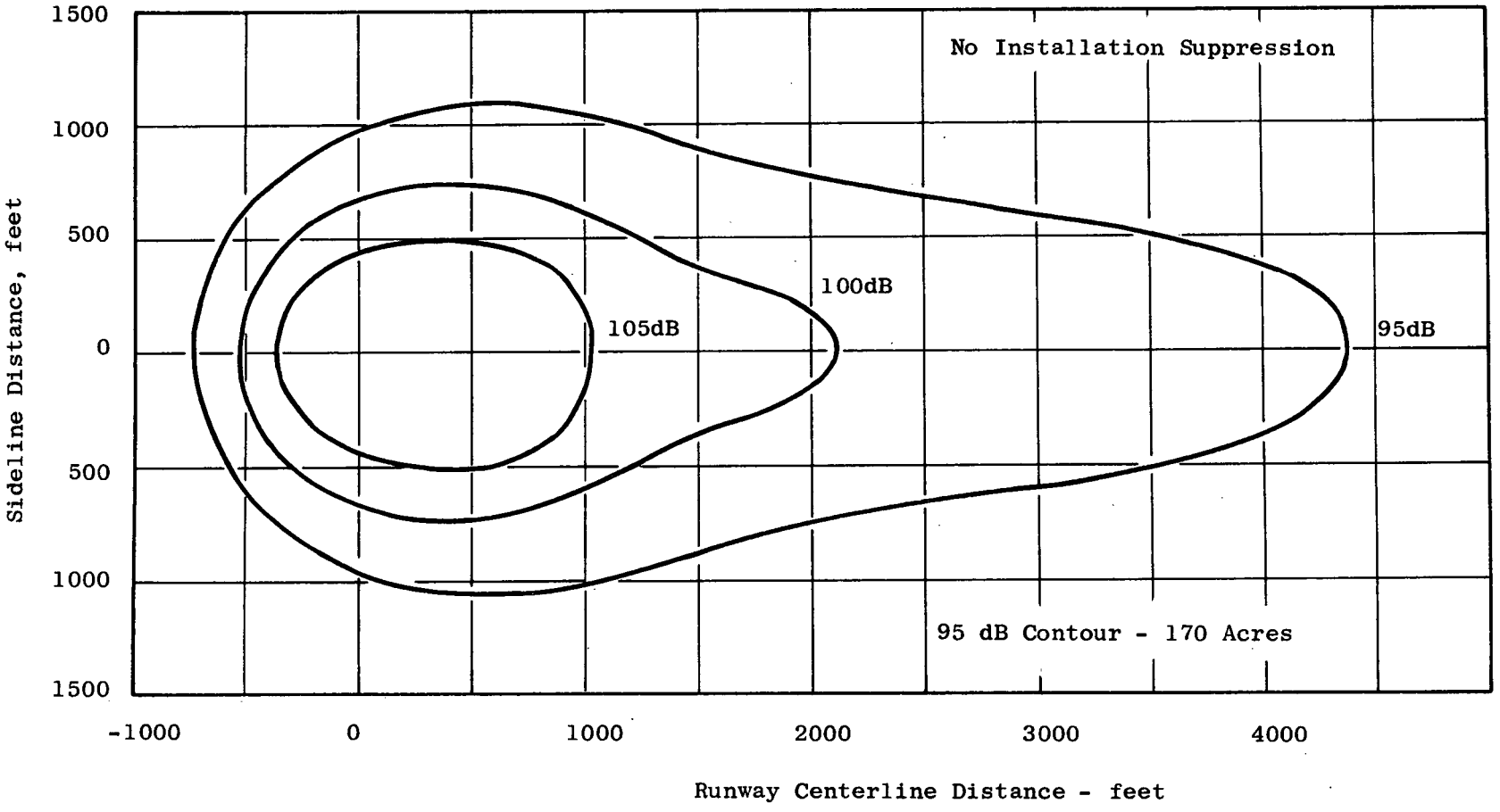

Figure 61. Noise Contour for North American Research Aircraft, No Installation Suppression, Steep Takeoff Path, All Fans at 10,500 pounds lift

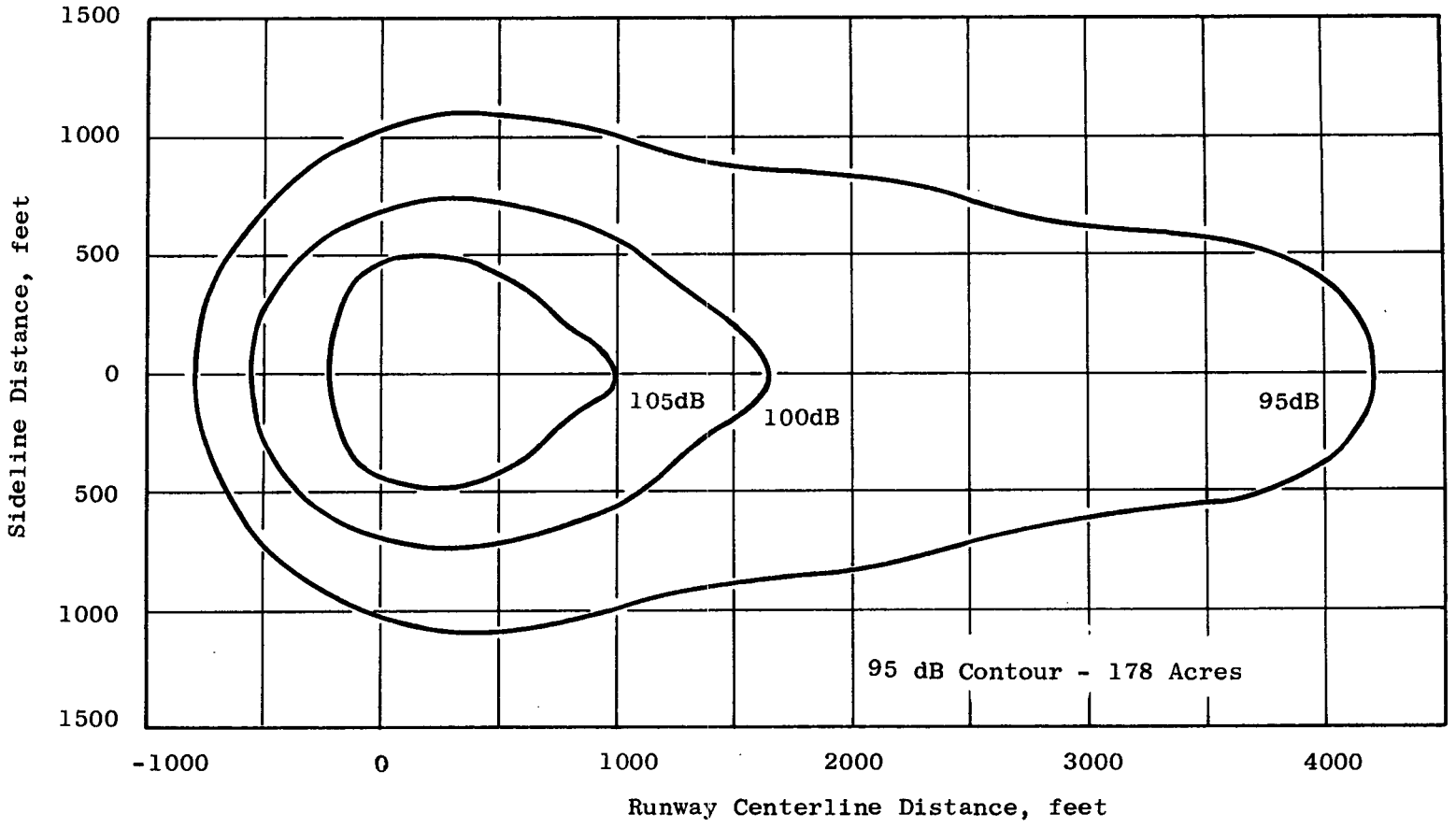

Figure 62. Noise Contour for Boeing Research Aircraft, No Installation Suppression, Steep Takeoff Path

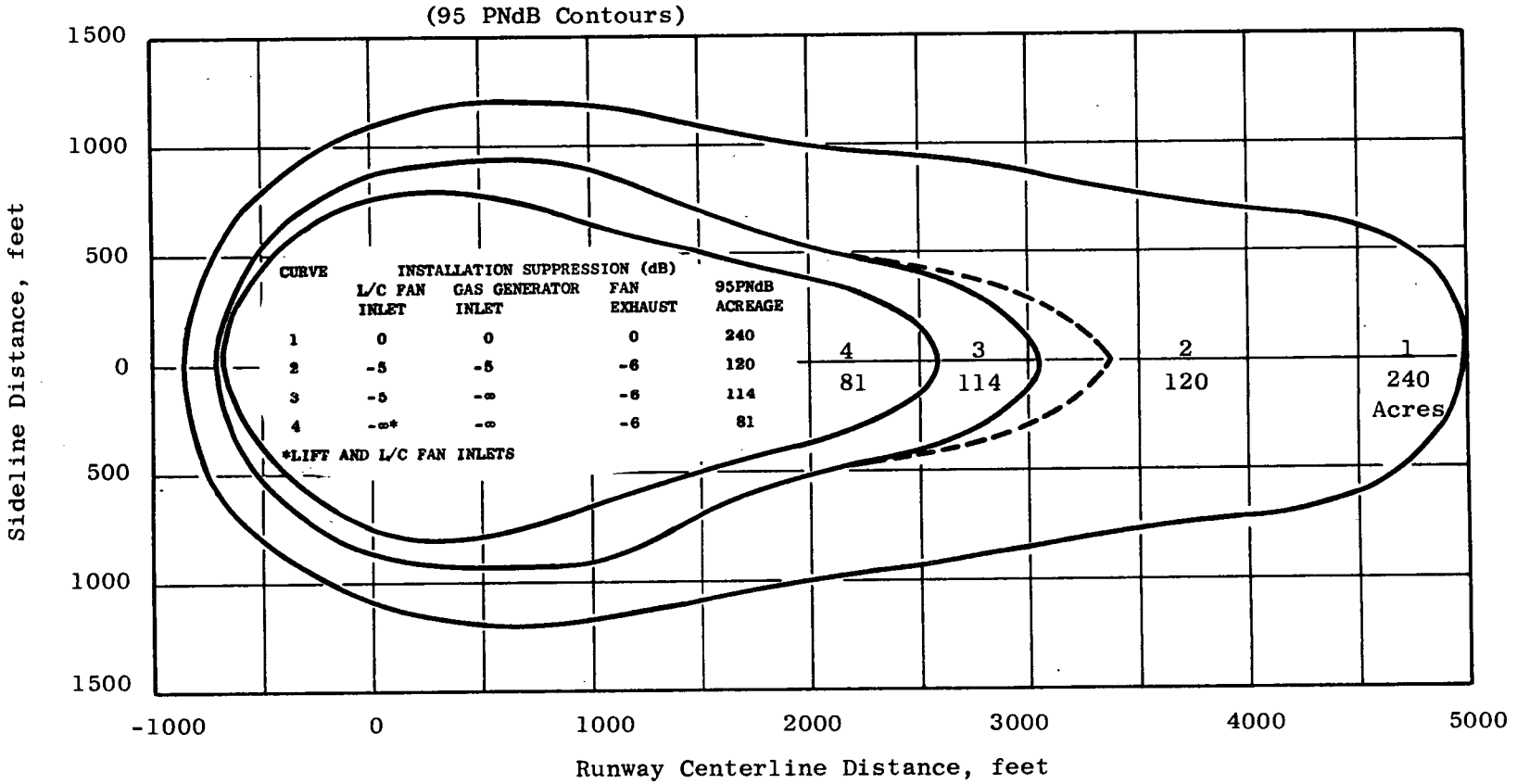

Figure 63. Contours for McDonnell Configuration showing Effects of Installation Suppression, Steep Takeoff Path

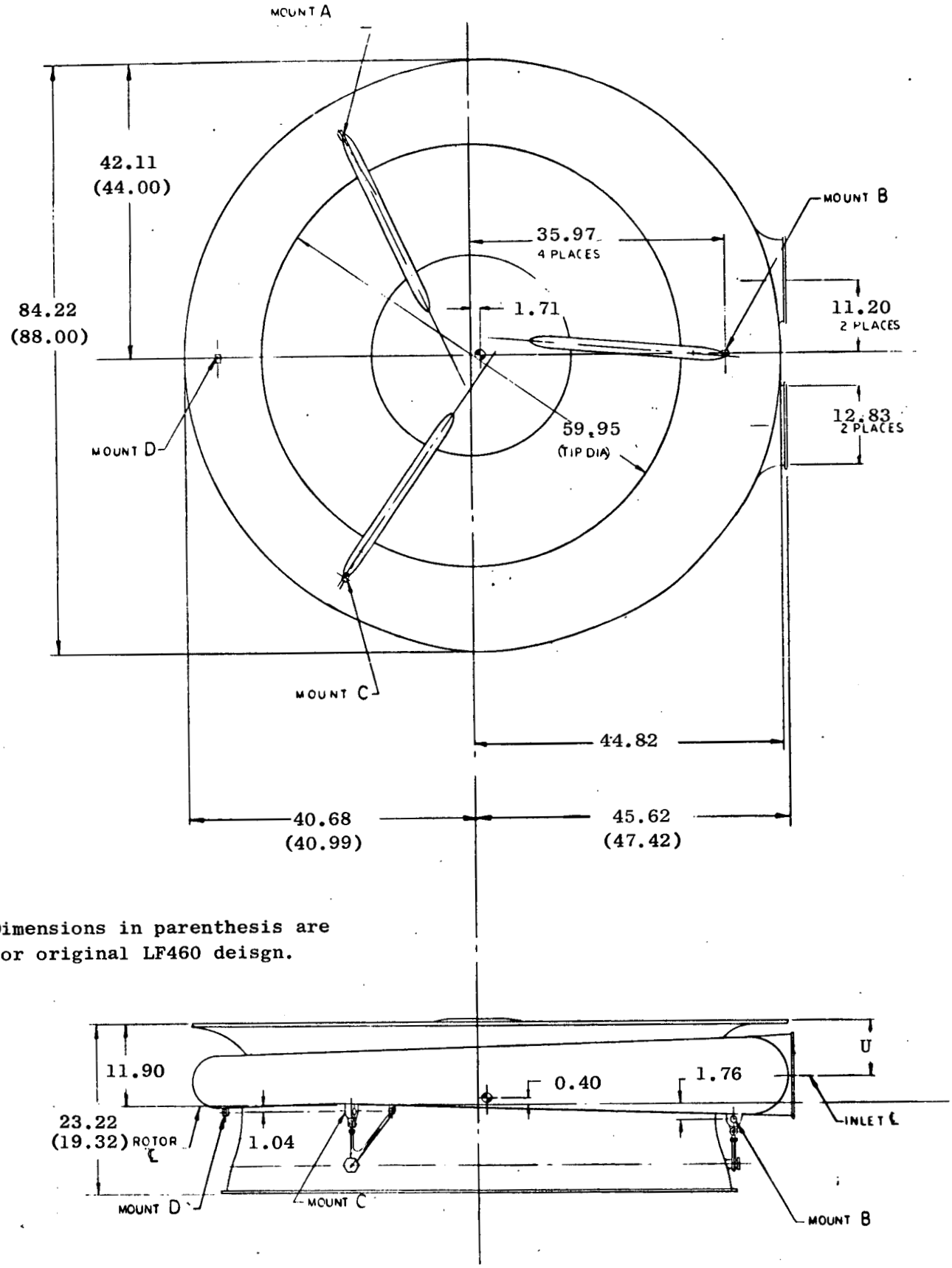

Figure 64. Installation Drawing of Modified LF460 Lift Fan

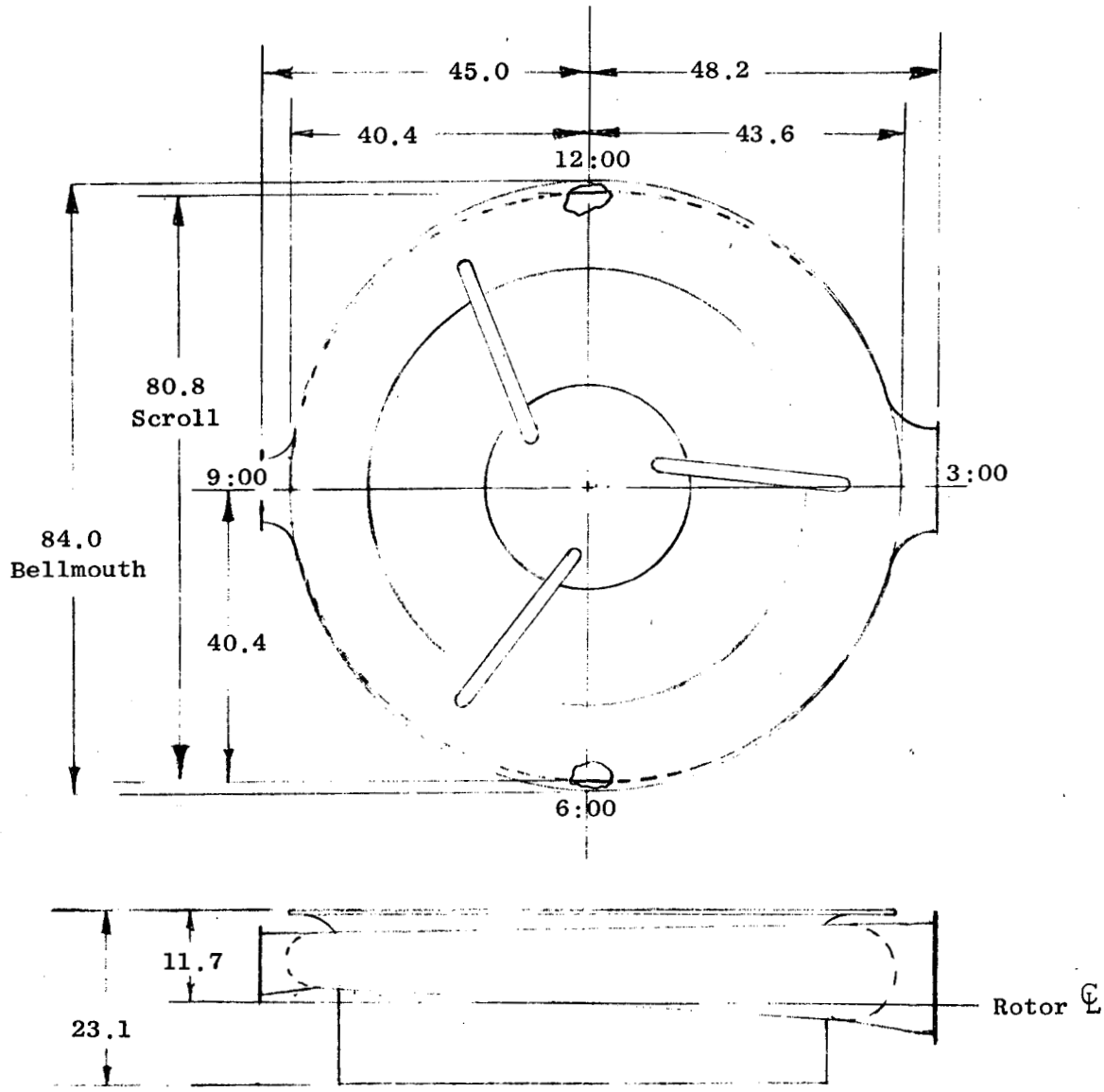

Figure 65. LF460 Single Bubble 75/25 Split - No Gooseneck

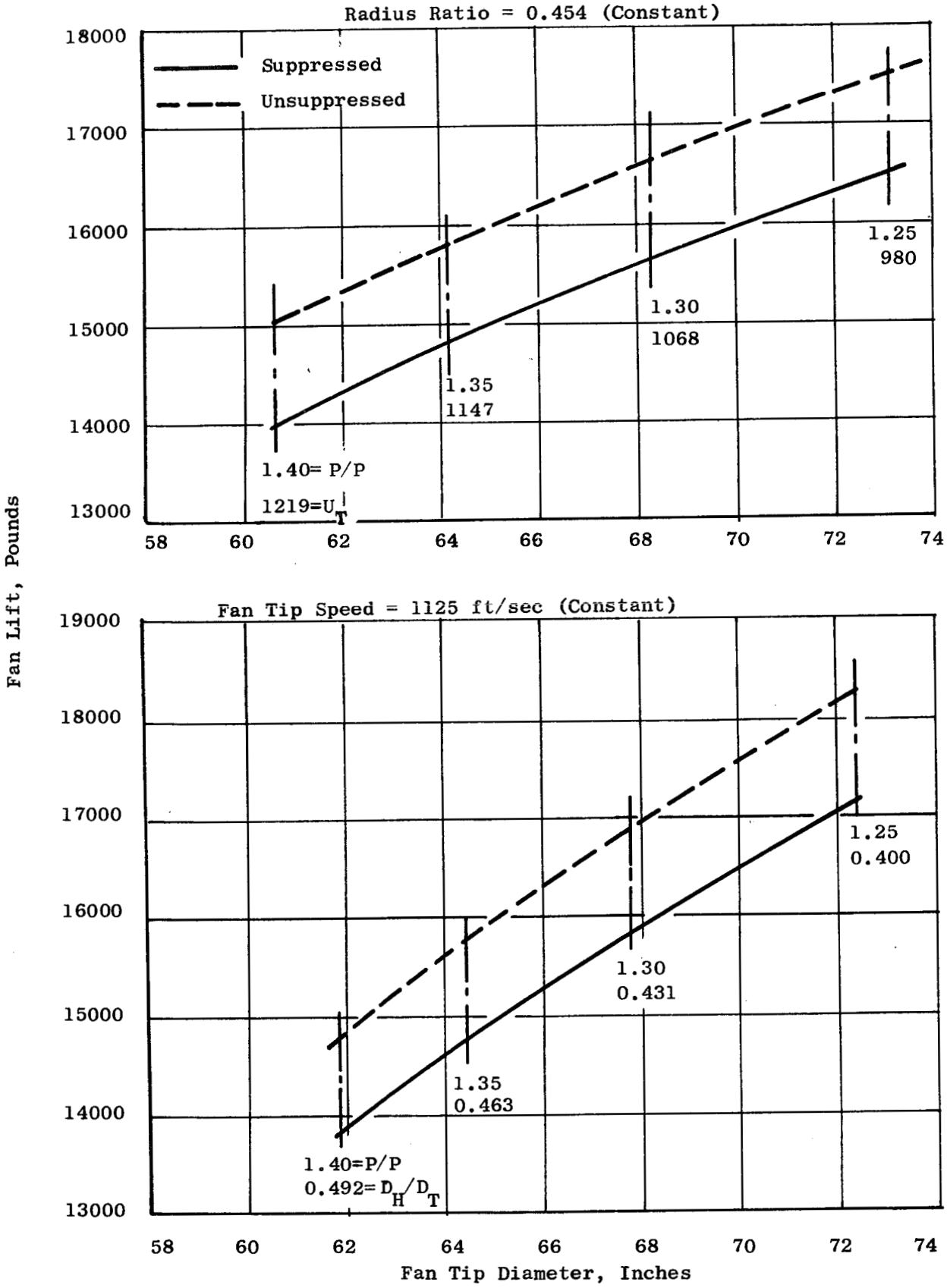

Figure 66. Parametric Fan Performance, Standard Day

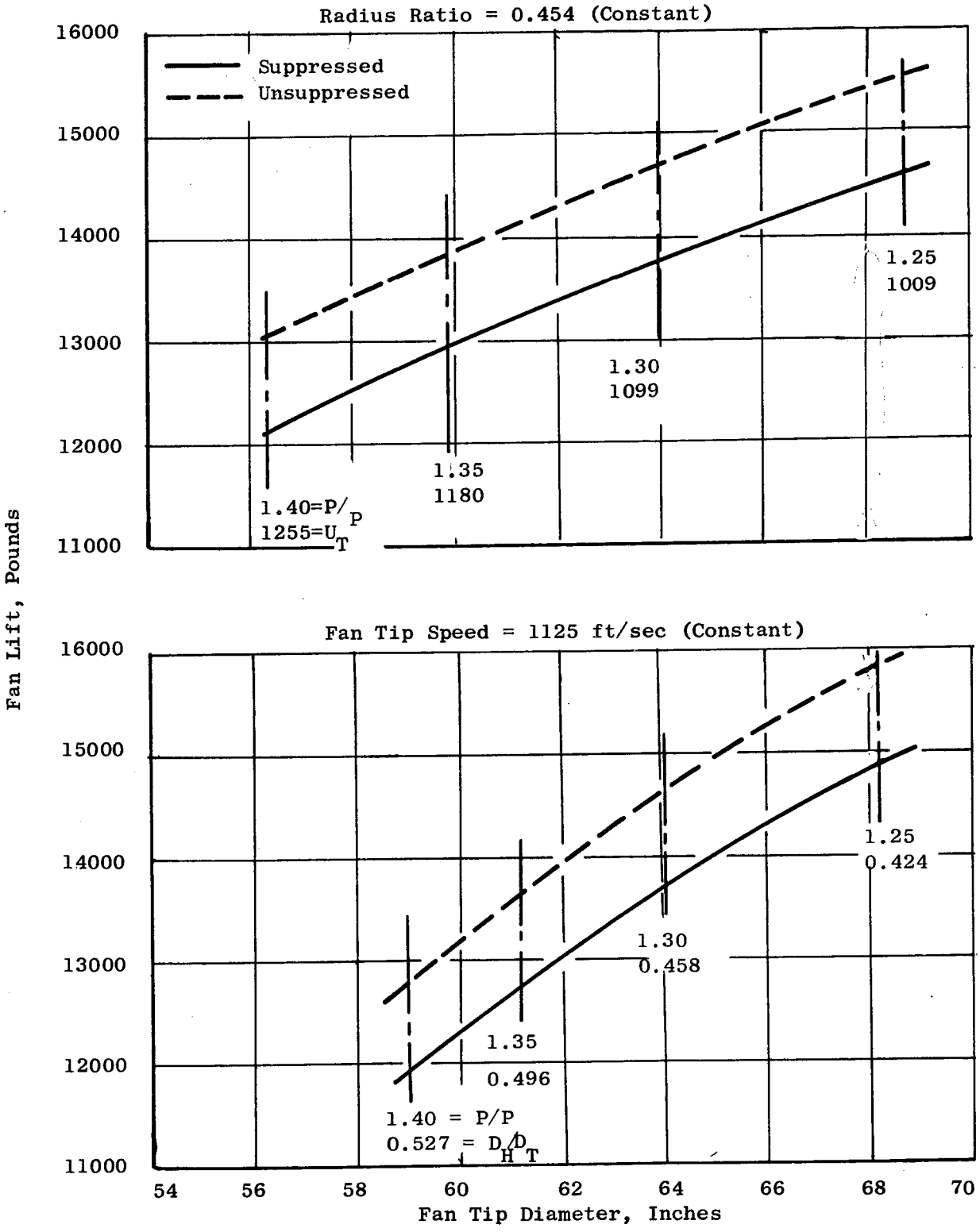

Figure 67. Parametric Fan Performance, 90°F Day

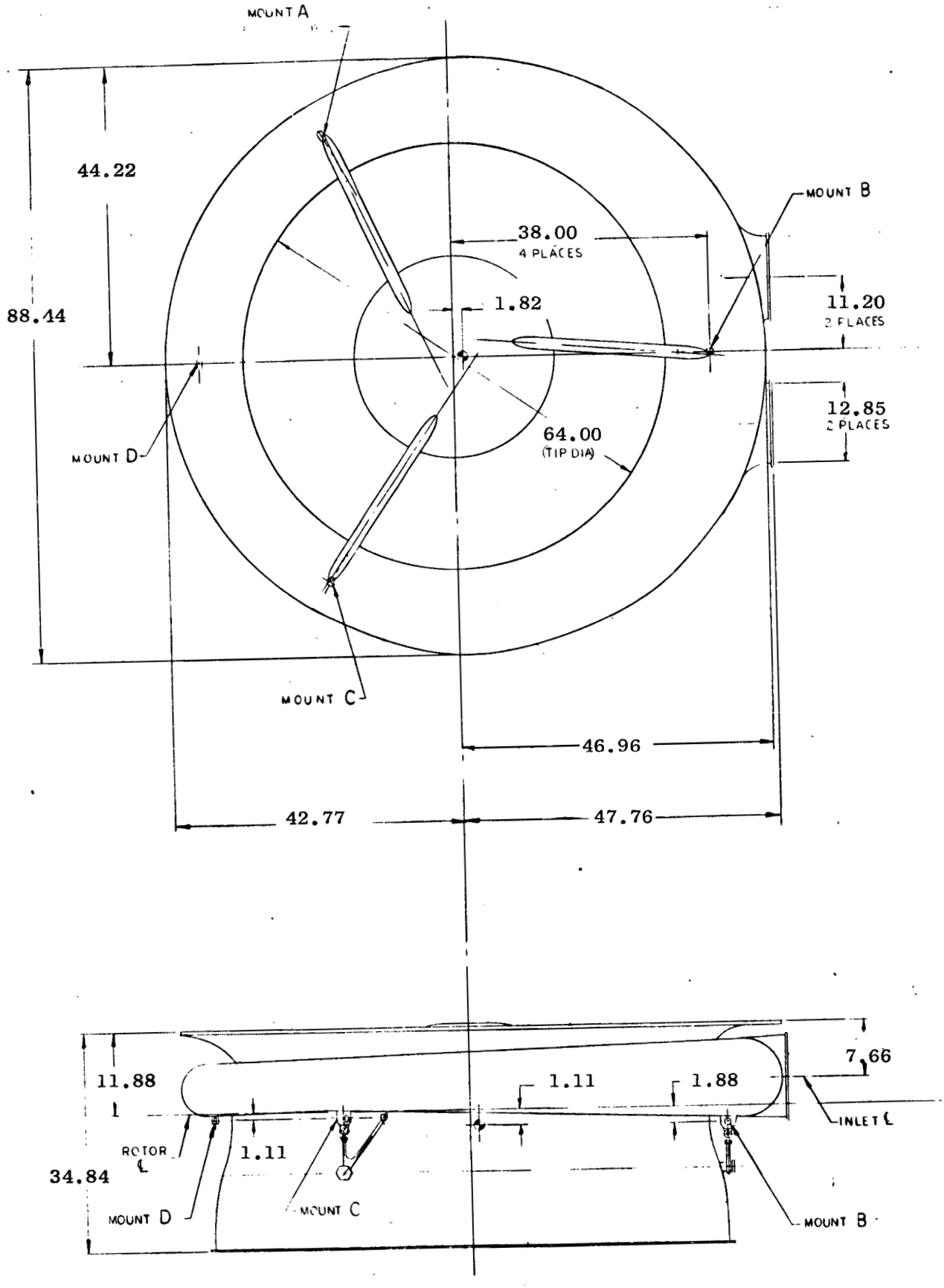

Figure 68. Installation Drawing of LF464, Heavy Suppressed, Lift Fan

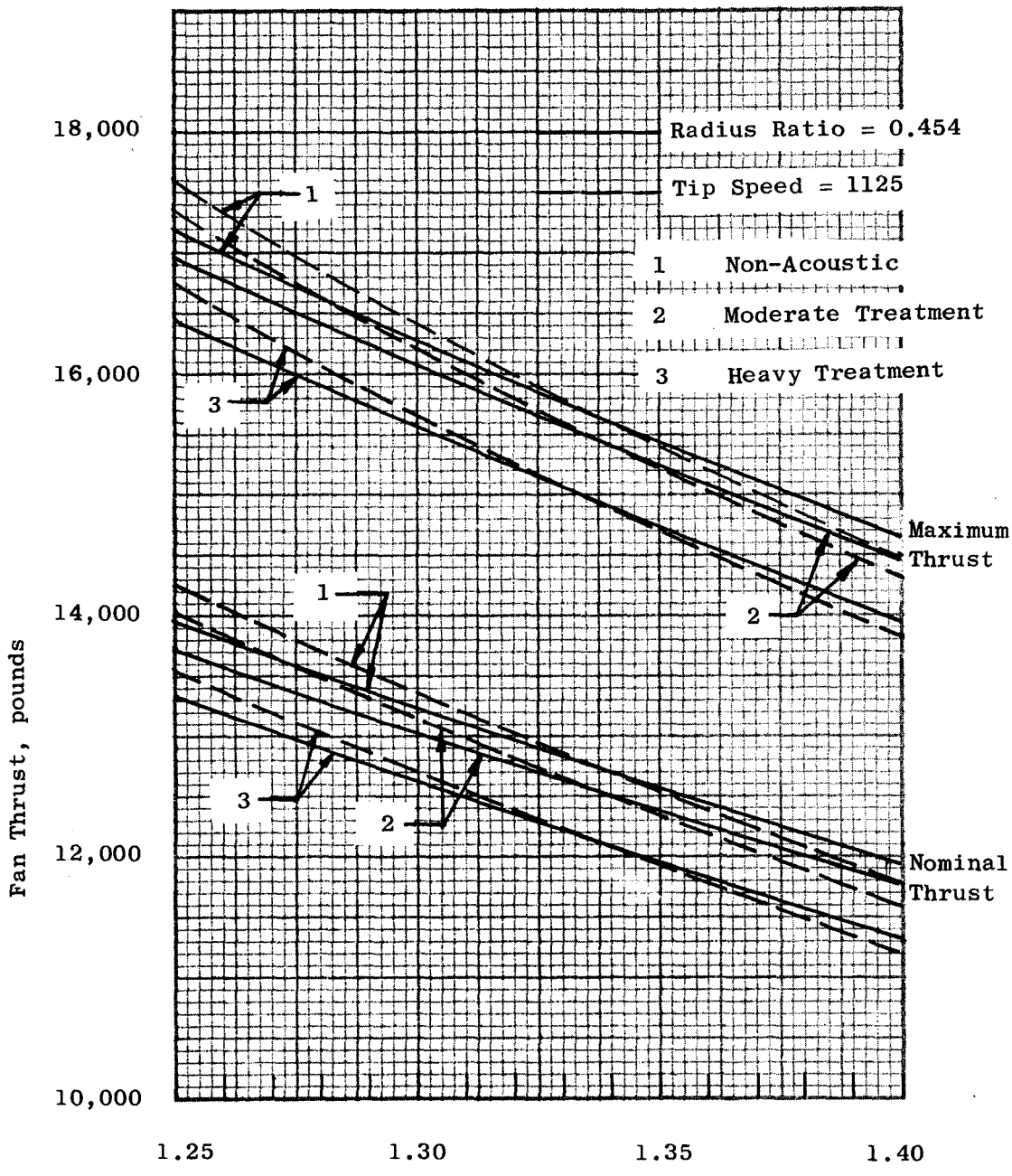

Figure 69. Fan System Thrust

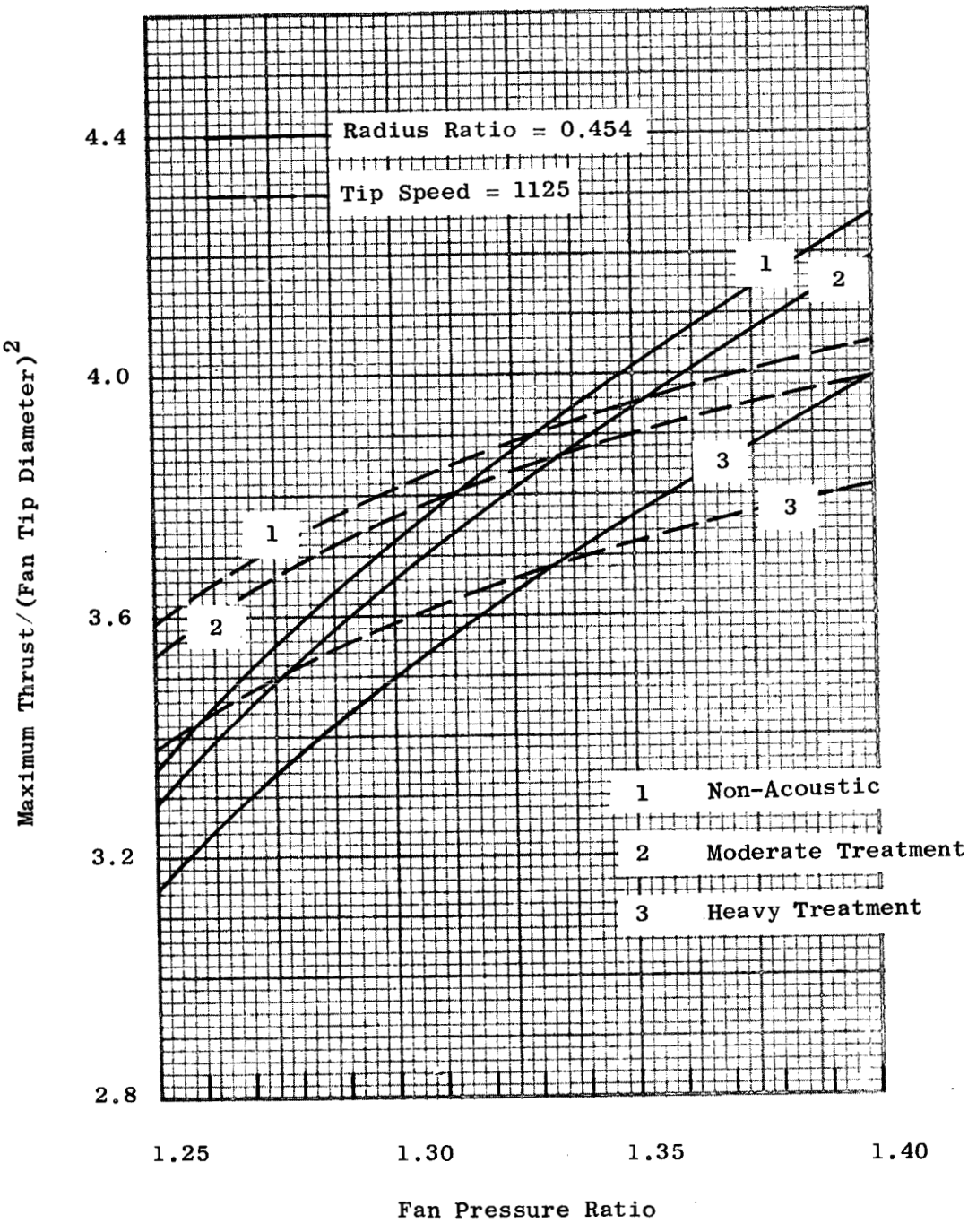

Figure 70. Fan System Sizing Parameter

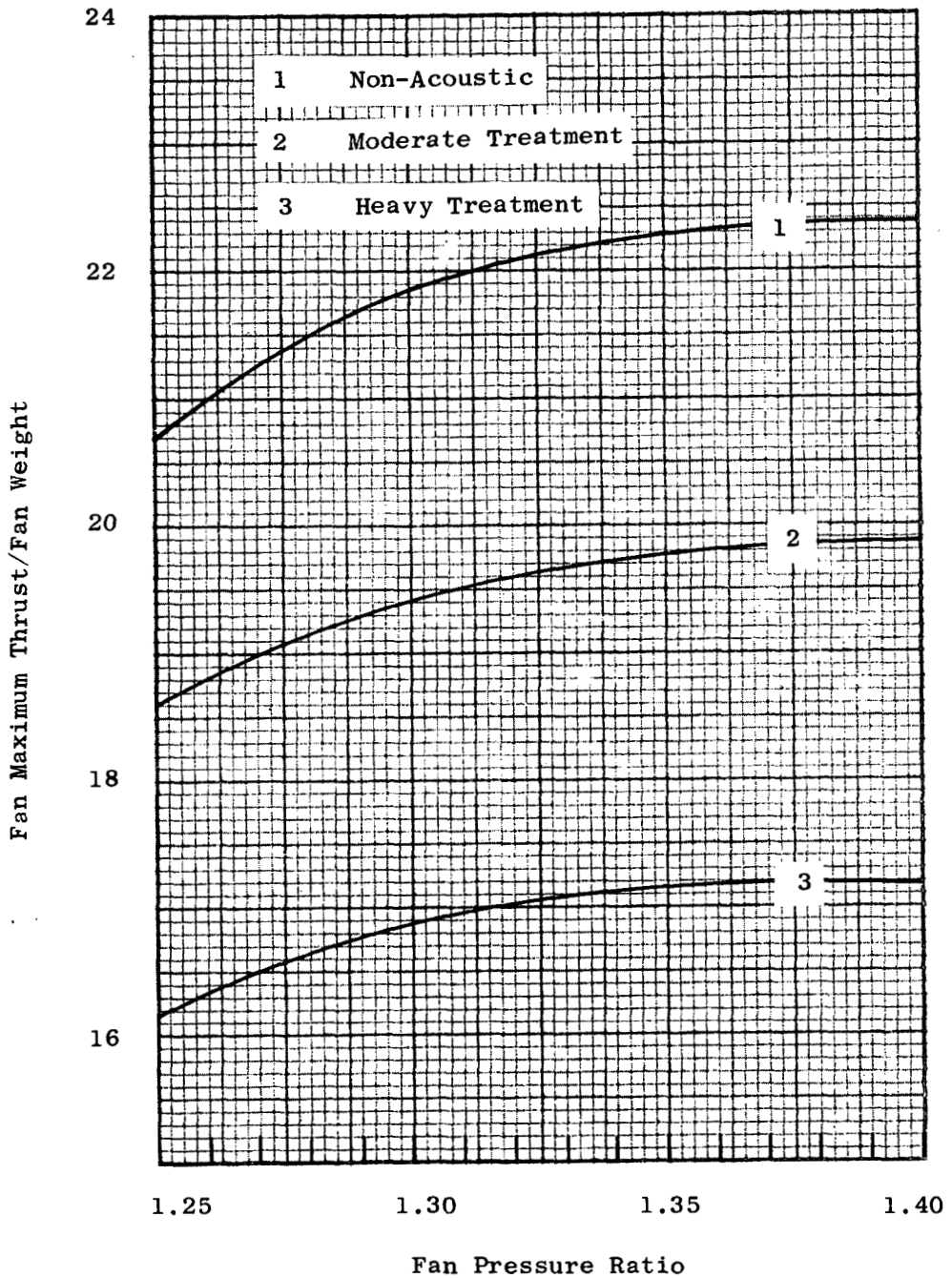

Figure 71. Fan Thrust-to-Weight

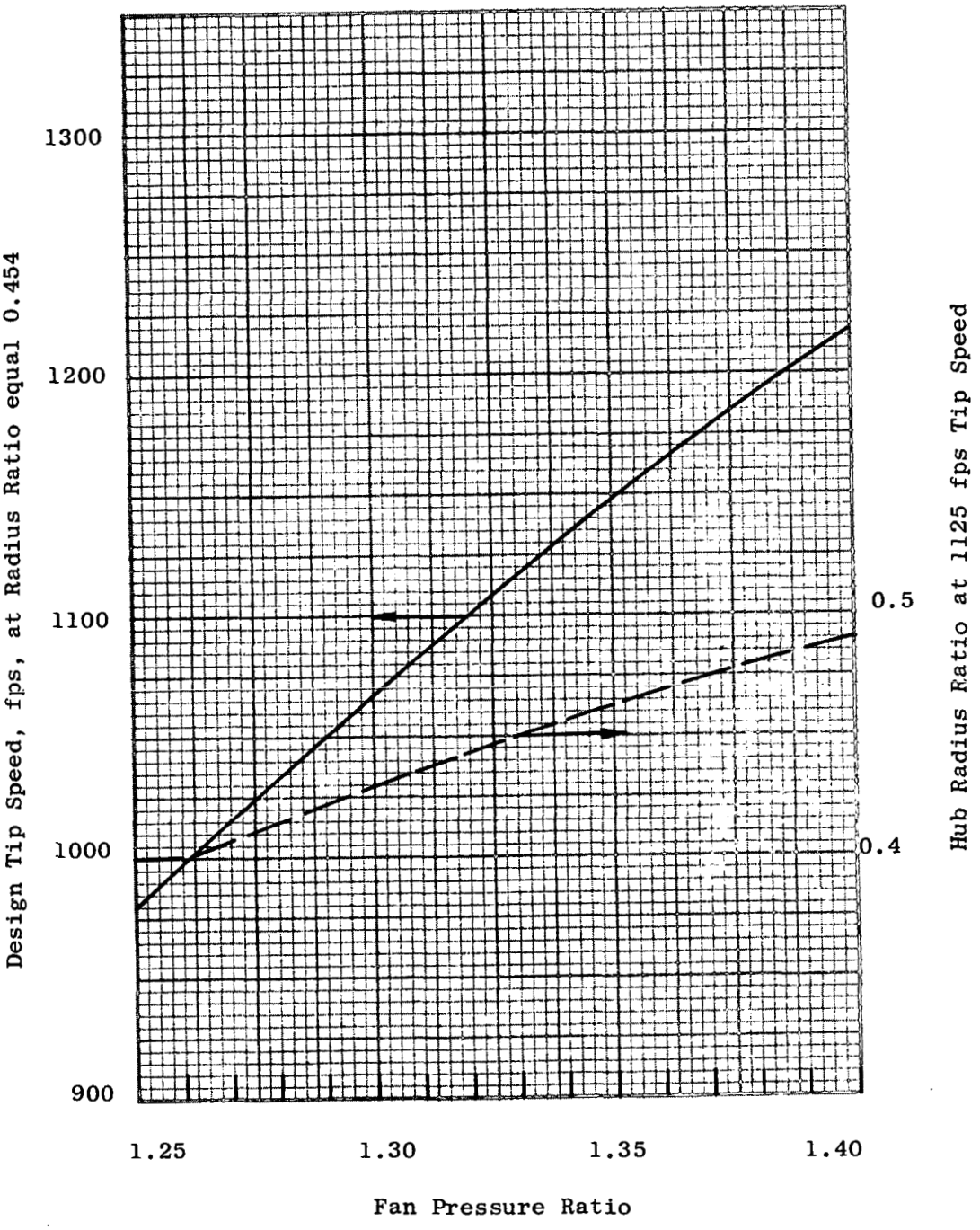

Figure 72. Fan Speed and Radius Ratio Variation with Design Pressure Ratio

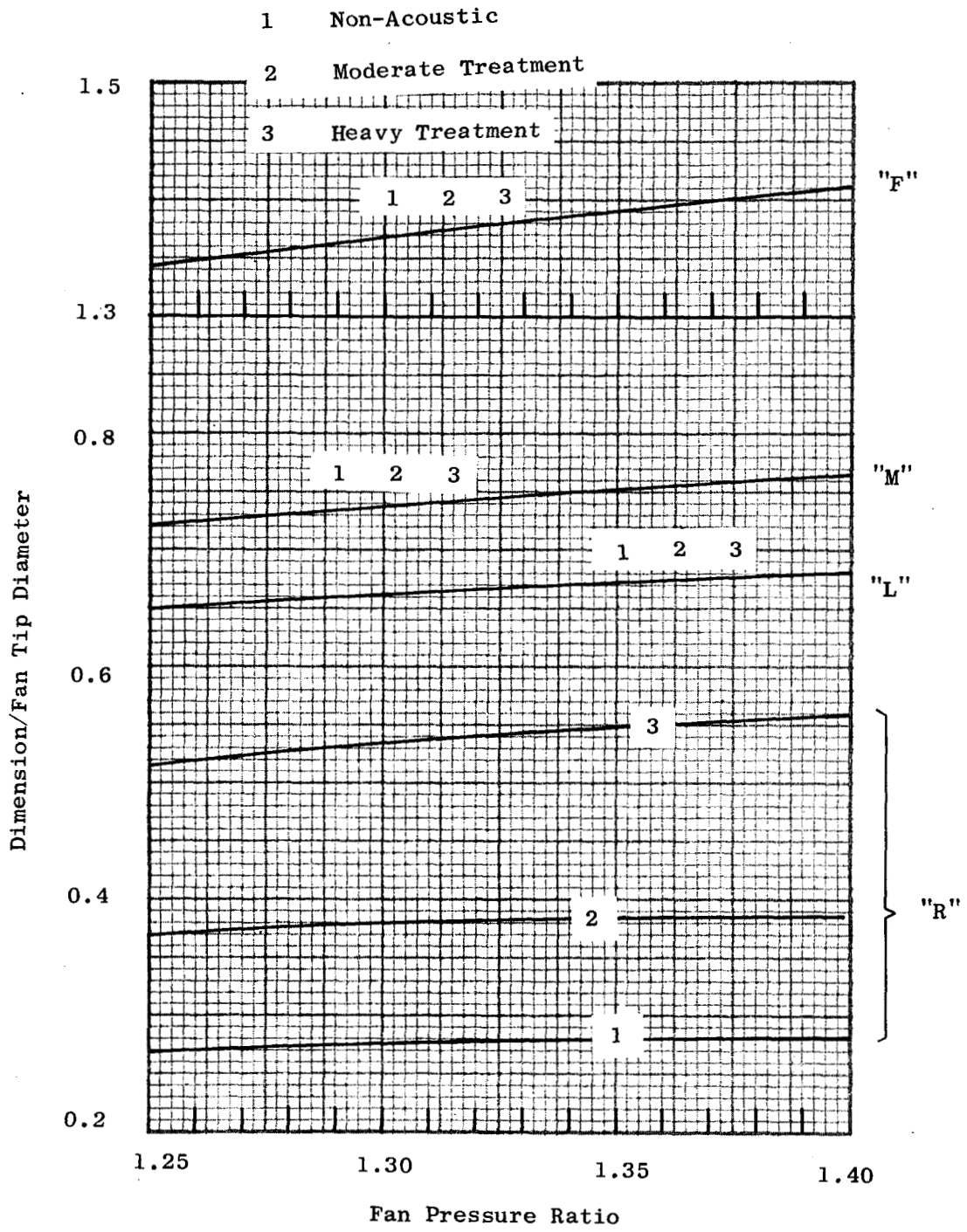

Figure 73. Installation Dimensions

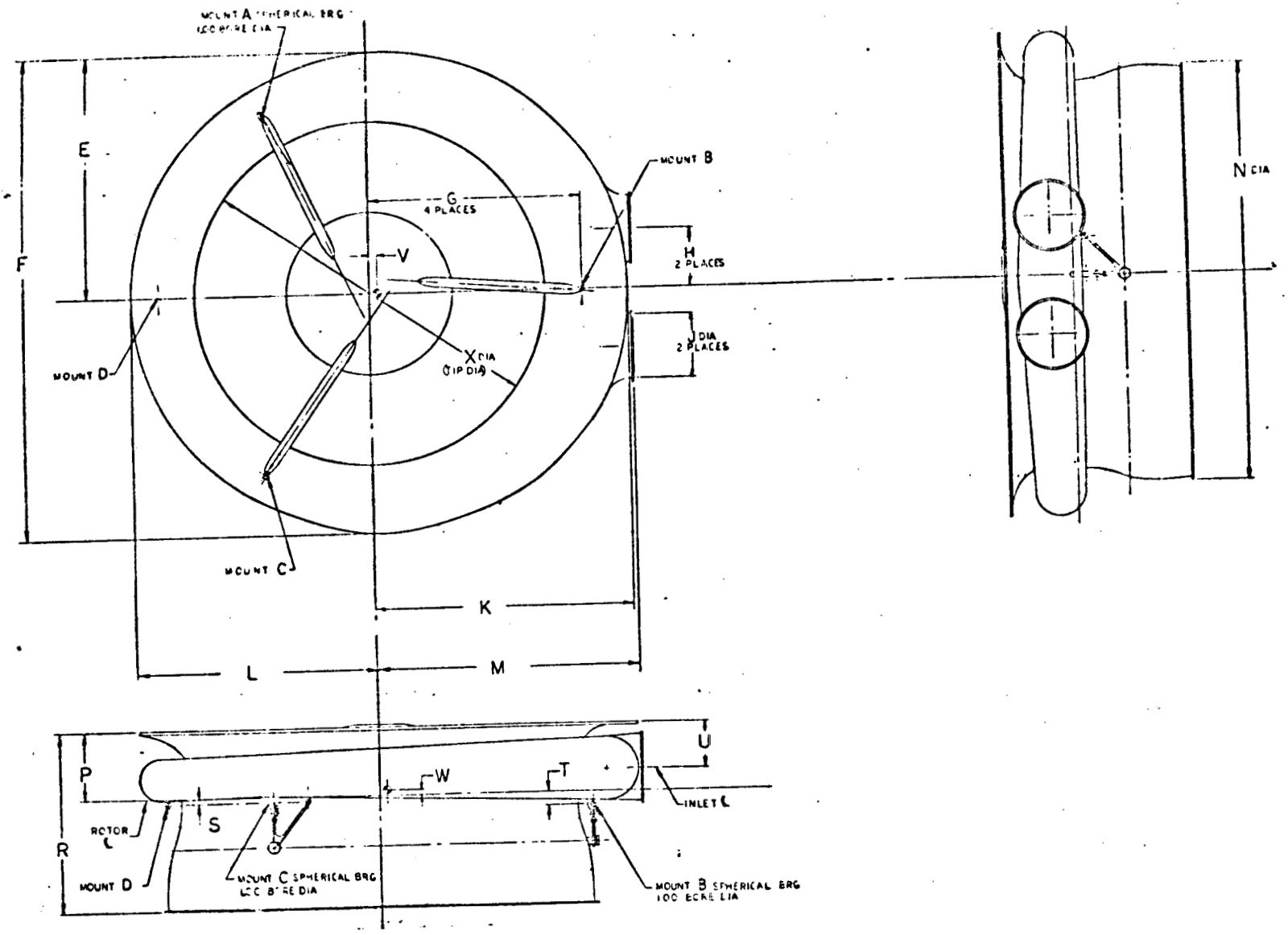

Figure 74. Installation Drawing

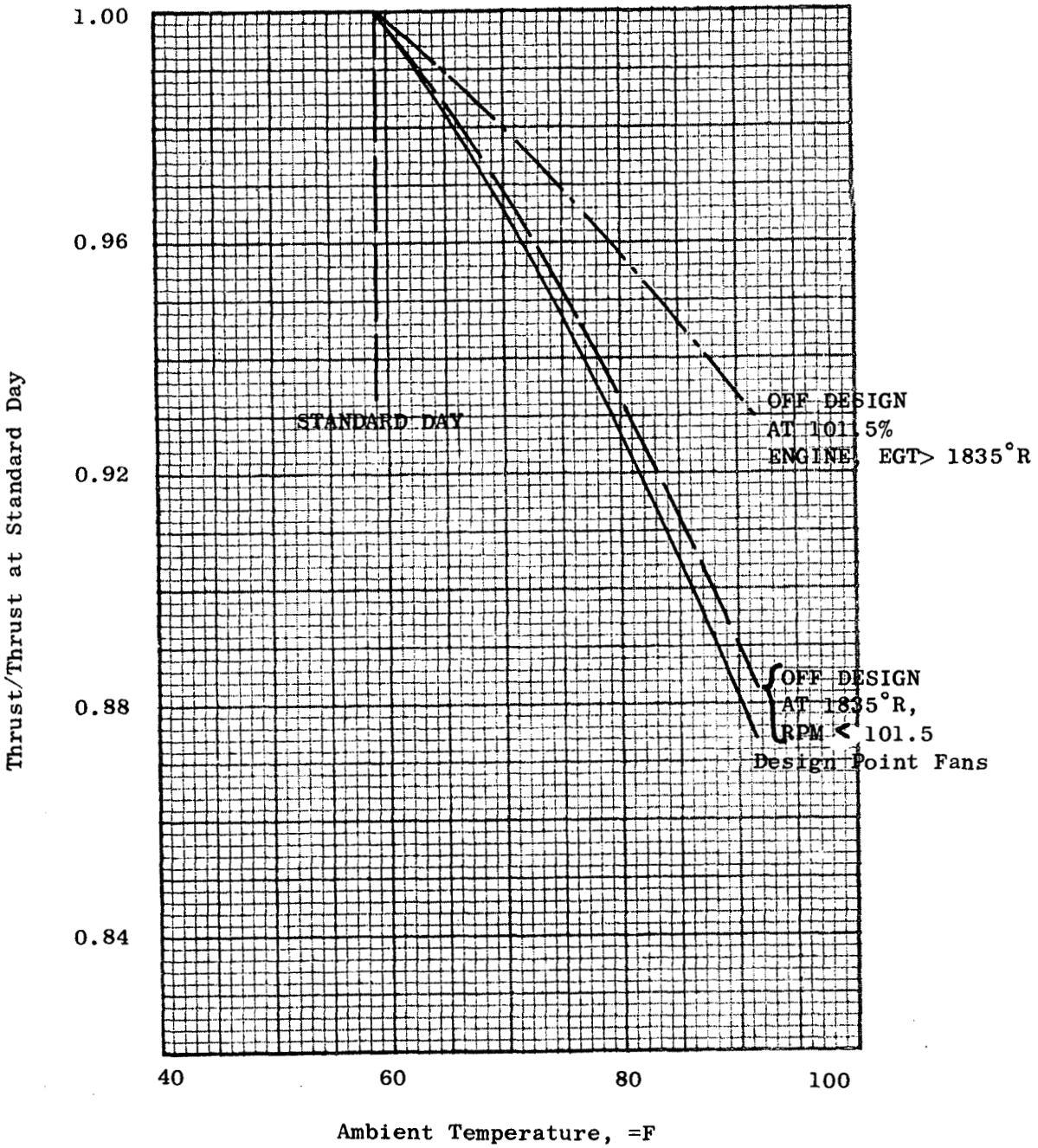

Figure 75. Corrections for Non-Standard Day Conditions

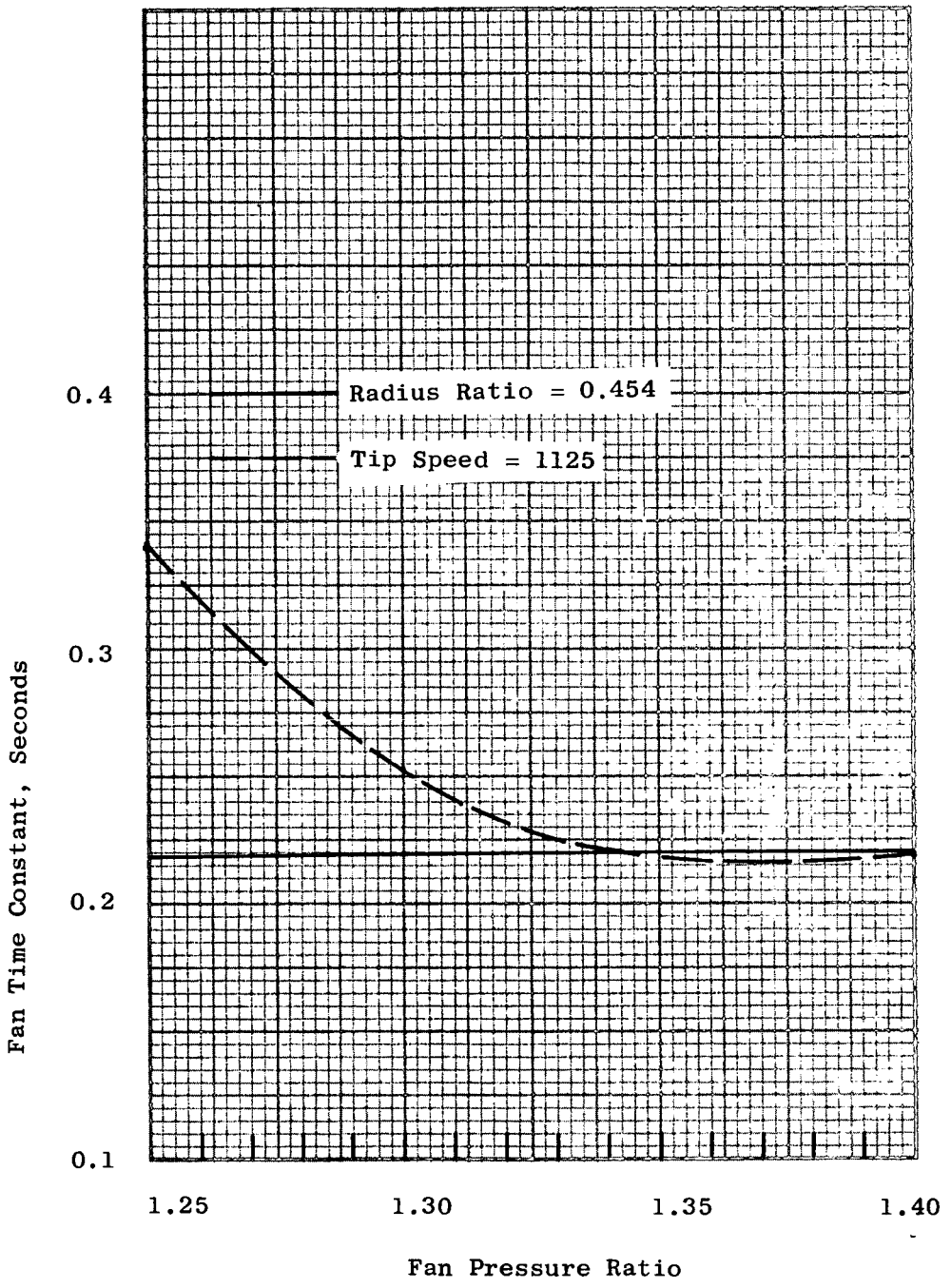

Figure 76. Fan Response Characteristics

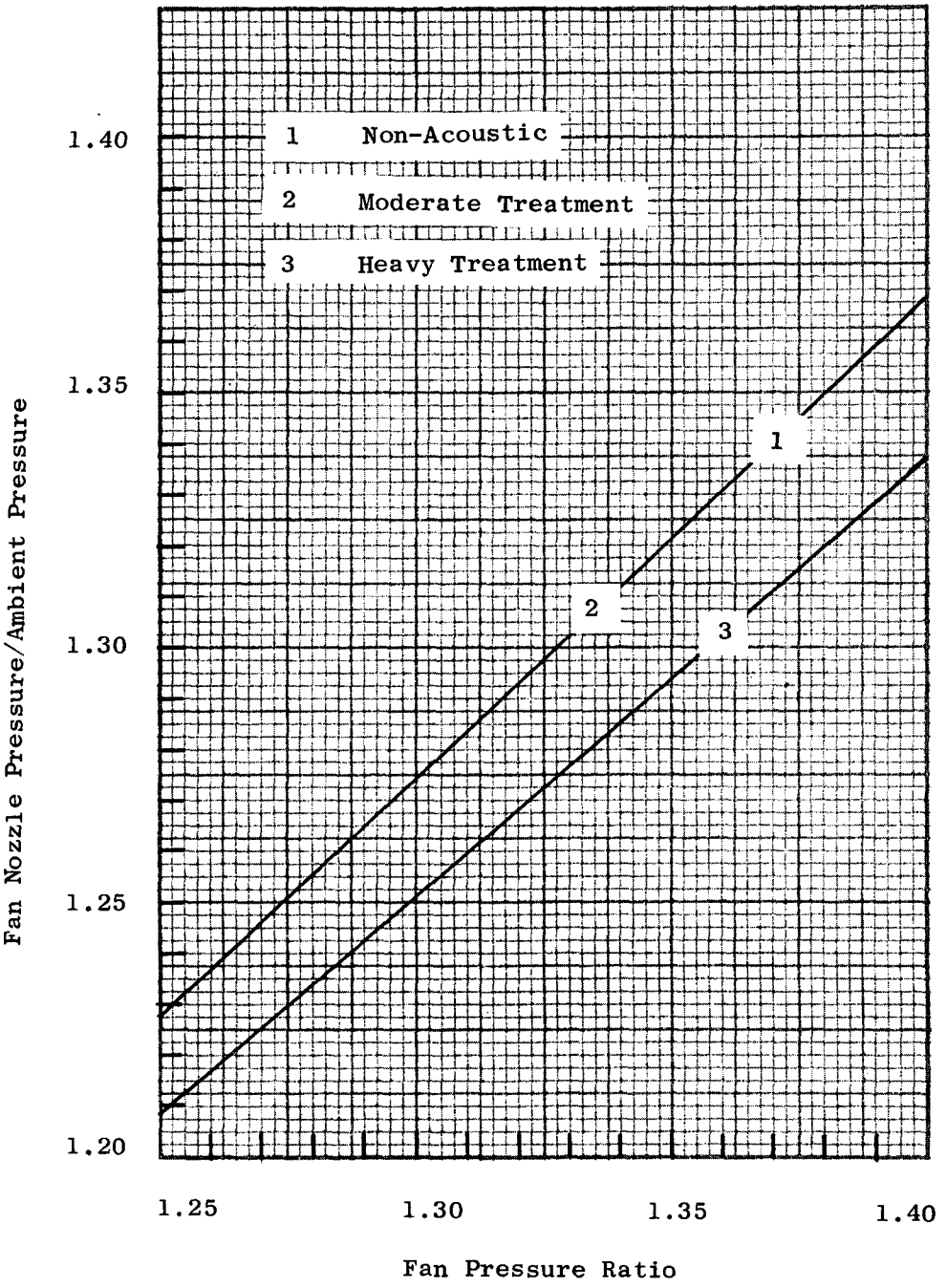

Figure 77. Fan Nozzle Pressure Ratio